

**Oscillatory patterns along the entire septo-temporal axis of the hippocampus in
behaving rats**

By Jagdish Patel

A Dissertation submitted to the
Graduate School-Newark
Rutgers, The State University of New Jersey
in partial fulfillment of the requirements
for the degree of
Doctor of Philosophy
Graduate Program in Integrative Neuroscience
written under the direction of
György Buzsáki
and approved by

Denis Paré, Ph.D.

André Fenton, PhD.

Laszlo Zaborszky, Ph.D.

Farzan Nadim, Ph.D.

György Buzsáki, Ph.D.

Newark, New Jersey
May, 2013

©2013

Jagdish Patel

ALL RIGHTS RESERVED

Abstract of the Dissertation

Oscillatory patterns along the entire septo-temporal axis of the hippocampus in behaving
rats

By Jagdish Patel

Dissertation Director:

György Buzsáki

The hippocampus exhibits two major modes of activity: Theta oscillations during the “online” active behavior and sharp-wave associated ripples during the “offline” inactive state. The rodent hippocampus is a complex C- shaped structure with a longitudinal axis (LA) of approximately 10mm. While theta and ripples oscillations have been extensively studied over the last 4 decades with strong evidence of their role in hippocampal memory functions, the organization of these oscillatory patterns along the LA has never been studied before. This lacuna is striking because there are genomic, anatomic, cellular, synaptic, and functional differences along its LA.

My dissertation investigated the organization of theta (5-10Hz) and sharp wave associated ripple (140 -200Hz) oscillations along the entire LA of the hippocampus in behaving rats. Using multiple drives I simultaneously recorded local field potentials and single unit activity from multiple locations along the LA.

The first study examined traveling theta waves. While the frequency of theta oscillations remained similar, theta amplitude and coherence between recording sites decreased from the dorsal to the ventral hippocampus. Theta phase shifted monotonically along the LA, reaching a maximum of 180° . While the majority of single units were phase-locked to the local field at all dorso-ventral segments, approximately 25% of single units from the ventral segment were phase locked to the dorsal hippocampal theta. Ventral hippocampal theta was weakly correlated with the locomotion velocity and varied independently of dorsal hippocampal theta. Thus, theta oscillations can temporally integrate or segregate neocortical representations along the LA of the hippocampus.

The second study examined the local generation and spread of ripples. Qualitatively similar ripples occurred at all levels of the LA and propagated in both directions: septally or temporally, with an average speed of 0.35m/sec. While ripples propagated smoothly in the septal 2/3rd of the hippocampal tissue, ripples in the ventral segment remained isolated. These findings suggest that the septal hippocampus can use ripples to combine the information before transferring integrated signals to downstream targets. However, because ripples occur at different times in the ventral and dorsal segments, they broadcast independent information to their non-overlapping cortical and subcortical targets.

Acknowledgements

Thank you to György Buzsáki for giving me the opportunity to take on this wild journey and for your support and wisdom throughout. I hope to have learned the virtue of patience and high energy levels. I pray to find the focus and passion as deep as yours.

Thank you to Bhagvanji Patel for believing in me, for giving me the freedom to pursue my dreams and for your bottomless well of love and support. Thank you to Lilavanti Patel for instilling in me the value of a simple life and for sharing with me your endless optimism and for your bottomless well of love and support. Thank you to Nisha Patel for your unquestioning belief, support and encouragement. Thank you to Ritesh Mishra for encouraging and inspiring as only a friend can.

Table of Contents

Chapter 1.0 - Introduction

1.1 - Overview	1
 1.2 – Hippocampal organization along the septo-temporal axis	2
<i>1.2.1 Anatomy: Afferent connectivity along the septo-temporal axis.....</i>	<i>2</i>
<i>1.2.2 Anatomy: Intrinsic connectivity along the septo-temporal axis</i>	<i>3</i>
<i>1.2.3 Anatomy: Neuro-modulatory connectivity along the septo-temporal axis....</i>	<i>4</i>
<i>1.2.4 Anatomy: Efferent connectivity along the septo-temporal axis</i>	<i>5</i>
<i>1.2.5 Genomic variation along the septo-temporal axis</i>	<i>6</i>
<i>1.2.6 In-Vitro electrophysiology: Cellular and Circuit properties along the septo-temporal axis.....</i>	<i>6</i>
<i>1.2.7 Lesion Studies involving different segments along the septo-temporal axis.....</i>	<i>7</i>
<i>1.2.8 In-Vivo electrophysiological recordings from different hippocampal segments along the septo-temporal axis</i>	<i>9</i>
 1.3 Hippocampal electrical activity.....	10
<i>1.3.1 - Rhythmic slow activity: Theta oscillations</i>	<i>10</i>
<i>1.3.2 – Large Irregular activity: Sharp waves</i>	<i>12</i>
 1.4 Health Relevance	13

Chapter 2.0 – Methods

2.1 Methods: General

<i>2.1.1 - Animals and Chronic Surgery</i>	15
<i>2.1.2 – Behavioral Training.....</i>	17
<i>2.1.3 – Histological and physiological verification of recording sites.....</i>	18
<i>2.1.4 - Data acquisition, processing and analysis.....</i>	20
<i>2.1.5 – Spike sorting and cell classification.....</i>	21

2.2 – Methods: Theta

<i>2.2.1 – Detection of theta periods.....</i>	22
<i>2.2.2 – Spectral analysis.....</i>	22
<i>2.2.3 – Theta amplitude and phase.....</i>	23
<i>2.2.4 – Unit analysis.....</i>	23
<i>2.2.5 – Permutation test.....</i>	24

2.3 – Methods: Ripples

<i>2.3.1 – Ripple event detection</i>	24
<i>2.3.2 – Wavelet analysis</i>	25
<i>2.3.3 – Ripple synchrony measure</i>	26
<i>2.3.4 – Relative ripple amplitude</i>	26
<i>2.3.5 – Unit analysis.....</i>	26
<i>2.3.6 – Permutation test.....</i>	26
<i>2.3.7 – 3-way ANOVA</i>	27

Chapter 3.0 – Results

3.1 Traveling theta waves along the entire septo-temporal axis of the hippocampus

3.1.1 - Abstract	28
3.1.2 - Introduction	29
3.1.3 - Results	30
<i>3.1.3.1 – Frequency, Power, Coherence, and Phase Shift of Theta Oscillations along the CA1 Septo-temporal Axis</i>	<i>33</i>
<i>3.1.3.2 – Theta Phase Locking of Neuronal Firing along the Septo-temporal Axis</i>	<i>38</i>
<i>3.1.3.3 – Co-modulation of Theta Power along the Septo-temporal Axis and the Effect of Speed on Power.....</i>	<i>40</i>
3.1.4 – Supplementary figures.....	43

3.2 – Local Generation and Spread of Ripples along the Septo-temporal Axis of the Hippocampus

3.2.1 - Abstract	50
3.2.2 - Introduction	51
3.2.3 - Results	53
<i>3.2.3.1 – Ripples along the Septo-temporal Axis of the CA1 pyramidal layer.....</i>	<i>54</i>
<i>3.2.3.2 – Spread of Ripples along the Septo-temporal Axis.....</i>	<i>60</i>

Chapter 4.0 – Discussion	69
4.1 Main Results: Theta oscillations	69
4.2 Main Results: Sharp-wave associated ripple oscillations	70
4.3 General discussion	71
4.4 Theta oscillations along the entire septo-temporal axis of the hippocampus ..	73
<i>4.4.1 – Mechanisms of Traveling Theta Waves along the Septo-temporal Axis</i>	<i>76</i>
4.5 Sharp wave-associated ripple oscillations along the entire septo-temporal axis of the hippocampus	79
<i>4.5.1 – Ripples are locally generated</i>	<i>80</i>
<i>4.5.2 – Propagating sharp wave ripples along the Septo-temporal Axis</i>	<i>82</i>
<i>4.5.3 – Hippocampal-neocortical communication by ripples</i>	<i>83</i>
4.6 Outstanding questions	
<i>4.6.1 – How strict is the dorsal-intermediate-ventral functional boundary/ Is the hippocampus a functionally unified network or two relatively separate, inter- connected networks?</i>	<i>86</i>
<i>4.6.2 – Is the ventral hippocampus functional distinction concerning sharp-wave ripples due to the ‘gap’ in anatomical sampling?</i>	<i>87</i>

4.6.3 – <i>How can the dorsal and ventral hippocampal circuits influence each other?</i>	88
4.6.4 – <i>How might the hippocampal poles integrate and segregate information?....</i>	89
4.6.5 - <i>How can these findings relate to the knowledge of theta generation and furthermore how do these findings impact behavior?</i>	90
4.7 Overall Summary	93
Chapter 5.0 – Bibliography	95
Chapter 6.0 – Appendix	115
Chapter 7.0 – Curriculum Vitae	116

List of Abbreviations:

CA1: Cornu Ammonis 1

CA2: Cornu Ammonis 2

CA3: Cornu Ammonis 3

DG: Dentate Gyrus

EC: Entorhinal Cortex

LIA: Large Irregular Activity

LFP: Local Field Potential

LT: Longitudinal Axis

REM: Rapid Eye Movement

RSA: Rhythmic Slow Activity

ST: Septo-Temporal Axis

TA: Transverse Axis

Chapter 1.0 - Introduction

1.1 - Overview

The hippocampus has long been assumed to play a key role in certain forms of memory (Scoville and Milner, 1957; Squire, 1992). Studies have shown that the hippocampus is critical for multiple forms of memory (Berger et al., 1983; Eichenbaum and Cohen, 1988; Eichenbaum et al., 1987; Squire, 1992; Wible et al., 1986; Wiener et al., 1989; Young et al., 1994) including spatial mapping (Maguire et al., 2000; Muller et al., 1987; O'Keefe and Dostrovsky, 1971; O'Keefe and Nadel, 1978), odor discrimination (Eichenbaum et al., 1988; Eichenbaum et al., 1989), configural discrimination (Rudy and Sutherland, 1989; Sutherland et al., 1989), and encoding of verbal and visual information (Fernandez et al., 1998; Rombouts et al., 1997; Stern et al., 1996), usually referred to as “declarative” memory in humans i.e. memories that can be consciously recollected (Squire, 1992). Hippocampal lesions produce wide ranging impairments including spatial and non-spatial deficits, confirming the role of hippocampus in multiple forms of memory (Gray, 1982). The range of impairments associated with hippocampal damage cannot be explained with a single theory and suggests functional differentiation within the hippocampus. The hippocampus could serve these diverse functions in one of at least two ways. Either the entire hippocampus could be devoted to a single very general type of memory with multiple subtypes, or the diverse forms of memory could depend on separate intra-hippocampal circuits, either overlaid or segregated.

1.2 Hippocampal organization along the septo-temporal axis

The rodent hippocampus is an elongated 3-dimensional structure, the dorsal/anterior/medial portion of which is known as the dorsal or septal pole while the other end, located more ventrally is known as the ventral or temporal pole. The hippocampus along this long axis is known as the septo-temporal (ST) axis or the dorso-ventral axis or the longitudinal axis (LA), while the hippocampus at an axis perpendicular to this septo-temporal axis is known as the transverse axis (TA). On its TA, the hippocampus primarily consists of the unidirectional excitatory pathways from the dentate gyrus (DG)-to-CA3-to-CA1-to-Subiculum. This intrinsic pattern of connectivity observed along the TA, repeats along the entire ST axis of the hippocampus (Amaral and Witter, 1989; Anderson, 1971). The lamellar organization of the intrahippocampal pathways combined with the parallel afferent and efferent connectivity of the hippocampus along the entire septo-temporal axis can be conceptualized to functionally subdivide the hippocampus along the long axis (Anderson, 1971). However, the longitudinally divergent connectivity of the CA3 recurrent collaterals, the CA3-CA1 schaffer collaterals and the CA3-CA1 associational system argues in favor of a functionally unified structure (Amaral and Witter, 1989; Li et al., 1994).

1.2.1 Anatomy: Afferent connectivity along the septo-temporal axis

All major cortical inputs to the hippocampus are conveyed via the entorhinal cortex (EC) which itself is divided into three parallel zones depending on its afferent connectivity, (Amaral and Witter, 1989), i.e., each zone receives a specific set of inputs from cortical

and subcortical areas, partly via the perirhinal and postrhinal cortices, (Burwell and Amaral, 1998; Naber et al., 1997). The sparse interconnectivity amongst these three entorhinal zones, (Dolorfo and Amaral, 1998a) suggests their possible role as separate functional units. In turn, these three entorhinal zones project in a topographic fashion to distinct regions of the hippocampus along the entire septo-temporal axis of the dentate gyrus: the caudolateral zone to the septal half, the intermediate zone to the adjacent quarter, and the rostromedial zone to the temporal quarter, (Dolorfo and Amaral, 1998b; Hargreaves et al., 2005; Ruth et al., 1982; Witter et al., 1989b). Such parallel, regionally specific afferent connectivity implies that specific information reaches specific division of the hippocampus along the septo-temporal axis, without prominent cross-talk, (Insausti et al., 1987; Room and Groenewegen, 1986a, b).

1.2.2 Anatomy: Intrinsic connectivity along the septo-temporal axis

Although specific information reaches different segments of the hippocampus along the septo-temporal axis, this information can be mixed within the hippocampus through the longitudinally divergent intrinsic connections of dentate gyrus to CA3, the CA3 recurrent collaterals or the CA3 projections to the CA1, which make-up the intrinsic connections within the hippocampus (Witter et al., 1989a). These connections have been reported to be longitudinally divergent: i.e. each downstream neuron in the trisynaptic loop connects to longitudinally wide-ranging upstream neurons (Amaral and Witter, 1989; Li et al., 1994). However, the same studies also reported that despite the longitudinal divergence of these intrinsic connections, they still form an arbitrary boundary at septal 2/3rd of the hippocampus, thereby essentially dividing the hippocampus into 2 segments: the septal

2/3rd and the temporal 1/3rd segments (Amaral and Witter, 1989; Fricke and Cowan, 1978; Li et al., 1994). This suggests that not only the different segments of the hippocampus along the septo-temporal axis receive information from different cortical areas, but that this information is kept segregated within the hippocampus (Insausti et al., 1987; Room and Groenewegen, 1986b).

1.2.3 Anatomy: Neuro-modulatory connectivity along the septo-temporal axis

Numerous studies have shown that almost all neuromodulators, including various neuro peptides project differentially and in a continually graded manner, to different segments of the hippocampus along the septo-temporal axis. Morphological differences along the septo-temporal axis include higher level of septal cholinergic innervation (Amaral and Kurz, 1985; Milner et al., 1983), higher receptor levels for substance P (Roberts et al., 1984), neuropeptide Y (Kohler et al., 1987), and oxytocin (van Leeuwen et al., 1985), higher number of calretinin positive mossy cells (Blasco-Ibanez and Freund, 1997) and higher density of dopaminergic (Verney et al., 1985), noradrenergic (Gage and Thompson, 1980; Haring and Davis, 1985), serotonergic (Gage and Thompson, 1980), vasopressinergic (Caffe et al., 1987) and enkephalinergic (Gall et al., 1981) terminals in the ventral part of the hippocampus. Such differences between the dorsal and ventral hippocampus are consistent with the notion that the dorsal and ventral hippocampal segments play different functional roles.

1.2.4 Anatomy: Efferent connectivity along the septo-temporal axis

Under such an organization where the information that reaches the hippocampus is kept segregated and is likely processed differently in different segments of the hippocampus along the septo-temporal axis, the outputs to different downstream targets may still overlap, thereby de-signifying the function of the segregated afferent and intrinsic connections to/within the hippocampus. The specificity in afferent connectivity observed along the septo-temporal axis is preserved on the efferent side. Both output regions, the CA1 and subiculum, project topographically onto the entorhinal cortex i.e., cells along the septo-temporal axis of the hippocampus project along the lateral to medial axis of the entorhinal cortex, (Cenquizca and Swanson, 2007; van Groen and Wyss, 1990). Furthermore, the entorhinal cortex has topographic projections to perirhinal cortex, which connects back to the same cortical areas from which the afferent information originated (Insausti et al., 1987). Information thus flows in dedicated lines along the transverse axis throughout the septo-temporal axis of the hippocampus without significant overlap. In addition, only ventral CA1 cells project to the medial prefrontal cortex (Ferino et al., 1987; Jay et al., 1989; Jay and Witter, 1991; Swanson, 1981; Thierry et al., 2000), the bed nucleus of stria terminalis and amygdala (Amaral, 1986; Petrovich et al., 2001; Pitkanen et al., 2000). Ventral CA1 also projects, selectively and topographically, to the subcortical structures associated with the hypothalamic-pituitary-adrenal axis (Jacobson and Sapolsky, 1991; Siegel and Tassoni, 1971). In addition, the dorsal, intermediate and ventral hippocampi project to cyto-architectonically different regions of the lateral septum, which in turn innervate specific sets of hypothalamic nuclei (Risold and Swanson, 1996, 1997). Such segregated and parallel input and output connections suggest

that different segments of the hippocampus along the septo-temporal axis may be processing different information.

1.2.5 Genomic variation along the septo-temporal axis

Genetic markers reveal distinct spatial expression patterns with domains and subdomains along the septo-temporal axis of the CA1 pyramidal layer, (Dong et al., 2009; Thompson et al., 2008). Furthermore, downstream subcortical brain regions display distinct gene expression patterns. This suggests that the spatial domains in the CA1 region are genetically wired in a manner as to form independent and distinct functional networks. The evidence of genomic variation along the septo-temporal axis suggest regional selectivity of functions along the long axis (Fanselow and Dong, 2010).

1.2.6 In-Vitro Electrophysiology: Cellular-circuit properties along the septo-temporal axis

Hippocampal neurons along the septo-temporal axis exhibit different electrophysiological properties. These differences include increased tendency of multiple population spikes (Gilbert et al., 1985) and lower threshold epileptiform after discharges in ventral CA1 segment (Racine et al., 1977). Differences in event related potentials (Brazier, 1970), vulnerability to ischemia (Ashton et al., 1989), short-term synaptic plasticity (Papatheodoropoulos and Kostopoulos, 2000b), long-term potentiation, (Maggio and Segal, 2007; Maruki et al., 2001; Papatheodoropoulos and Kostopoulos, 2000a), paired pulse facilitation, (Maruki et al., 2001) and synaptic inhibition (Papatheodoropoulos et al., 2002) have also been observed between the dorsal and the ventral CA1 regions.

Overall, the differences in electrophysiological properties in the dorsal and ventral segments suggest that the hippocampus may consist of two or more independent modules along its septo-temporal axis.

1.2.7 Lesion Studies involving different segments along the septo-temporal axis

Many early behavioral experiments based on lesions, hinted at potential functional differences between the dorsal and ventral hippocampus (Hughes, 1965; Stevens and Cowey, 1973). Later studies using aspiration lesions of confined septo-hippocampal segments showed that spatial learning was severely impaired in the Morris water maze task following dorsal lesions but not following ventral lesions of the same size (Moser et al., 1993). The impairment also correlated with the size of the dorsal hippocampal lesion. These findings were replicated with fiber-sparing ibotenic acid lesions (Moser et al., 1995). The threshold volume of damage to the dorsal area necessary to produce a deficit was very high, and spatial learning could occur with only 20-30% of the dorsal segment. Subsequent studies using selective lesions of dorsal or ventral CA1 regions confirmed that the dorsal part of the CA1 region plays a critical role in a variety of spatial memory tasks compared to ventral CA1 (Bannerman et al., 2002; Bannerman et al., 2003; Bannerman et al., 1999; Hock and Bunsey, 1998; Pothuizen et al., 2004; Zhang et al., 2004). Overall, these studies implied a selective role of the dorsal hippocampal neurons in spatial learning and memory under different experimental conditions. In contrast, these studies found that neurons in the ventral pole of the hippocampus are not critical for either spatial working or spatial reference memory. Therefore, separate kinds of computation might be performed by the two poles of the hippocampus. On the other

hand, numerous behavioral studies have implicated ventral hippocampus in anxiety-related behavioral responses (Bannerman et al., 2004; Degroot and Treit, 2004; Hock and Bunsey, 1998; Kjelstrup et al., 2002; McHugh et al., 2004; Richmond et al., 1999). These studies found that rats with selective ventral hippocampus lesions show reduced hyponeophagia i.e., they are quick to eat in potentially anxiogenic and unfamiliar environments, have increased social interactions, are quick to cross compartments in a two compartment box test, spent more time in anxiogenic arms of the elevated plus maze, have reduced levels of defecation in anxiogenic environments and have reduced increase in plasma corticosterone levels following a stressful confinement period. Dorsal lesions in these studies had no effect on any of these parameters. However, lesion studies are often plagued by unintended effects on surrounding regions and fibers of passage, distal damage and compensatory processes (Bannerman et al., 2004; Moser and Moser, 1998). Indeed, spatial learning was found to be impaired following unilateral or bilateral lidocaine injections into the intermediate hippocampus to ventral hippocampus region (Poucet and Buhot, 1994; Poucet et al., 1991; Thinus-Blanc et al., 1991). Rats with excitotoxic dorsal lesions were also able to acquire spatial reference memory task in a Morris water maze, after sufficient training (de Hoz et al., 2003). In addition, increased *c-fos* activation subsequent to spatial training was found in both the dorsal and the ventral CA1 (Vann et al., 2000).

1.2.8 In-Vivo electrophysiological recordings from different hippocampal segments along the septo-temporal axis

If neural processing in the dorsal hippocampus is sufficient for spatial navigation, the firing correlates of the ventral pyramidal cells would be expected to be different from dorsal cells. In fact, a much lower proportion of neurons in the ventral hippocampus have spatial correlates (Colombo et al., 1998; Jung et al., 1994; Kjelstrup et al., 2008; Poucet et al., 1994; Royer et al., 2010), and their place fields tend to be broader with less spatial correlation (Jung et al., 1994; Kjelstrup et al., 2008; Royer et al., 2010). However, it is not clear whether the functional differentiation of the hippocampus along the septo-temporal is graded or discontinuous. One hypothesis is that the hippocampus works as a unitary structure wherein both, the dorsal and ventral pole participate in all hippocampal functions with varying effectiveness along the axis. For example, while the dorsal CA1 region may play a more significant role in spatial memory formation, the ventral CA1 region may be critical for encoding spatial memories involving anxiety. A second hypothesis suggests that the dorsal and ventral hippocampal segments are separate, relatively non-overlapping units processing qualitatively different kinds of information. Our study design allowed us to test these hypotheses (Patel et al., 2012; Royer et al., 2010). Furthermore, we still do not know what type of information is processed by the ventral hippocampus. While the oscillatory patterns of theta and sharp wave ripples from the dorsal hippocampus have been extensively studied, very little is known about the organization of these oscillatory patterns along the septo-temporal axis during different behavioral states. Oscillatory rhythms of the hippocampus are hypothesized to underlie information processing (Buzsáki, 2006) and synchronized patterns of particular rhythms

across regions would suggest functional kinship between them (Womelsdorf et al., 2007). Our recordings during exploratory activity allowed us to study the firing correlates of ventral and intermediate CA1 cells. We also measured and reported the organizing principles of theta waves along the entire septo-temporal axis of the hippocampus. No information is available about the distribution of SPW ripples along the length of the hippocampus. By recording during sleep and inactivity periods we examined how SPW ripples frequency, amplitude and occurrence rate varied as a function of electrode location along the entire septo-temporal axis. We also measured the temporal and spatial synchrony between ripples, their propagation direction and speed, and correlation with multi-unit activity at different levels along the septo-temporal axis. This helped us determine the differential methods of information processing used by neuronal populations along the septo-temporal axis of the hippocampus in behaving rats.

1.3 Hippocampal Electrical Activity

Based on the variations in local field potentials (LFP) and neuronal discharges, the hippocampus shows two major "modes" of activity: rhythmic slow activity (RSA) and large irregular activity (LIA).

1.3.1 - Rhythmic slow activity: Theta oscillations

Rhythmic slow activity occurs during the active "awake" state, and appears in the presence of voluntary movements, arousal, and during rapid eye movement (REM) sleep (Bland, 1986b; Green and Arduini, 1954; Sainsbury, 1998; Vanderwolf, 1969a). During

RSA, the LFP of the hippocampus exhibits theta oscillations (5-10 Hz). Theta oscillations have been seen in all mammals studied to date, including humans (Buzsaki, 2002; Kahana et al., 2001), although the prevalence of theta during immobile arousal states (Green and Arduini, 1954; Vanderwolf, 1969b), and possibly REM sleep (Bodizs et al., 2001; Cantero et al., 2003), varies to a large extent across species. Although theta oscillations are largest in CA1 lacunosum moleculare (Kamondi et al., 1998), they are present in every hippocampal region and have been observed in other structures, including the subiculum (Anderson and O'Mara, 2003), neocortex (Kahana et al., 2001), amygdala (Pare et al., 2002), striatum (DeCoteau et al., 2007), medial septum (Vinogradova, 1995), and hypothalamic nuclei (Vertes and Kocsis, 1997), but the local generation of theta oscillations must be carefully investigated to rule out effects of volume conduction (Sirota et al., 2008). During theta, hippocampal neurons show sparse population activity. In any short time interval, the great majority of cells are silent, while the small remaining fraction fire at relatively high rates, up to 50 spikes/sec (O'Keefe and Dostrovsky, 1971; O'Keefe and Nadel, 1978). An active cell typically stays active for half a second to a few seconds as the rat traverses the place field of the cell. As the rat explores, the overall percentage of active cells remains constant and as the currently active cells fall silent other cells become active. While the activity of pyramidal neurons is largely determined by the spatial location of the animal, other behavioral correlates have been identified, such as the grandmother cell.

1.3.2 - Large-amplitude irregular activity: Sharp-waves

Large-amplitude irregular activity represents an “offline” state of the animal, and accompanies “automatic” and consummatory behaviors such as grooming and eating, as well as the slow-wave stages of sleep (Buzsaki 1989; Vanderwolf 1969). Within the hippocampus, the LIA coincides with variable periods (100 msec - 10 sec) of relative inactivity among pyramidal neurons punctuated by strong bursts of activity originating in the CA3 region (Csicsvari et al. 2000). The coordinated burst of CA3 pyramidal neurons generates excitatory post-synaptic potentials (EPSPs) in CA1 neurons, creating a large (1-3mV) extracellular negativity in CA1 stratum radiatum that persists for approximately 50 to 100 msec. This leads to the brief emergence of a 120-200 Hz “ripple” oscillation in the CA1 pyramidal layer generated by the synchronized interplay between the pyramidal neurons and interneurons for the duration of the sharp wave (Buzsaki 1989; Buzsaki et al. 1992). The spiking activity of neurons within the hippocampus is highly correlated with sharp wave activity. While most neurons decrease their firing rate between sharp waves, during a sharp wave a dramatic increase in firing rate in up to 10% of the hippocampal population is reported (Buzsaki, 1986; Buzsaki et al., 1992; Csicsvari et al., 2000). These sharp wave/ripple complexes are correlated with the up-down state transitions in the cortex (Isomura et al. 2006) and are believed to aid the transfer of processed packets of information to the cortex (Chrobak and Buzsaki 1994; Siapas and Wilson 1998; Ylinen et al. 1995).

1.4 Health Relevance:

On the one hand, a rodent hippocampus is an elongated 3-dimensionally complex structure that sub-serves multiple forms of memories. On the other hand, numerous studies have shown that while the dorsal hippocampus is critical for spatial navigation based memories the ventral hippocampus is selectively associated with anxiety based responses. The ventral hippocampus has strong and specific efferent connections with several subcortical forebrain structures, including the rostral hypothalamus and amygdala, and may interact with a variety of autonomic, endocrine, defensive, social, reproductive and emotional control systems (Amaral, 1986; Risold and Swanson, 1996). The ventral hippocampus, through its specific projections to the neuroendocrine and pre-autonomic cell groups of the periventricular zone via the lateral septum, is suggested to be involved in the adaptation of the hypothalamus-pituitary axis to environmental information (Jacobson and Sapolsky, 1991; Risold and Swanson, 1997). Indeed, behavioral studies following ventral hippocampus lesions have indicated a specific role of the ventral hippocampus in anxiety. Many of the effects of ventral hippocampus lesions found in these studies were distinct from those of amygdala lesions (McHugh et al., 2004; Phillips and LeDoux, 1992). In particular, the ventral hippocampus and amygdala are suggested to contribute differentially and uniquely to the processing of anxiogenic and fearful stimuli, respectively. Moreover, it is the ventral segment of the rodent hippocampus that grows disproportionately to become the large body and uncus parts of the hippocampus in primates (anterior hippocampus). A better understanding of the ventral hippocampus will improve our knowledge of the hippocampus as a whole. Such wholesome mechanistic approach may not only uncover the functional organization

of the hippocampus but also help us understand how the hippocampus participates in multiple forms of memories. More specifically, studying the ventral hippocampus may broaden our neurobiological understanding of anxiety and may guide us towards more effective therapeutic interventions for disorders like depression, post-traumatic stress disorder, schizophrenia, autism, obsessive compulsive disorder and bipolar disorder. Our electro-physiological investigation of the differences and similarities between the electrical patterns in the dorsal, intermediate and ventral segments of the hippocampus constitute an important step in this direction.

Chapter 2: Methods

2.1 Methods: General

2.1.1 Animals and chronic surgery

Data were collected from 17 Long-Evans rats (male, 250-400g, 3-5 months old). The details of surgery and recovery procedures used have been described earlier (Csicsvari et al., 1998). In brief, animals were deeply anesthetized with isoflurane and up to four separate craniotomies were performed over the right hippocampus. In a total of 8 rats, two separate drives were implanted for electrophysiological recordings; one targeted the septal-intermediate 2/3rd and the other the ventral (4th quadrant) CA1 pyramidal layer. In the 9th rat (rat-11), the drive targeted only the septal 2/3 CA1 pyramidal layer. In the 10th rat (r-27), the septal drive was placed along the transverse axis in order to record activity along the subiculum-CA1-CA2-CA3 axis. In 2 additional rats (rat-29 & rat-30), 4 silicon probes (each with 8 vertical sites x 4 shanks; 20 μ m vertical site separation and 200 μ m intershank interval; shanks of each probe were placed along the transverse axis while the probes were placed along the longitudinal axis) were implanted in order to record the physiological activity in 3-D. In one rat (r-tn), a 256-site probe (32 sites on each of the 8 shanks with 50 μ m vertical site separation and 300 μ m intershank interval) was implanted along the TA in the dorsal hippocampus. This high-density probe was used to examine the theta phase shift in the CA1-CA3 pyramidal layer. In one more rat (rab), 2 separate 256-site probes, with similar configuration as described earlier, were implanted: one along the long axis and the other along the transverse axis. The electrodes, up to 10,

(tetrodes made from 12.5 μm nichrome wires, 6 rats; Royer et al., 2010 or single 50 μm tungsten wires, 3 rats) for recordings from the dorsal-intermediate CA1 segments were organized in a straight line and spanned upto 6.5 mm distance along the curvature of the CA1 pyramidal layer. These arrays were inserted parallel with the long axis of the hippocampus so that the tips arrived in the CA1 pyramidal layer at approximately the same distance from the subicular and CA3 borders at all septo-temporal levels. Ventral recordings were made with either tetrodes (2 rats) or single 50 μm wires (2 rats) or silicon probes (8 sites x 4 shanks, 10 rats), (Royer et al., 2010). The high-density 32-site silicon probe had 4-shanks with ‘octrode’ design (20- μm vertical site spacing in each shank and 200- μm inter-shank distance; NeuroNexus Technologies, MI), (Royer et al., 2010). All tetrodes and single wires were independently movable. The septal drive/s was/were placed between AP: 2.2 to 6.3 and ML: 0.8 to 6.0 while the ventral drive between AP: 4.5 to 6 and ML: 4 to 5.7. Prior to implantation, the electrode tips were gold-plated to reduce electrode impedances to $\sim 300\text{ k}\Omega$ at 1 kHz. Recordings, with tetrodes in 1 rat (r-27) and with multiple shank probes in 4 rats (r-tn, r-jc, r-s1 and r-s2) were used for theta wave analysis along the subiculo-fimbrial axis, 3 of which (r-jc, r-s1 and r-s2) were used in previous publications (Csicsvari et al., 2003; Montgomery et al., 2009). In all experiments, ground and reference screws were implanted in the bone above the cerebellum. After post-surgical recovery, recording wires were lowered over the course of several days in steps of 50 μm until large units and ripple activity were isolated at appropriate depths. The goal was to record, simultaneously, from at least 3 sites in the dorsal/intermediate CA1 pyramidal layer along the long axis, and at least 1 site in the CA1 pyramidal layer in the ventral pole (except 3 rats (r-27 and r-tn), in which recordings

were obtained only along the transverse axis and r-11, in which recordings were only obtained from the septal 2/3rd segment). All experiments were carried out in accordance with protocols approved by the Institutional Animal Care and Use Committee, Rutgers University.

2.1.2 Behavioral training

All animals were handled and trained in two mazes (an open field and a zigzag maze) for at least two weeks before surgery (Royer et al., 2010). The animals were water-restricted for 24 h before the tasks. The same behavioral procedures were used for training and testing. The apparatus was separated from the experimenter and recording equipment by a black curtain, which also served as a polarizing cue relative to the walls on the other two sides. The floor and walls of the mazes were washed between sessions.

Open maze. The animals were trained to forage for small pieces (~3 x 3 mm) of froot loops (Cereal Kelloggs) on the open maze (114 x 184 cm) thrown one at a time from behind a curtain. The open maze had 30 cm high side-walls on all 4 sides, tilting outward by 60°. The entire maze was painted black. The rat could freely see distant room cues.

Zigzag maze. By placing 5 roof-shaped partitioning walls into the open maze, it was converted into a zig-zag maze with 11 corridors. The walls were 30 cm high with a 24 cm base and painted black. The animals were trained to run back and forth between the 2 water wells, situated in the end compartments. 100 µl of water was delivered at each well, alternatively (Royer et al., 2010).

Homecage: All sleep sessions were recorded while the rats slept or were inactive in their homecage. Sleep sessions were recorded at the beginning of each day followed by a behavioral session, followed by more sleep sessions. Sleep sessions were terminated if the rat awakened and moved and continued only after a minimum waiting period of 15 minutes and when it returned to uninterrupted inactivity/sleep for at least 5 minutes.

2.1.3 Histological and physiological verification of recording sites

Since the main goal of the present experiments was to establish relationships among different frequency oscillatory signals recorded simultaneously along the septo-temporal axis of the hippocampus, the physical distances between the recording sites rather than the stereotaxic coordinates of the electrodes were used for comparing physiological features of electrical signals. In 2 separate rats, the hippocampi were removed following decapitation and placed in ice-cold cerebro-spinal fluid. The hippocampus was gently flattened and the distance between the anterior (septal) and posterior (temporal) poles was measured. In agreement with previous similar measurements (Amaral, 2007), the septo-temporal length of the adult hippocampus was approximately 10 mm. In all figures, the distances of the electrodes are given from the septal end of the hippocampus. These distances were determined from anatomically verified sites of the electrodes and the extrapolated distance of the stereotaxic coordinates of the electrode position from the septal pole (Paxinos and Watson, 2007), taking into account the curvature of the hippocampus.

The electrode tracks of both wire electrode and silicon probe shanks were determined from the histological sections. To identify the exact location of the recording sites, a small anodal current (5 μ A for 10 sec) was passed through the recording electrodes 2 days prior to sacrificing the animals (Fujisawa et al., 2008). The rats were deeply anesthetized and perfused through the heart: first with 0.9% saline solution and followed by 10% formalin solution. The brains were sectioned by a Vibratome (Leica, Germany) at 100 μ m, either along the longitudinal, transverse or coronal plane. Sections were mounted on the slides, Nissl stained, and cover-slipped. The tracks were typically reconstructed from multiple adjacent sections.

Since silicon probes have a fixed geometry, the recording sites can unambiguously inform the experimenter whether the sites are above, in or below the pyramidal layer with 20- μ m precision (within a 140 μ m span), (Mizuseki et al., 2011), i.e., better than what can be established by lesioning the sites (Fujisawa et al., 2008). Due to the fixed geometry of the recording sites and shank distances, the relative depths of the recording sites can be reliably determined even if only one unambiguous histological verification is available for only one or two shanks (Csicsvari et al., 2003; Mizuseki et al., 2011; Montgomery et al., 2009). Within the CA1 pyramidal layer, the electrodes were advanced until sharp wave-ripples, associated with unit firing in the CA1 pyramidal layer, were detected during sleep in the home cage. During subsequent recording sessions, the electrodes were further adjusted to obtain largest amplitude ripples, corresponding to the middle of the pyramidal layer (Mizuseki et al., 2011). To facilitate visual comparison of

the recording sites and LFP events, the silicon probe tips were superimposed on the histological sections.

Only data with verified electrode tracks and physiological recordings of ripples and unit firing were included in the analyses. Due to these strict criteria, data obtained from 29 dorsal/intermediate sites and 17 ventral sites were excluded from further analysis because the electrode tracks were outside the CA1 pyramidal layer (in CA1 radiatum, CA2, subicular region) or because the tracks could not be verified reliably. Occasionally, the electrodes moved the tissue a bit deeper. Such tissue ‘dragging’ was observed mainly with blunt single wire electrodes and tetrodes, appearing as indentation of the pyramidal cell layer. In the dorsal (septal) hippocampus, pushing the pyramidal layer into the stratum radiatum, in principle, could lead to an artificial theta phase measure reducing the magnitude of the D-V phase shift. There are two arguments against the effects of tissue dragging in our experiments. First, the theta phase shift below the pyramidal layer is gradual and reaches $\sim 90^\circ$ in mid-radiatum (Winson, 1974). Such large indentation has never been observed. Second, the middle of the pyramidal layer was determined by the maximum of ripple power (Mizuseki et al., 2011). This latter observation would suggest that even if the pyramidal layer is moved deeper, most of the LFP activity still reflects the nearby current sources, i.e., the pyramidal layer.

2.1.4 Data acquisition, processing and analysis

During the recording session the rat was connected to a light-weight, counter-balanced cable that allowed the animal to move freely in the apparatus or to sleep comfortably in

the homepage. During the recording sessions in 11, neurophysiological signals were amplified (20 X), band pass filtered (1 Hz - 9 kHz), acquired continuously at 32 kHz on a 128-channel DigiLynx System (24-bit resolution; NeuraLynx, MT) and stored for offline analysis. During recordings made from additional 6 rats, the neurophysiological signals were preamplified (400 X), band pass filtered (0.3 Hz - 10 Hz), multiplexed at the head stage, acquired continuously at 20 kHz per channel on a 256 channel KJE-11001 system (Ampliplex, Hungary), and stored for offline analysis. All raw data were preprocessed using custom-developed suite of programs (Csicsvari et al., 1998). The wide-band signal was low pass filtered and down sampled to 1252 Hz (or 1250 Hz) to generate the local field potential and was high-pass filtered (>0.8 kHz) for spike detection. For tracking the position of the animals, two small light emitting diodes, mounted above the headstage, were recorded by a digital video camera and sampled at 30 Hz. Malfunctioning recording sites (due to high impedance, cross-talk, short circuit) or sites without large units and ripples were removed from the analysis.

2.1.5 Spike sorting and cell classification

Spike sorting was performed offline using a semiautomatic, custom-developed clustering analysis program (<http://klustakwik.sourceforge.net>), (Harris et al., 2000), followed by manual adjustment of unit clusters, aided by autocorrelation and cross-correlation functions as additional separation tools (<http://klusters.sourceforge.net>; <http://neuroscope.sourceforge.net>), (Hazan et al., 2006). Only clusters with clear refractory periods and well-defined boundaries in at least one of the projections were included in the single unit analysis (Harris et al., 2000). The tip of the electrodes either

moved spontaneously between sessions or was moved by the experimenter. We cannot exclude the possibility that some neurons recorded in different sessions were partially overlapping because spikes from each session were clustered separately.

2.2 Methods: Theta

2.2.1 Detection of theta periods: Theta periods were detected automatically using the ratio of the power in the theta band (5-10 Hz) to the power of the nearby bands (1-4 Hz, 12-15 Hz) from either the most dorsal or the most ventral CA1 sites in each rat. This was followed by manual adjustment based on the visual inspection of whitened power spectra (using a low-order autoregressive model), (Mitra and Pesaran, 1999) and the raw EEG (Sirota et al., 2008). The manual adjustment was especially necessary in behavioral sessions to remove the falsely detected short segments containing movement artifacts. Theta periods of duration <4 seconds for REM periods and <2 seconds for RUN sessions were further removed. Theta periods, detected in both behavioral and sleep/inactivity sessions, were analyzed further.

2.2.2 Spectral Analysis: Detected theta periods were concatenated to form a continuous signal and whitened using an autoregressive model, using a 1-second window. The autoregressive model generated from the 1st channel was then re-used for whitening all other channels from the same session in order to maintain the scale. Signals thus produced were used for the measurement of power. All coherence estimates and phase estimates were performed from non-whitened signal. All spectral analysis employed

multitaper direct spectral estimates method. Since our analysis was focused on the theta frequency band, we used a window size of 1 second with 5 tapers. Phase shifts along the septo-temporal axis were measured taking the most ventrally located channel as reference, while phase shift along the subiculo-fimbrial axis was measured taking the most distally located CA1 site as the reference channel.

2.2.3 Theta amplitude and phase: LFP from all channels was theta filtered between 5-10 Hz using a Butterworth filter with a 1-second window. Instantaneous amplitude and phase of theta oscillations were derived from Hilbert transformation of the filtered LFP trace, following Siapas et al. (Siapas et al., 2005). Local minima were detected from the filtered signal of the reference channel to generate trough-triggered field averages for all channels. Multiple unit activity was extracted from all channels. Instantaneous phase of the local channel was used to assign theta phases to spikes.

2.2.4 Unit Analysis: Because single units cannot be reliably identified from single wire recordings (Harris et al., 2000), and because we wanted to generate group data from all rats, unit firing vs. theta phase relationship was first analyzed for multiple unit data. Multiple unit was obtained by removing the noise cluster from the data and combining all spikes into a single spike series. Single units were identified from the ventral recording sites and segregated into putative pyramidal cells or interneurons, based on firing rates. Cells with firing rates < 5 Hz were classified as putative pyramidal cells and all others as putative interneurons (Royer et al., 2010). Only single units with at least 100 spikes and a firing rate of $> .1$ Hz were used to test their phase locking. Rayleigh test for the uniformity

of the phase of firing was used to identify phase-modulated pyramidal cells. Pyramidal cells with a P value of <0.05 were considered to be significantly phase-locked.

2.2.5 Permutation test: A permutation test was used to assess the statistical significance of the difference of theta phase shift slopes between different brain states (i.e. REM and RUN). First, the regression coefficients between phase shifts and anatomical distances were calculated for data from each brain state, using a multiple linear regression model. Second, to form the surrogate data sets, each label (i.e. REM and RUN) of each data point in the original data set was randomly shuffled. Next, the regression coefficients were estimated for these surrogate data sets and the difference of slopes for the two states was noted. This process was repeated independently to generate 10,000 counts of slope differences. Finally, the phase shift difference between REM and RUN were determined to be statistically significant if they were atypical with respect to those constructed from the shuffled data sets.

2.3 Methods: Ripples

2.3.1 Ripple Event Detection: The following step-by-step procedure was used for each individual session to detect ripple events.

- 1) The wide-band (1 Hz – 5 kHz) recorded data were low pass (0.5 Hz - 1252/1250 Hz) filtered.
- 2) Slow wave sleep (SWS) periods were extracted from sleep recordings by removing REM theta periods, detected using theta/delta power ratio (Csicsvari et

al., 1999). SWS periods of <4 seconds were further removed.

- 3) The select SWS periods were concatenated and narrow band-pass filtered (between 100 to 250 Hz).
- 4) The power (root mean square) of the filtered signal was calculated for each electrode.
- 5) The mean and standard deviation (SD) of the power signal were calculated to determine the detection threshold.
- 6) Oscillatory epochs with a power larger than 1.5, 2, and 3 SD above the mean for at least 20 msec were detected. Each detected epoch was also required to cross a higher threshold of 3, 5, and 7 SD, respectively. The beginning and the end of oscillatory epochs were marked at points at which the power reduced below the lower threshold values.
- 7) The time of the peak integrated power was detected and surrounding this peak, the trough and the peak of the ripple wave were identified and saved.
- 8) Ripple event was defined as the trough of the largest amplitude ripple wave for each detected ripple.

2.3.2 Wavelet Analysis: Morlet wavelet transforms were generated for each detected ripple epoch for ± 50 msec period surrounding the ripple event for frequencies 1-250 Hz. Peak values from the wavelet transforms were defined as peak ripple amplitude values. Peak ripple frequency was identified as the frequency bin in which the wavelet transform peaked. Average frequency and amplitude was calculated over each session.

2.3.3 Ripple synchrony measure: For this analysis we used pairs of electrodes, one was a reference electrode and the other was a referred electrode. Using ripple event times as central time points, we measured how often a ripple occurred within ± 1 msec in other referred channels, and converted it to percentage (ripple wave synchrony). We repeated the same analysis with a wider time window of ± 50 msec to measure the ripple event synchrony.

2.3.4 Relative ripple amplitude: This analysis was conducted in electrode pairs. Using the morlet wavelet amplitudes we determined the amplitude values in all referred channels and plotted them as a function of distance from the reference electrode.

2.3.5 Unit Analysis: Multiple unit activity was obtained by removing the noise cluster from the data and combining all spikes into a single spike series.

2.3.6 Permutation test: A permutation test was used to assess the statistical significance of the difference of ripple propagation speed slopes between ripple events detected with different SDs and ripples propagating in different directions. First, the regression coefficients between propagation speed and anatomical distances were calculated, using a multiple linear regression model. Second, to form the surrogate data sets, each label (i.e. different SDs used to detect ripples or ripple propagation direction) of each data point in the original data set was randomly shuffled. Next, the regression coefficients were estimated for these surrogate data sets and the difference of slopes for any two amplitudes/propagation directions was noted. This process was repeated independently to

generate 10,000 counts of slope differences. Finally, the ripple speed difference was determined to be statistically significant if they were atypical with respect to those constructed from the shuffled data sets.

2.3.7 3-way ANOVA: For calculating the statistical significance of ripple length, frequency, amplitude and ripple rate values over location along the septo-temporal axis, and for the factor of SDs used to detect ripples, 3-way ANOVA method was used.

Chapter 3.0 – Results

3.1 – Traveling theta waves along the entire septo-temporal axis of the hippocampus

In Press: Patel, Fujisawa, Berenyi, Royer & Buzsaki, Neuron

3.1.1 – Abstract

A topographical relationship exists between the hippocampus-entorhinal cortex and the neocortex. However, it is not known how these anatomical connections are utilized during information exchange and behavior. We recorded theta oscillations along the entire extent of the septo-temporal axis of the hippocampal CA1 pyramidal layer. While the frequency of theta oscillation remained the same along the entire long axis, the amplitude and coherence between recording sites decreased from dorsal to ventral hippocampus (VH). Theta phase shifted monotonically with distance along the longitudinal axis, reaching $\sim 180^\circ$ between the septal and temporal poles. The majority of concurrently recorded units were phase-locked to the local field theta at all dorso-ventral segments. The power of VH theta had only a weak correlation with locomotion velocity, and its amplitude varied largely independently from theta in the dorsal part. Thus, theta oscillations can temporally combine or segregate neocortical representations along the septo-temporal axis of the hippocampus.

3.1.2 - Introduction

The elongated hippocampus communicates with the neocortex via the entorhinal cortex interface (Witter et al., 1989a). Both hippocampal ‘representation’ of neocortical information and re-routing of hippocampal messages to the neocortex are topographically organized (Amaral, 2007; Witter et al., 1989b). The septal (or ‘dorsal’, DH) and intermediate (IH, or posterior) segments receive visuo-spatial inputs mainly via the dorsolateral band of the medial entorhinal cortex, and the temporal segment (or ‘ventral hippocampus’, VH) from the ventromedial band of the entorhinal cortex (Dolorfo and Amaral, 1998b; Witter et al., 1989b). In addition, the temporal segment is innervated by amygdalar and hypothalamic afferents carrying emotional and other non-spatial information (Petrovich et al., 2001; Risold and Swanson, 1996) and has characteristically distinct gene profiles (Dong et al., 2009; Thompson et al., 2008). In return, the septal and temporal segments of the hippocampus broadcast to different streams of structures (Amaral, 2007; Cenquizca and Swanson, 2007). In contrast to its afferent and efferent connections, the internal organization of the hippocampus suggests that the widespread neocortical representations are integrated (Bast et al., 2009; Moser et al., 2008; Royer et al., 2010; Small, 2002) by the extensive recurrent collateral system of CA3 pyramidal neurons (Ishizuka et al., 1990; Li et al., 1994).

The physiological mechanisms of communication between the hippocampus and the neocortex are not well understood. Neuronal recording studies from the septal and more temporal segments of the hippocampus are controversial, and range from emphasizing the

unity of hippocampal operations (Bullock et al., 1990; Colombo et al., 1998; Jung et al., 1994; Kjelstrup et al., 2008; Lubenov and Siapas, 2009; Maurer et al., 2005; O'Keefe and Nadel, 1978) to more localized and specialized computations (Hampson et al., 1999; Royer et al., 2010; Segal et al., 2010; Wiener, 1996). A fundamental mode of hippocampal operations is reflected by theta oscillations during explorative behavior and REM sleep (5-10 Hz), (Buzsaki, 2002). In a recent elegant study, Lubenov and Siapas (2009) have observed that the phase of theta waves advances systematically in the dorsal hippocampus (Lubenov and Siapas, 2009) and hypothesized a full cycle (i.e., 360°) phase shift between the septal and temporal poles. The implication of a full cycle phase shift of theta waves is that outputs from the two poles of the hippocampus would affect their joint targets in a temporally synchronous manner, while the intermediate parts would remain temporally segregated from either pole. To examine the spatial organization of theta patterns, we recorded LFP and neuronal discharge activity in the subiculo-fimbrial (transverse) axis and from the entire length of the septo-temporal (longitudinal) axis of the hippocampal CA1 pyramidal layer during behavioral exploration and REM sleep.

3.1.3 Results

LFP and unit activity were recorded during REM sleep in the home cage and during navigation (RUN sessions) either while the rat was chasing small fragments of randomly dispersed food loops on an open field and/or running for a water reward in an 11-compartment zig-zag maze (Royer et al., 2010). Since the phase of theta oscillation in the CA1 region varies along the somatodendritic (depth), subicular-CA3 (transverse) and

septo-temporal (dorsoventral or longitudinal) axes (Buzsaki, 2002; Lubenov and Siapas, 2009), (Patel et al., 2008), we examined phase shifts in each direction using multiple site

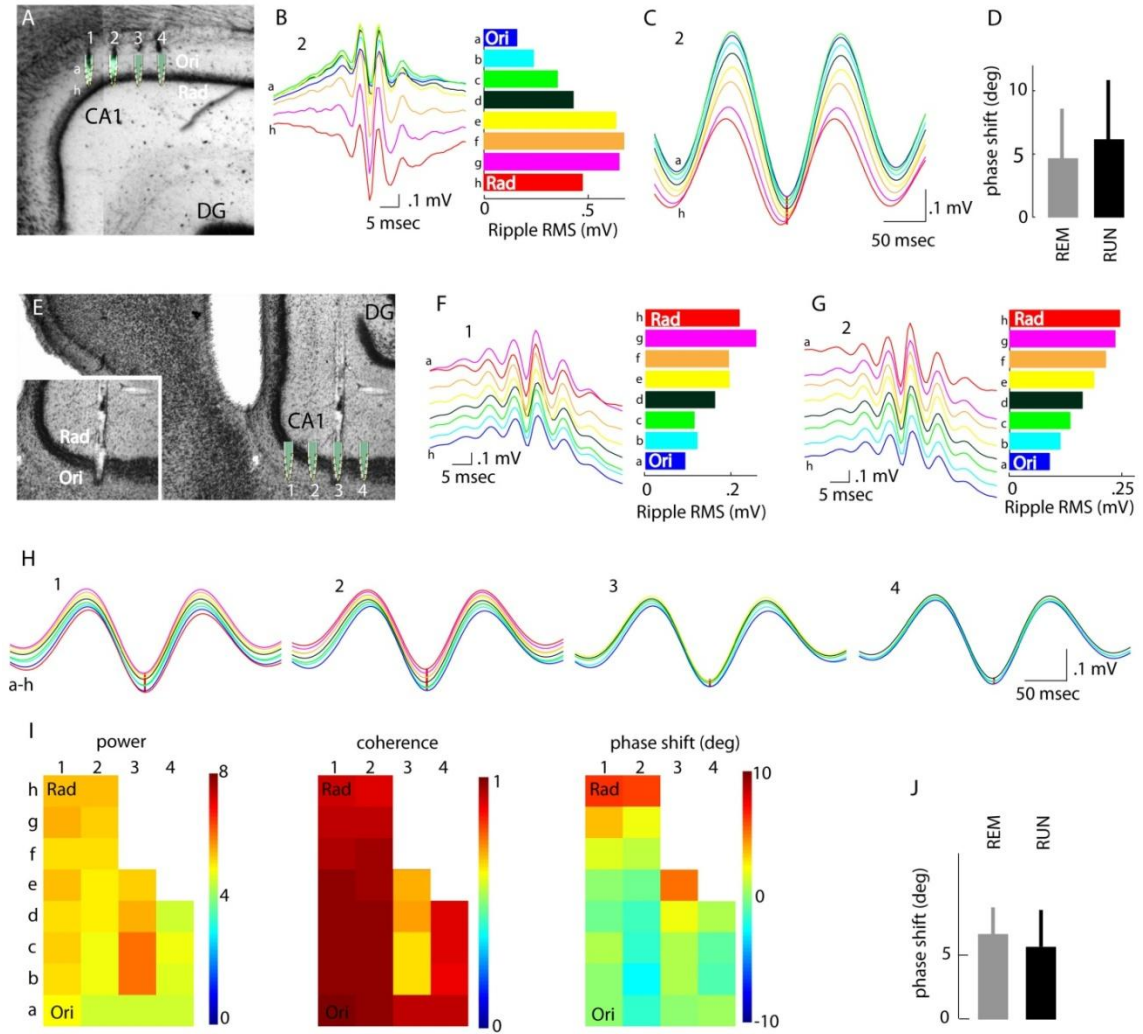


Figure 1. Similar theta phases in the str. oriens and pyramidale of both dorsal and ventral hippocampus. (A) 4-shank silicon probe tips superimposed on the histologically recovered tracks. Ori, stratum oriens. Rad, stratum radiatum. (B) Average filtered (100–250 Hz) ripple traces from each of the 8 recording sites (on shank 2) triggered by ripple troughs. Right, ripple power at each recording site. The recording site with the largest ripple power identifies the middle of the pyramidal layer. (C) Averaged filtered (5–10 Hz)

theta waves during REM, from the same sites in the same session. Same color-coding as in B. (D) Mean (+ std. dev.) theta phase shift between mid-pyramidal layer and str. oriens locations (REM: n=41 pairs from 8 sessions in 6 rats; RUN: n=62 pairs from 10 sessions in 5 rats). (E) 4-shank silicon probe in the CA1 pyramidal layer of ventral hippocampus. (F and G) Average filtered ripples and ripple power at all sites of shank 1 (F) and 2 (G). (H) Average filtered theta waves recorded from all good channels on each of the 4-shanks. Averages recorded by the same shank are superimposed. (I) Theta power, coherence and phase-difference as a function of depth (8 sites; 20 μ m intervals) and lateral distance (shanks are 200 μ m apart). Malfunctioning sites are white. (J) Mean (+ std. dev.) theta phase shift between mid-pyramidal layer and s. oriens locations (REM: n=40 pairs from 14 sessions in 3 rats; RUN: n=22 pairs from 8 sessions in 3 rats).

silicon probes and independently movable wire electrode arrays (See Experimental Procedures). Theta phase difference between the alveus and the CA1 pyramidal layer in both the dorsal (Figures 1A-D) and ventral (Figures 1E-J) segments of the hippocampus was constant ($<10^\circ$). Therefore, in all experiments recordings were made from the middle of the pyramidal cell layer (Figures 1A, 1E, 2A, S1, S2A, S3B and S4B). The electrodes were advanced until sharp wave-ripples (Buzsaki et al., 1992; O'Keefe, 2006), associated with unit firing in the CA1 pyramidal layer, were detected during sleep in the home cage. During subsequent recording sessions, the electrodes were further adjusted to obtain largest amplitude ripples, corresponding to the middle of the pyramidal layer. The phase difference along the transverse axis, i.e. from the subicular end to the fimbrial end of the CA1 pyramidal layer, was approximately 40° (Figure S2).

3.1.3.1 Frequency, power, coherence and phase shift of theta oscillations along the CA1 septo-temporal axis

To accurately assess the changes in LFP theta oscillations along the septo-temporal axis of the CA1 region, electrodes were positioned at approximately the same distance from the CA1-subicular border (Figures 2A, S1 (r-25) and S3B). The frequency and regularity of theta oscillations in the dorsal and intermediate hippocampus were similar at all recording sites, with the phase of theta gradually shifting from the dorsal (septal) to intermediate sites of the CA1 layer (Figure 2E, 3F and S3). Theta waves were phase shifted by approximately a half cycle, i.e., 180° between the septal and ventral (temporal) sites (Figures 3F, 3G and S4). Theta oscillations were less regular, lower in amplitude and more intermittent at the ventral sites, with episodes of no recognizable rhythm at times of regular theta oscillation at dorsal locations (Figures 2F, 2G1 and S4C; Royer et al., 2010). While coherence of theta waves was relatively high between septal and intermediate sites, it decreased to <0.5 between septal and ventral sites (Figures 2D and 3E).

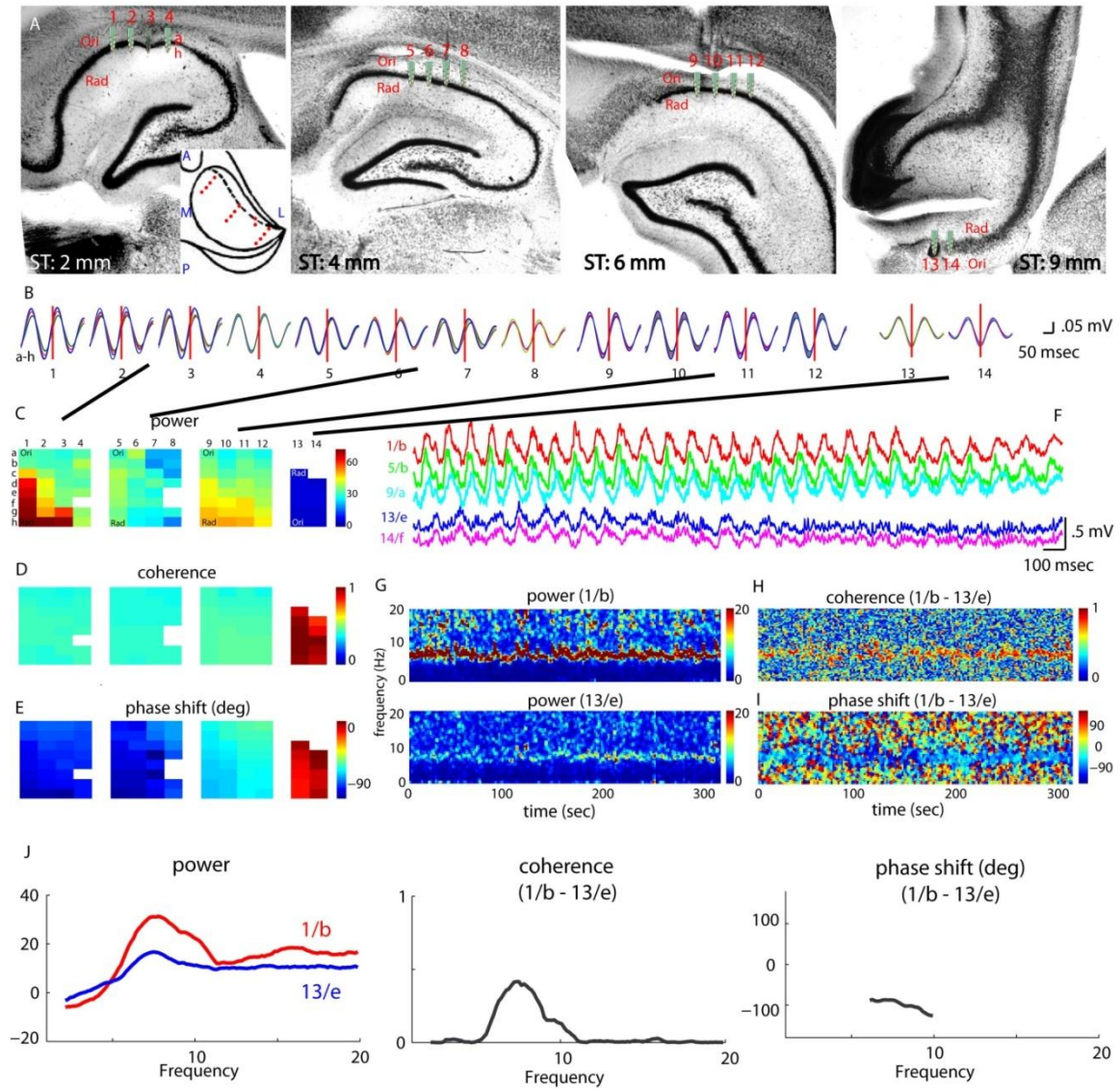


Figure 2. Three-dimensional distribution of theta waves in the CA1 pyramidal layer.

(A) Inset: top-down view of the right hippocampus. The positions of the recording probes and shanks are shown (red dots). Histological sections were cut along the transverse axis. Silicon probe tips superimposed on the histologically recovered tracks in the dorsal (1st panel), intermediate (2nd and 3rd panels) and ventral (4th panel) segments. Ori, stratum oriens. Rad, stratum radiatum. a-h, recording sites on each shank. (B) Average filtered (5-10 Hz) theta waves during REM from all 14 shanks. Average traces from recordings sites (a-h) from the same shank are superimposed. (C-E) Power, coherence and phase-shift as

a function of depth (a-h; 20 μm intervals) and transverse axis distance (1-4, 5-8, 9-12, 13-14; shanks are 200 μm apart). Malfunctioning sites are white. (F) Three-second long wide-band LFP traces during REM theta from selected sites at four septo-temporal levels. (G) Time-resolved power spectra during REM periods concatenated over the entire session from the most septal (dorsal) and most temporal (ventral) probes. Coherogram (H) and phase shift spectrum (I) calculated between sites shown in G and H. (J) Average power, coherence and phase spectra for sites shown in G. Phase is shown where coherence is >0.1 .

Data recorded from 45 histologically verified electrode locations in the dorsal and intermediate hippocampus and 19 histologically verified electrodes from the ventral hippocampus (n=10 rats) were included in the analysis. For group comparison, the recording sites were categorized into dorsal (0-3.0 mm), intermediate (3.1-6.5 mm) and ventral (8.0-10.0 mm) segments. Because the most ventral electrode in each animal was positioned in a relatively similar plane (between 9th and 10th mm along the septo-temporal axis), the ventral CA1 sites were used as reference for coherence and phase shift measurements. The group analysis confirmed that the frequency of theta oscillations remained the same along the entire septo-temporal axis but differed significantly between REM sleep and maze behavior (RUN) (Figure 3C; REM – DH: 6.97 ± 0.35 ; IH: 7.07 ± 0.32 ; VH: 7.00 ± 0.44 Hz, mean & SD, n=42 sessions in 10 rats; RUN - DH: 7.53 ± 0.31 ; IH: 7.82 ± 0.26 ; VH: 7.64 ± 0.32 Hz, mean & SD, n=28 sessions in 7 rats; recording location effect $P=0.21$; state effect: $P=0.008$; 2-way ANOVA). Identifiable

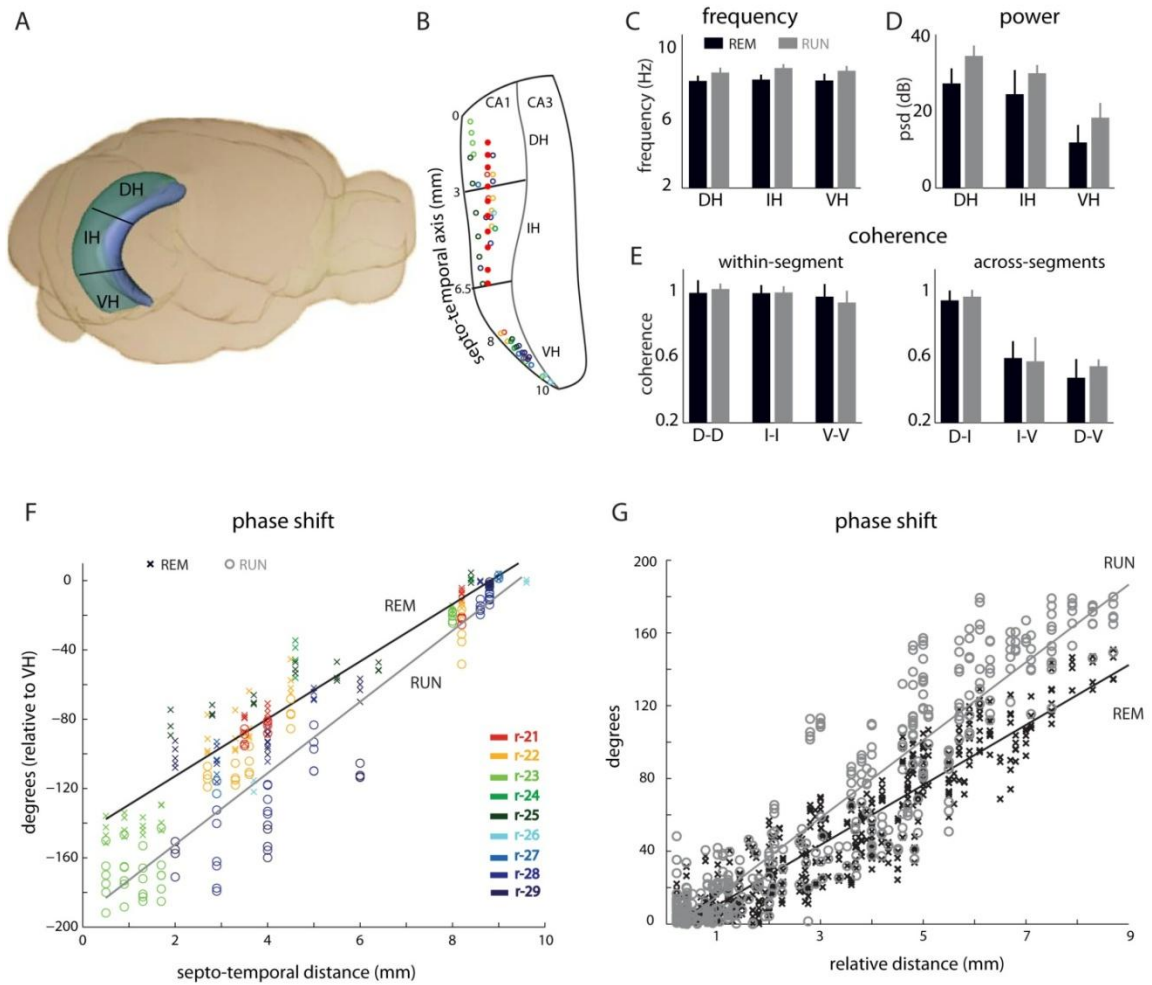


Figure 3. State and location-dependent features of phase-shifting theta waves. (A) Schematics of the dorsal (DH), intermediate (IH) and ventral (VH) divisions of the hippocampus, respectively. (B) Flattened map of the CA1-CA3 regions. Dots indicate the tip of the recording sites in the CA1 pyramidal layer. (C) frequency (mean + std. dev. of peak theta frequency, across 42 sessions in 10 rats - REM and 28 sessions in 7 rats - RUN), (D), power (mean + std. dev. of average theta power around ± 1 Hz of peak theta frequency) and (E), coherence (mean + std. dev.) of theta oscillations in the dorsal (DH; 0-3 mm), intermediate (IH, 3.1-6.5 mm) and ventral (VH, 8.0-10.0 mm) segments of the CA1 region. Results are shown separately from RUN and REM sessions. (F) Phase shift

of theta oscillations in single rats (color symbols) as a function of septo-temporal distance. In these comparisons, the reference site was the ventral-most electrode. Distances are measured from the septal end of the CA1 pyramidal region (0 mm). Note up to 180° phase shift between the ventral-most and septal-most (dorsal) sites during RUN and significantly less steep phase shift during REM. (G) Theta phase shift as a function of electrode distance. All possible electrode pair comparisons (relative distance) are shown.

theta oscillations in the ventral hippocampus (See Experimental Procedures) were present ~60% of the time during prominent theta waves in the dorsal hippocampus (RUN: $63.3 \pm 22.11\%$; REM: $58.1 \pm 16.14\%$; $P=0.31$). The power of theta oscillations decreased from dorsal to ventral sites (Figure 3D; REM - DH: 27.24 ± 3.93 ; IH: 24.43 ± 6.30 ; VH: 11.87 ± 4.57 , mean & SD, $n=42$ sessions in 10 rats; RUN - DH: 34.44 ± 2.70 ; IH: 29.92 ± 2.15 ; VH: 18.34 ± 3.84 , mean & SD, $n=28$ sessions in 7 rats; recording location effect, $P=0.003$; 2-way ANOVA), and was significantly smaller during REM sleep compared to RUN (state effect, $P=0.006$, 2-way ANOVA). Within-segment coherence in the theta band was high along the long axis and during different behaviors: REM and RUN (Figure 3E –left panel, recording location effect, $P=0.23$; behavioral state effect, $P=0.89$; 2-way ANOVA). In across-segment comparisons, coherence remained high between dorsal and intermediate sites (Figure 3E –right panel, mean coherence $c > 0.88$ for both REM and RUN), but it was significantly smaller between ventral and intermediate (Figure 3E; $c=0.46 \pm 0.12$, REM; $c=0.44 \pm 0.17$, RUN) and ventral and dorsal locations (Figure 3E; $c=0.32 \pm 0.13$, REM; $c=0.41 \pm 0.05$, RUN; location effect, $P=0.009$; 2-way ANOVA). Across-segment coherence was similar during RUN and REM ($P=0.45$; 2-way ANOVA). The slope of theta phase-shift vs distance, referenced to the most ventral

site in each rat, was significantly more shallow during REM sleep ($16.53^{\circ}/\text{mm}$; reaching 150° between the most ventral and most septal parts of the hippocampus) than during RUN ($20.58^{\circ}/\text{mm}$; reaching 180° ; $P < 0.00001$; permutation test; Figure 3F). In addition, we calculated phase differences between all possible pairs of recording sites at all septo-temporal levels (Figure 3G). The slopes based on these latter comparisons yielded similar values (REM: $16.48^{\circ}/\text{mm}$; RUN: $21.36^{\circ}/\text{mm}$; $P < 0.00002$; permutation test). The above comparisons were independent of whether epochs were selected based on the presence of theta waves at the ventral (Figures 3F and 3G) or dorsal (Figures S5A and S5B) recording sites. While theta phase shift was monotonous in the septal 2/3rd, it accelerated between the intermediate and ventral segments (Figure S6).

3.1.3.2 Theta phase-locking of neuronal firing along the septo-temporal axis

The temporal shifts of the LFP theta along the septo-temporal axis were mirrored by similar phase shifts of unit firing in the CA1 region (Figure 4). At all locations, majority of both multiple units and single pyramidal cells fired preferentially near the trough of the local LFP theta (Figures 4A-C and 4E). Theta phase preference of ventral neurons was more variable and a fraction of ventral pyramidal cells preferred the peak of the local theta cycle (Figure 4E). This peak preference of ventral neurons was not due to improper positioning of the electrode within the CA1 pyramidal cell layer or misclassification of the unit identity because even well-isolated pyramidal cells, recorded simultaneously by the same probe and referenced to LFP from the same recording site, often showed different theta phase preferences (Figure 4D). Thus, while pyramidal neurons were largely phase-locked to the local theta waves, their spiking activity was phase-distributed

when referenced to the theta cycle recorded from a single site. Assuming an 8-Hz theta signal (125-msec period) and a 10mm flattened distance between the septal and temporal poles, the half-theta cycle septo-temporal phase shift of population unit firing between the two poles corresponds to 0.16 m/sec velocity of activity travel, comparable to the speed of traveling activity observed in visual areas (Benucci et al., 2007).

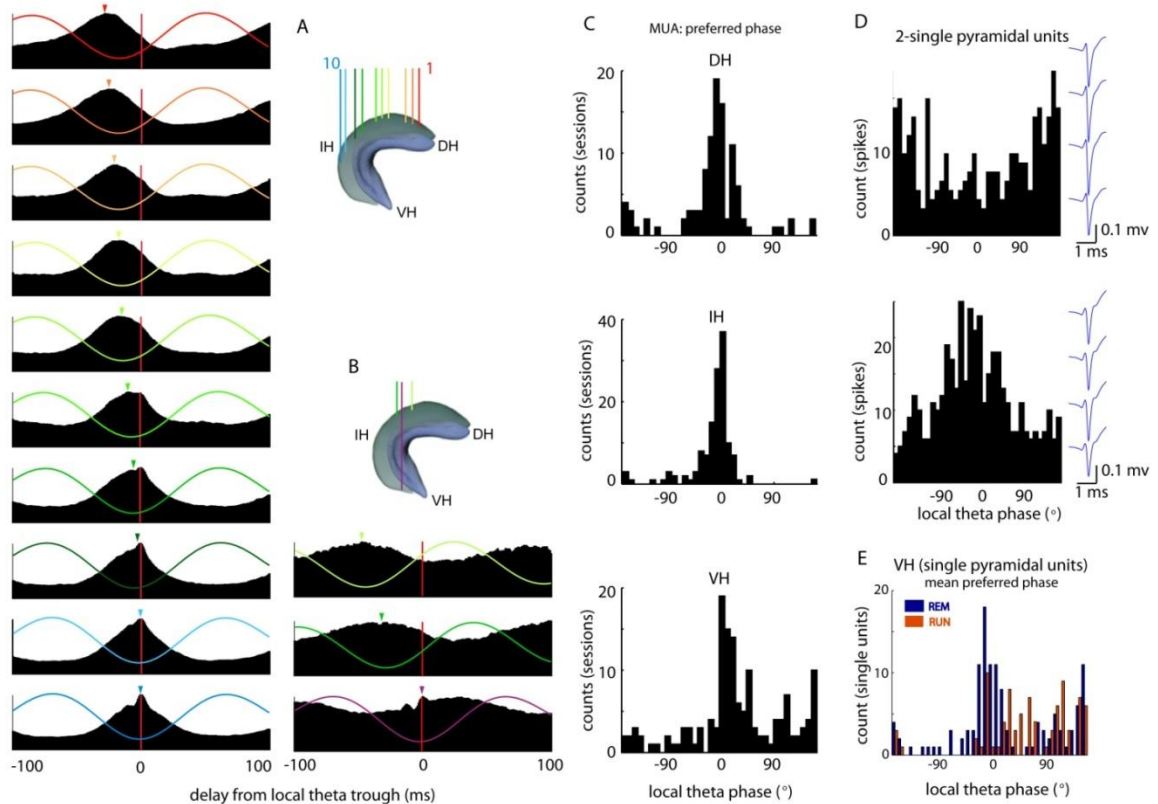


Figure 4. Theta phase shift of unit firing along the septo-temporal axis is in register with phase shifting theta waves. (A). Theta trough-triggered LFP (colored line) and corresponding local multiple unit firing histogram (r-11). LFP and units signals are referenced to the theta troughs (zero on the x -axis), detected at the most ventral electrode. (B). Similar, field and unit histograms from the dorsal and ventral regions, referenced to the trough of ventral theta (r-28). Note time-shifted LFP average theta

waves and corresponding preferred discharge of multiple unit activity at the trough of local theta. (C). Distribution of preferred theta phases of multiple unit firing, referenced to the troughs of local theta waves, in the dorsal (DH), intermediate (IH) and ventral (VH) segments from all animals. Each count is the preferred phase of multiple unit activity (MUA) from an electrode for that session. (D). Two simultaneously recorded putative pyramidal cells from the same tetrode in the ventral CA1 region. Note that of the two neurons, one fires preferentially on the peak and the other at the trough of the local theta cycle, respectively. Waveforms of units (wide band: 1 Hz-5 kHz). (E). Distribution of preferred theta phases of isolated pyramidal neurons from the ventral hippocampus, shown separately for RUN and REM sessions (overlaid). Only cells with significant theta modulation of firing ($P < 0.05$, Rayleigh test) were included. Pyramidal cells with < 100 spikes during a session were not included in the analysis.

3.1.3.3 Co-modulation of theta power along the septo-temporal axis and the effect of speed on power

While theta coherence remained moderately high ($c > 0.4$; Figure 3E) along the entire long axis of the CA1 pyramidal layer, theta amplitude (or power) varied extensively (Figures 5A and 5B). Theta power between sites of the same hippocampal segment (Figure 5C; $R > 0.81$ REM; $R > 0.75$ RUN; $P = 0.3$, 2-way ANOVA) and between the dorsal and intermediate segments (Figure 5D; $R = 0.66 \pm 0.132$ REM; $R = 0.64 \pm 0.134$ RUN) co-varied reliably. In contrast, co-variation of theta power between ventral sites versus intermediate and dorsal hippocampal locations was significantly lower during both REM (Figure 5D; V-I: $R = 0.39 \pm 0.18$; V-D: $R = 0.32 \pm 0.14$; $P < 0.001$; 2-way ANOVA) and RUN (Figure 5D; V-I: $R = 0.16 \pm 0.14$; V-D: $R = 0.09 \pm 0.082$; $P < 0.001$; 2-way ANOVA). A potential source of theta power modulation in different hippocampal segments is a ‘speed signal’, since the locomotion velocity of the animal is known to affect the amplitude of theta

(McFarland et al., 1975). There was a significant correlation between running speed and theta power in the dorsal and intermediate segments (Figures 5E and 5F), (Maurer et al., 2005; Montgomery et al., 2009) but not in the ventral segment (Figures 5E and 5F; $P < 0.0001$; ANOVA).

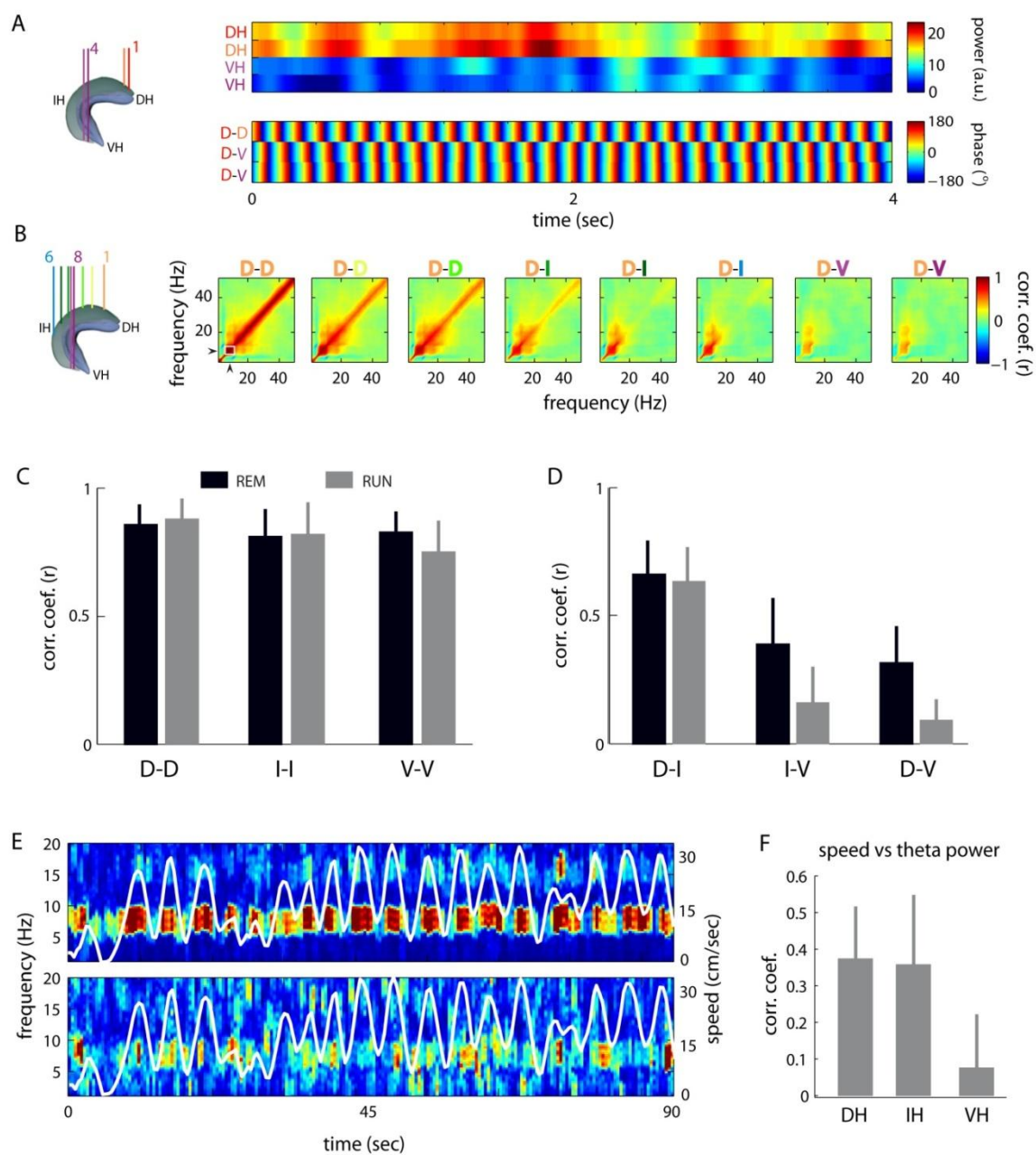


Figure 5. Power variability and speed-dependence of theta power. (A). A 4-sec LFP segment showing instantaneous theta amplitude and phase relationships between electrodes in the dorsal and ventral CA1 pyramidal layers. Note high theta power correlation between sites in the dorsal CA1 pyramidal layer and virtually independent power fluctuation in sites in the ventral CA1 pyramidal layer (top), while theta phase relationship between dorsal and ventral sites is highly consistent and well preserved during the same period. (B). Power-power correlation between the most dorsal CA1 pyramidal layer recording site (red) and seven other sites in the dorsal (DH), intermediate (IH) and ventral (VH) CA1 pyramidal layers from an example REM session (r-25). (C & D) Group data of power-power correlations. Note high power correlations within the same segments (C) and strongly decreased power correlations between the ventral vs. intermediate and dorsal sites (Mean + std. dev.). (E). Examples of time-resolved power spectra from the dorsal and ventral CA1 pyramidal layer electrodes (rat-27) and concurrent running speed (superimposed, white) during open field exploration. Note striking correlation of theta power fluctuation with running speed in the dorsal hippocampus and a less reliable relationship in the ventral part. (F). Mean (+SD) of correlation coefficient values between theta power and speed from all sessions (n=19 sessions from 5 rats), grouped as dorsal (DH), intermediate (IH) and ventral (VH) hippocampus. While theta power from the dorsal and intermediate sites was equally and strongly correlated with speed, theta power from the ventral sites showed significantly less correlation with speed than sites in the septal 2/3rd.

3.5 Supplementary figures

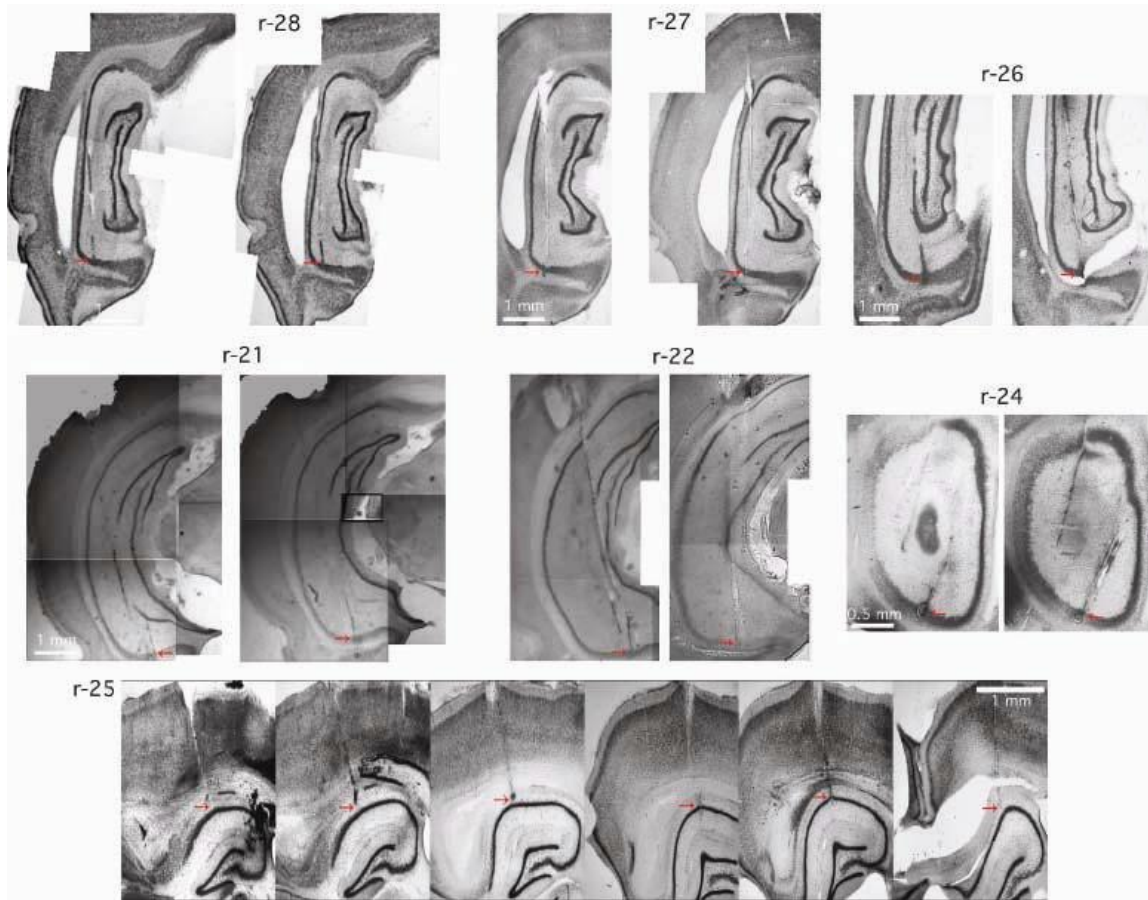


Figure S1. Histological reconstruction of the recording tracks. Red arrows indicate the extrapolated or verified (lesion) tip. Every rat has at least one clearly identified lesion site. All rat brains were sectioned along the transverse axis i.e. axis perpendicular to the LA, except of rat r-24 which was cut in the coronal plane. The distance between the first and last recording electrode in r-25 is 4.5 mm (0.9 mm gaps between electrodes). This figure provides supplementary information to Figures 1-5.

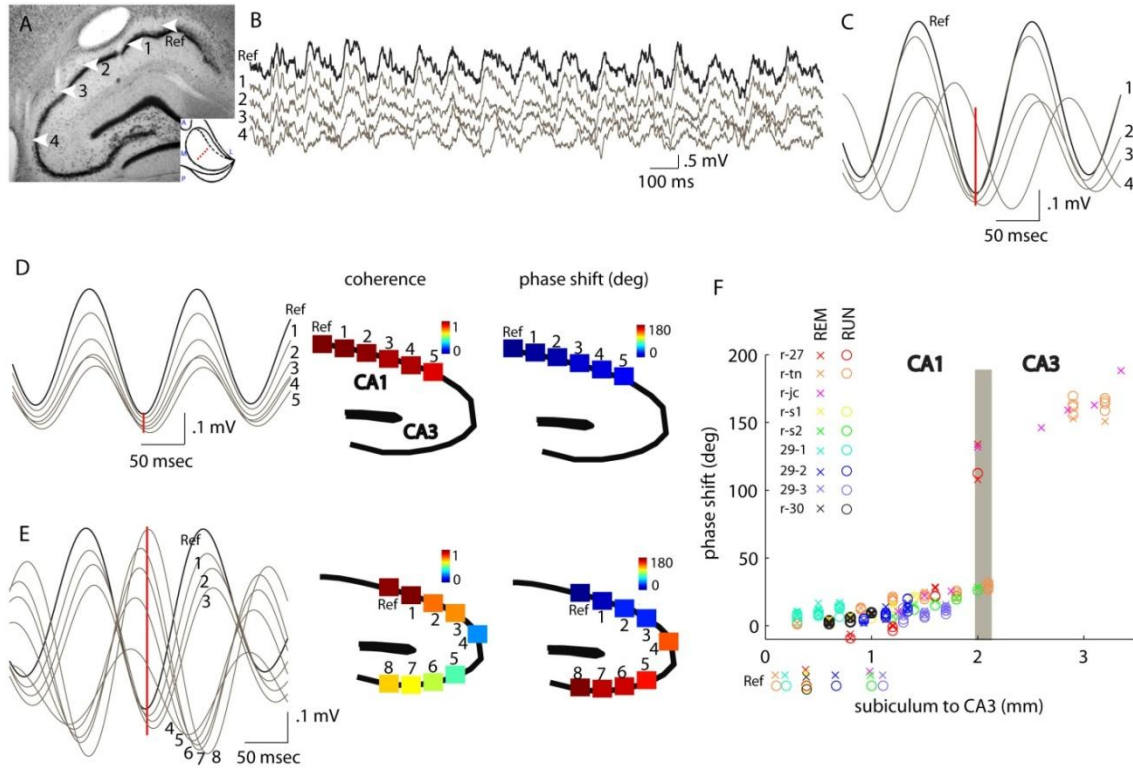


Figure S2. Theta phase shift in the subiculo-fimbrial axis. (A) Histological reconstruction of 5 tetrode tracks in the subiculo-fimbrial axis (reference, Ref and 1-4; rat-27). Sections were cut along the transverse axis of the hippocampus. Inset: Top-down view of the right hippocampus illustrating tetrode placement along the transverse axis. (B) Two-second long wide-band LFP traces during theta from the sites shown in A. (C) Average filtered (5–10 Hz) theta waves during RUN from the same recording sites as in A and B. (D) left: Average filtered theta waves during RUN. middle and right: coherence and phase shift against the most medial reference (Ref) site. Note phase-shifted theta waves in the CA1 pyramidal layer along the subiculo-fimbrial axis relative to the most distal (subicular) CA1 reference. Silicon probe recordings with 300 μ intershank distance (r-sm2). (E) Same as in D from another rat (r-jc) equipped with a 96-site silicon probe (REM). Note large phase shifts of theta waves between the CA1 and CA3 sites. (F) Group data of phase shifts during REM (X) and RUN (O). Different colors code for different rats. Reference locations are shown below the x axis. Note moderate phase shift in the subiculo-fimbrial axis of CA1 pyramidal layer and phase reversal of theta waves

between CA1 and CA3. This figure complements Figures 1 and 3.

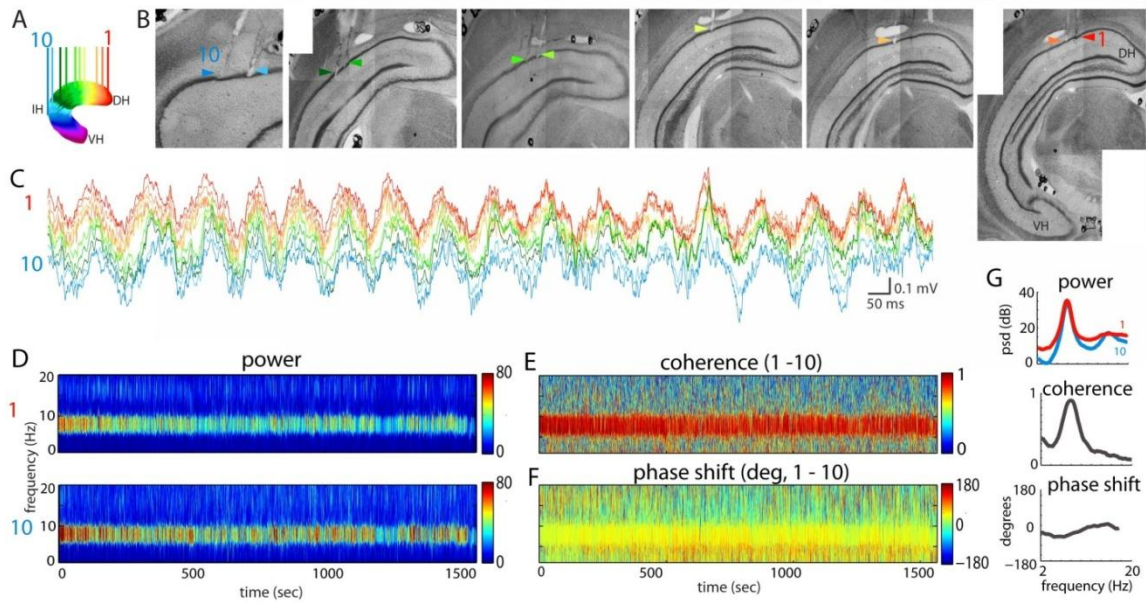


Figure S3. Theta oscillations in the dorsal and intermediate hippocampus. (A). Top-down view of the right hippocampus illustrating electrode placement along the long axis. Each colored dot indicates one electrode. (B) Histological sections showing ten recordings sites from the dorsal (DH) and intermediate (IH) parts of the CA1 pyramidal layer (r-11). Sections were cut parallel with the LA of the hippocampus. Arrowheads, tips of the electrodes. Color-coding of the electrodes applies also to parts B, C, D and G. (C) Two-second long wide-band LFP traces during RUN theta from all recording locations. (D). Time-resolved power spectra during run periods concatenated over the entire session, from the most septal (dorsal) and intermediate electrodes. Coherogram (E) and time-resolved phase (difference) spectra (F) calculated between channels shown in D. (G) Average power, coherence and phase spectra for the sites shown in D. Phase is shown where coherence is >0.1 . This figure is supplementary to Figure 2.

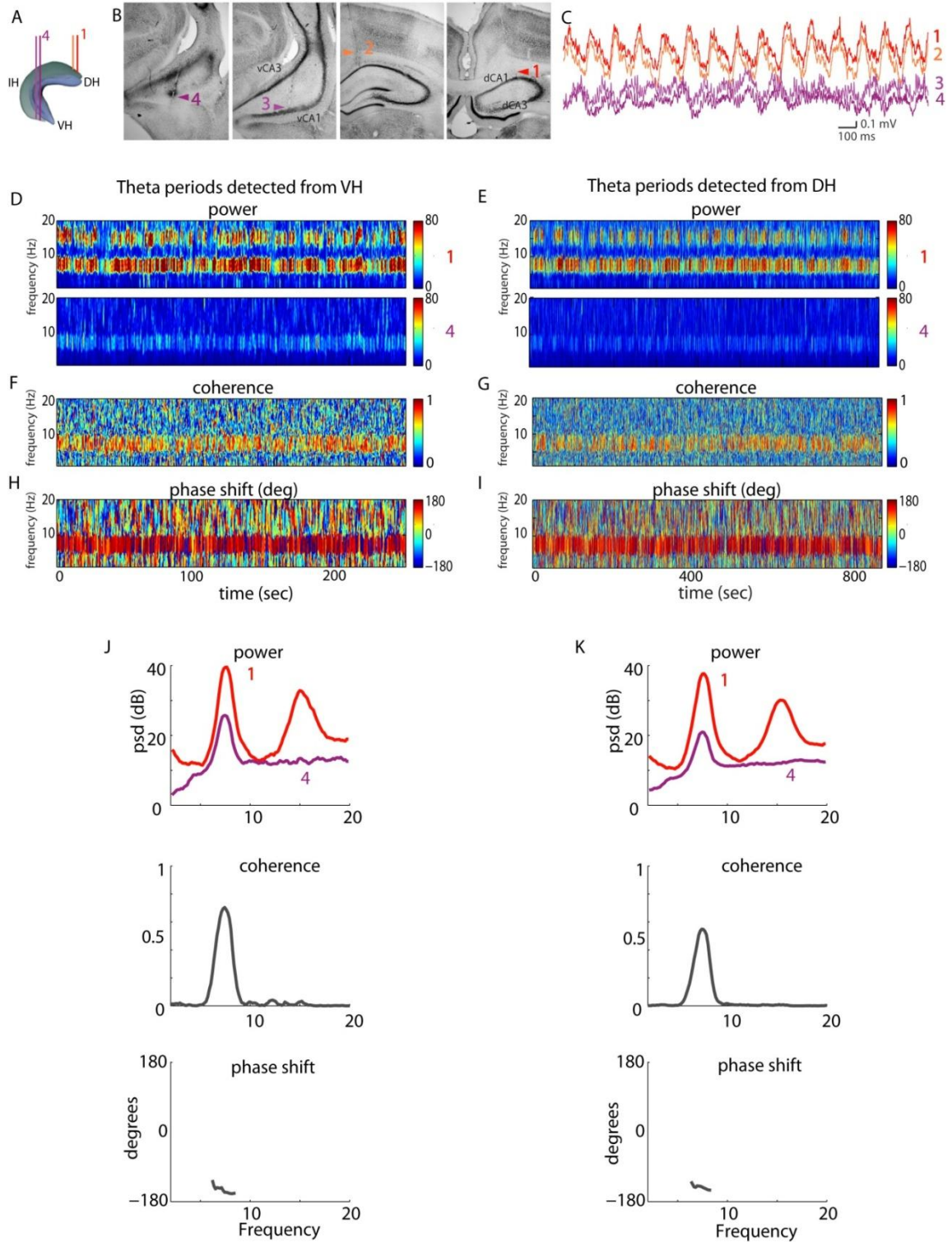


Figure S4. Largely independent amplitude variability in the DH and VH. (A). Schematics of the recording sites in the dorsal and ventral segments of the hippocampus

(r-23). Color-coding of recording sites also applies to traces in parts B and C. (B). Transverse sections (cut perpendicularly to the LA) showing two recording sites in the ventral and two sites in the dorsal CA1 pyramidal layer. (C) A short segment of LFP during RUN. Note approximately half cycle (180°) phase shift of theta oscillations between the most dorsal and most ventral CA1 pyramidal layers. (D, F, H) Time-resolved power, coherence and phase spectra for RUN theta periods, referenced to theta epochs detected from the ventral hippocampal site (VH). (J) Average power, coherence and phase spectra (E, G, I, K) Same as D, F, H and J but theta epochs were detected from the dorsal hippocampal site (DH). Note reduced theta power in the VH and lower theta coherence when theta periods are detected from DH. Note also that reference theta site selection bias does not affect theta phase difference (Phase shift is shown only when coherence is >0.1). This figure is supplementary to Figures 1, 2, 3 and 5.

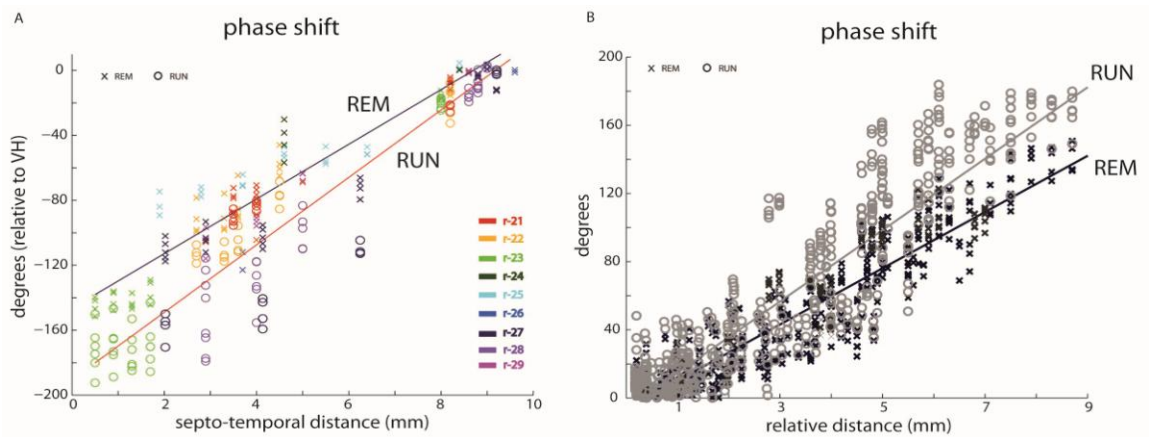


Figure S5. Traveling theta waves along the septo-temporal axis. Here, theta epochs were selected from the recordings from the dorsal hippocampus (in Figure 3, the inclusion criterion was the presence of thresholded theta power from the ventral hippocampus). (A). Phase shift of theta oscillations in single rats (color symbols) as a function of septo-temporal distance. Note up to 180° phase shift between the ventral-most and septal-most (dorsal) sites during RUN and significantly less steep phase shift

during REM. (B). Theta phase shift as a function of electrode distance. All possible electrode pair comparisons (relative distance) are shown. This figure is supplementary to Figures 3F and 3G, respectively.

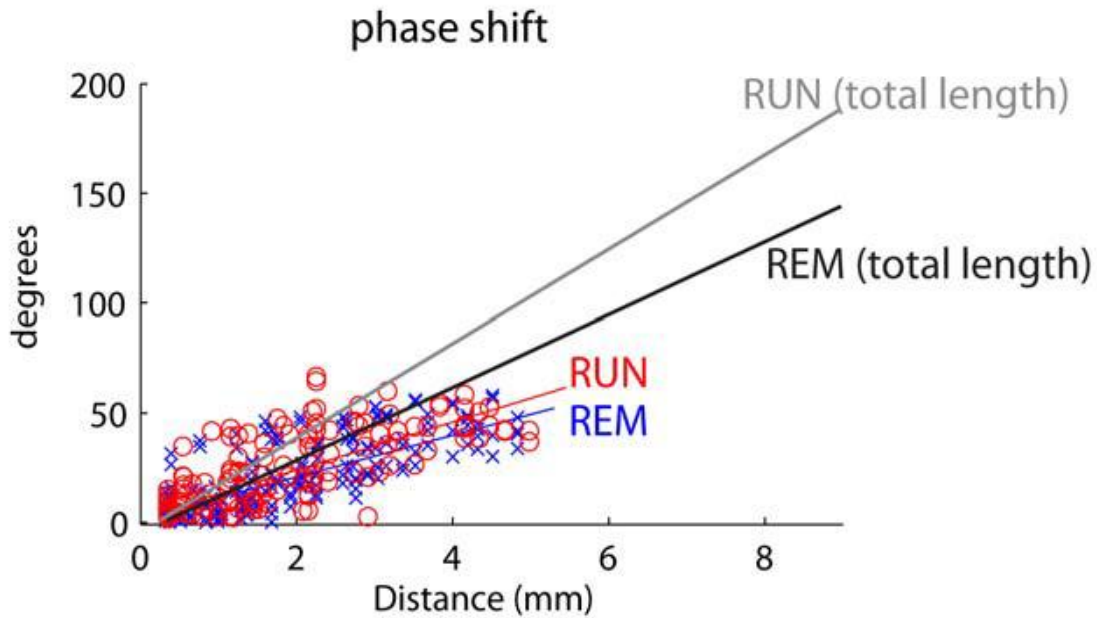


Figure S6. Discontiguity of theta coherence between intermediate and ventral segments of the hippocampus. Phase shift slopes measured separately for data points in the septal 2/3rd alone compared to data along the whole long axis. Note that the slope of theta phase vs distance from ONLY septal data is less steep compared to the slope obtained from data all along the LA (gray lines). This difference suggests that the speed of theta wave travel is slower in the septal-intermediate segments of the hippocampus and accelerates between the intermediate and ventral segments. This figure is supplementary to Figure 2.

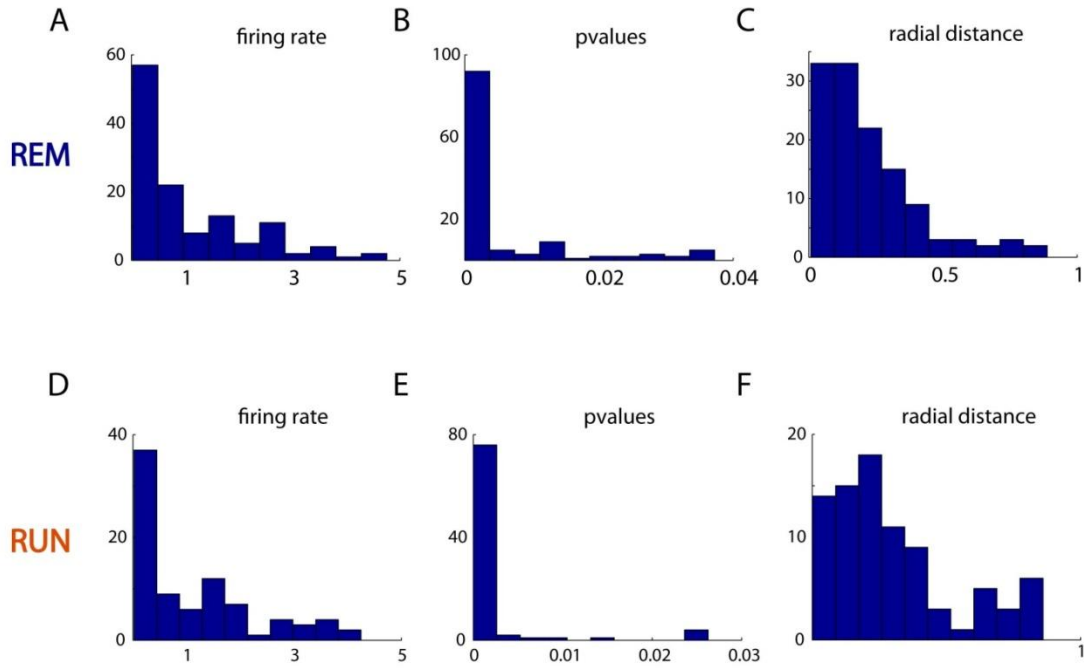


Figure S7. Ventral hippocampal single units. A) Distribution of firing rates of isolated single units from VH during REM sleep theta. B) Distribution of p-values for the significantly phase preferring single units from VH during REM, measured using Rayleigh test for circularity. C) Distribution of true radial distance measures for each significantly phase preferring isolated single unit from VH, during REM. D,E,F) Significantly phase preferring neurons from VH. Same, respectively, as A,B,C, but during running behavior.

Section 3.2 – Local generation and spread of ripples along the septo-temporal axis of the hippocampus

Submitted: Patel, Berenyi, Schomburg, Fujisawa & Buzsaki, J. Neuroscience

3.2.1 - Abstract

A topographical relationship exists between the septo-temporal segments of the hippocampus and their entorhinal-neocortical targets. However, the functional organization of the hippocampal networks along the septo-temporal axis is poorly understood. We recorded sharp-wave-ripple patterns during sleep from the entire septo-temporal axis of the hippocampal CA1 pyramidal layer. Qualitatively similar ripples emerged at all levels of the septo-temporal axis. From the local seed, ripple events propagated septally or temporally (with an average speed of ~ 0.35 m/sec), with a spatial reach proportional to ripple magnitude. While ripples propagated smoothly across the dorsal and intermediate segments of the hippocampus, ripples in the ventral segment most often remained isolated. These findings show that ripples can combine information from the entire dorsal and intermediate hippocampus and transfer integrated signals downstream. In contrast, because ripples emerge in the ventral and dorsal poles at different times, they broadcast largely independent information to their cortical and subcortical targets.

3.2.2 – *Introduction*

During immobility, consummatory behaviors and slow wave sleep, co-incidental activity at multiple locations in the excitatory recurrent networks of the hippocampal CA3 region gives rise to a convergent depolarization of CA1 neurons (i.e., the sharp wave), (Buzsaki et al., 1983). The excitatory drive, in turn, triggers a transient interaction between CA1 pyramidal cells and interneurons in the form of a fast oscillatory event (140-180 Hz), known as a “ripple” (Buzsaki et al., 1992; Csicsvari et al., 2000; O’Keefe and Nadel, 1978; Ylinen et al., 1995). Neuronal composition of the sharp wave ripple (SPW-R) is shaped by previous experience (Buzsaki, 1989; Diba and Buzsaki, 2007; Dupret et al., 2010; Foster and Wilson, 2006; Karlsson and Frank, 2009; Kudrimoti et al., 1999; Lee and Wilson, 2002; O’Neill et al., 2006; O’Neill et al., 2008; Singer and Frank, 2009; Skaggs and McNaughton, 1996; Wilson and McNaughton, 1994). Mainly because of the effective hippocampal-neocortical communication during ripples and their behaviorally relevant spike content, SPW-Rs have been postulated to play an important role in memory consolidation (Buzsaki, 1989; 1996; Wilson and McNaughton, 1994; Ji and Wilson, 2007; McClelland et al., 1995; Siapas and Wilson, 1998; Axmacher et al., 2008; Eschenko et al., 2008; Mölle et al., 2009; Ramadan et al., 2009; but see Lubenov and Siapas, 2009). In support of this hypothesis, selective elimination of ripples during post-learning sleep results in impairment of memory performance (Ego-Stengel and Wilson, 2010; Girardeau et al., 2009; Nokia et al., 2012). Despite progress on the potential physiological-behavioral role of ripples, it is not well-understood what fraction of neurons along the long axis of the hippocampus is engaged during the ripple events and

whether ripple events remain largely localized or engage multiple segments along the septo-temporal axis of the hippocampus (Chrobak and Buzsaki, 1996; Ylinen et al., 1995). Such information is critical to determine whether the different segments of the structure send outputs to different streams or whether sharp waves combine intrahippocampal information from all segments and transmit this combined pattern.

Several recent experiments have emphasized physiological differences between different segments of the hippocampus along its septo-temporal axis (Adhikari et al., 2011; Deadwyler et al., 1996; Hampson et al., 1999; Jung et al., 1994; Lubenov and Siapas, 2009; Maurer et al., 2005; Patel et al., 2012; Royer et al., 2010; Segal et al., 2010; Wiener, 1996). However, the conditions which confine or allow for the propagation of ripple events along the septo-temporal axis are largely unknown (Chrobak and Buzsaki, 1996; Csicsvari et al., 2000; Ylinen et al., 1995). Since projections from different segments of the hippocampus communicate with different territories of the neocortex through the entorhinal cortex (Amaral, 2007), ripples that emerge from the septal, intermediate and ventral segments of the CA1 region may broadcast different information to their targets at the same or different times. To examine the spatial organization of SPW-R patterns, we recorded LFP and neuronal discharge activity along the entire septo-temporal axis of the hippocampal CA1 pyramidal layer in sleeping rats.

3.2.3 Results

Local field potential (LFP) and unit activity were recorded in the home cage while the rat was sitting still or sleeping. To characterize ripples along the septo-temporal axis, recordings were done with a combination of multiple, individually movable wire electrodes, tetrodes and silicon probes (4, 6 and 8 shank silicon probes; see Methods) inserted into the CA1 pyramidal layer parallel to the septo-temporal axis (n=15 rats), (Patel et al., 2012). The electrodes were advanced until ripples (Buzsaki et al., 1992; O'Keefe, 2006), associated with unit firing in the CA1 pyramidal layer, were detected during immobility periods and sleep in the home cage. During subsequent recording sessions, the electrodes were further adjusted to obtain largest amplitude ripples, corresponding to the middle of the pyramidal layer (Mizuseki et al., 2011; Patel et al., 2012). In rats with silicon probe recordings, only sites with the maximum ripple power in the pyramidal layer were included for analysis (Patel et al., 2012). Only recordings which met the inclusion criteria (large amplitude ripples with associated strong unit firing and subsequent anatomical verification of the recording tracks) were analyzed further (59 out of 119 recording sites in septal hippocampus and 24 out of 54 recording sites in ventral hippocampus; n=15 rats; 2 to 6 sleep sessions per rat; see Methods).

3.2.3.1 Ripples along the septo-temporal axis of the CA1 pyramidal layer

Sharp wave-ripple complexes are initiated by the coincident discharge of pyramidal cells in the CA3 region. The CA3 output generates strong depolarization in the apical dendrites of CA1 pyramidal cells and interneurons, which is reflected extracellularly as a sharp wave in the str. radiatum (Fig. 1A), (Buzsaki et al., 1983; Sullivan et al., 2011). In turn, the interactions between CA1 pyramidal cells and interneurons give rise to a transient fast oscillation, the ripple (Buzsaki et al., 1992). While sharp waves and ripples are distinct events, their cross-frequency coupling is reflected by the similar time course of the two

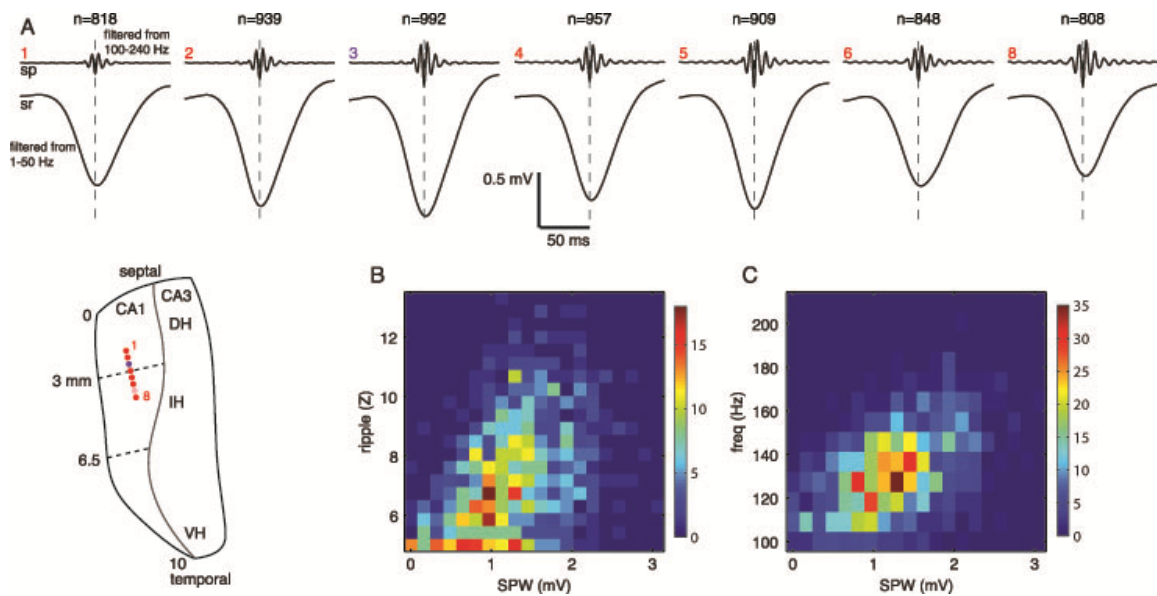


Fig. 1 Sharp waves and ripples in the CA1 region. (A) Ripples and sharp waves recorded from seven pairs of sites (red dots in inset) in the pyramidal layer (pyr) and middle of stratum radiatum (rad) along the septo-temporal axis. Each pair is an independent average of >807 (actual number given on top of each shank) events, triggered by the trough of the largest amplitude ripple wave of the locally recorded ripple

events. Flat map shows the position of the CA1 and CA3 regions. Numbers on left (in mm) and dashed lines indicate the approximate boundaries between the dorsal (DH), intermediate (IH) and ventral (VH) segments of the CA1 region. (B) Correlation between the peak amplitude of sharp waves (SPW) and ripple magnitude (root mean square of the filtered event). Colors indicate the density of points. (C) Correlation between the peak amplitude of sharp waves (SPW) and ripple frequency.

events and the correlation between the amplitude of the sharp waves and the magnitude and frequency of the ripples (Fig. 1B, C), (Buzsaki, 1986; Sullivan et al., 2011). Because of the strong correlation between the two events, and because in most experiments only recordings from the CA1 pyramidal layer were available at multiple locations, the magnitude of the ripple episodes was used as a proxy for sharp waves in the quantification of their spread along the septo-temporal axis. A ripple episode consists of multiple ripple waves (4-10), whose envelope defines the ripple event. Therefore, we discuss the spatial relationship between *ripple waves* and *ripple events* separately.

To quantify ripples, fast frequency events were first detected independently at each recording site. Oscillatory episodes in which the amplitude of the ripple band-filtered trace (100-250 Hz) is >3 standard deviations (SD) above the session background mean were identified as ripple events and subsequently separated into 3 to 5, 5 to 7 and >7 SD groups (see Methods). The recording sites along the septo-temporal axis were divided into dorsal (0-3.25 mm) intermediate (3.26-6.5 mm) and ventral (8.0-10.0 mm) segments. Figure 2A and 2C illustrates recordings from the CA1 pyramidal layer at multiple sites in the septal 2/3rd segment and the ventral segment, respectively. Ripples emerged at each

location with comparable amplitude, duration and shape but showed large inter-electrode distance-dependent variability from one event to the next (Fig. 2B and 2E). When filtered LFP ripples (100-250 Hz, SD <7) and ripple triggered multiunit activity were compared at different locations, the locally recorded events were virtually identical at all recordings sites from the septal to the temporal pole of the CA1 pyramidal layer (Fig. 2B and 2E, leftmost columns). However, when the LFPs and unit firing histograms were aligned relative to ripple times at a single reference site, while the ripple coherence decreased precipitously with distance (Figure 2B and 2E, central column), a broad ripple event-related increase in firing rates persisted for longer distances (up to 5.5 mm; Figure 2B, rightmost column). However, the ripple event-related increase in the septal hippocampus failed to spread to the ventral segment (Figure 2E, rightmost column).

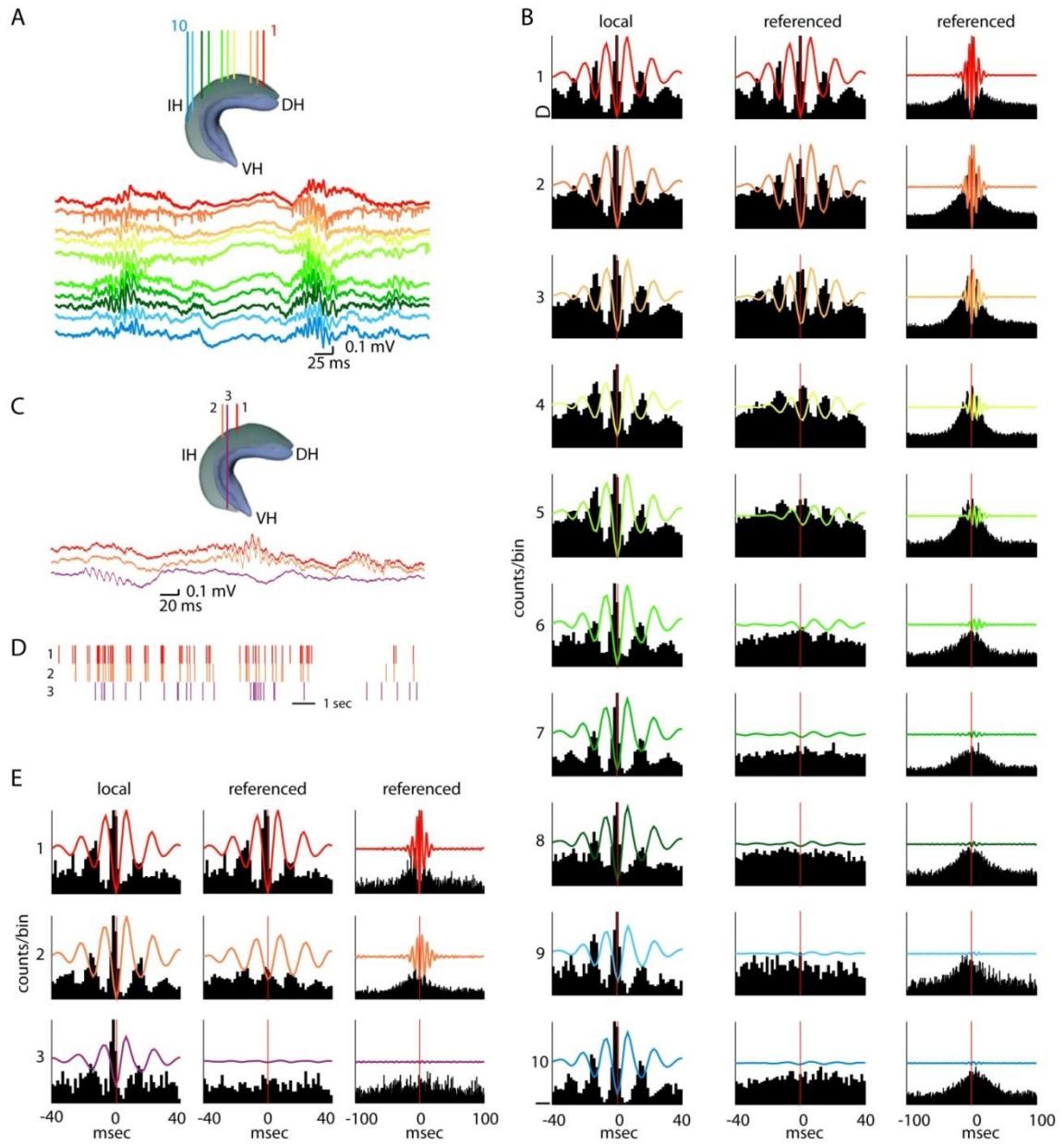


Fig. 2. Ripples occur along the entire septo-temporal axis of CA1. (A) Cartoon of the hippocampus indicating the locations of 10 recording electrodes along the septo-temporal axis. DH, dorsal; IH, intermediate; VH, ventral hippocampus. Ripples recorded from the CA1 pyramidal layer as in A. (B). Left panel: Ripple trough-triggered LFP (100-250 Hz band pass) and correlated multiple unit activity during ripples detected on each electrode (left column; same color code as in A). Middle and right columns show averaged LFP

and MUA, but the ripple event times were taken from the most septal reference site (1, reference). The two time scales emphasize ripple wave (middle) and ripple event (right) relationships. Note rapid loss of ripple wave modulation of neuronal firing with distance, whereas ripple events have a larger spatial spread. (C-E) Same as in A-B but showing traces from two dorsal (DH) and one ventral (VH) CA1 pyramidal layer locations. (D) Temporal relationship of ripple events at the 3 locations. (E) Locally recorded LFP ripples and unit firing are similar at dorsal and ventral locations (left). In contrast, ripples recorded at dorsal sites and at the ventral tip of the CA1 region are largely independent (middle and right columns).

Next we quantified various ripple parameters, including duration, frequency, amplitude and rate of occurrence at different locations along the septo-temporal axis. The duration of the ripple event was defined as the time difference between the tails of the detected ripples where the power of the filtered trace exceeded and returned below the threshold (Fig. 3A, B; see Experimental Procedures). A ripple event consisted of 4 to 9 oscillatory waves of increasing and decreasing amplitude. The number of waves (i.e. ripple length or duration) increased (i.e., the ripple event was longer) as a function of the ripple event amplitude (Fig. 3C; $P < 0.001$; 3-way ANOVA). The duration of the ripple event within the same amplitude group was remarkably similar in the dorsal, intermediate and ventral segments ($P = 0.41$, location effect; distance-amplitude group interaction: $P < 0.0002$; 3-way ANOVA). Within-ripple event frequency, quantified from the morlet wavelet transform surrounding the ripple peak amplitude, showed a moderate but monotonic decrease from the dorsal to the ventral pole ($P < 0.001$, septo-temporal axis effect; 3-way ANOVA) and also depended on the magnitude of the ripple (SD group effect: $P < 0.001$;

septo-temporal axis-SD group interaction: $P < 0.0005$; 3-way ANOVA). The magnitude of the ripple event was determined from the morlet wavelet transform in the ± 50 ms time window surrounding the ripple event (Fig. 3D; see Experimental Procedures). The amplitude of the ripple event remained relatively constant or slightly decreased in the

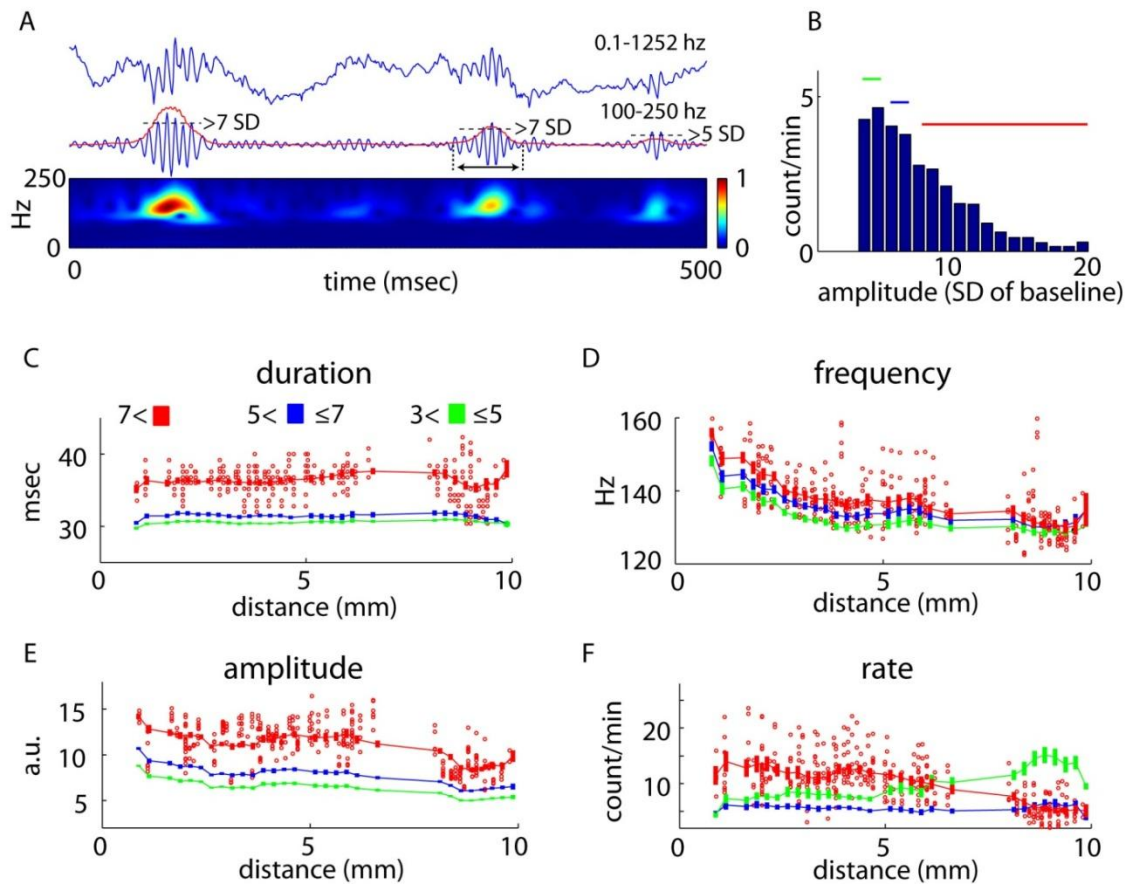


Fig. 3. Parameters of ripples. (A) Three successive ripple events and their filtered derivatives. Red line represents the root mean square (magnitude) of the ripple events. Dotted lines illustrate ripple events >7 standard deviation (SD) and >5 SD above the session mean baseline. The duration of the ripple event is determined as the interval where the magnitude exceeds and goes below 1.5SD (double arrow under the 2nd ripple). Bottom, morlet wavelet decomposition of the events. (B) Amplitude distribution of ripple

events from an example session at a dorsal CA1 location. Color lines indicate 3-5SD (green), 5-7SD (blue) and >7SD (red) events. (C-F) Group data for duration, frequency, amplitude and rate of ripple events. Each red dot is a session mean of ripple events recorded by a given electrode. The x-axis provides the location of the electrodes along the septo-temporal axis, from the septal pole (0 mm) to the temporal pole (10 mm). Red line, running average (pooled across sessions and rats) for ripple events >7SD. For the smaller amplitude events (3-5SD and 5-7SD), only the running averages are shown.

dorsal-intermediate axis but was significantly lower in the ventral third (Fig. 3E; SD group effect: $P < 0.001$; axis effect: $P < 0.001$; axis-SD group interaction: $P < 0.001$; 3-way ANOVA). Ripple event rate (event/min) showed a strong axis-SD group interaction ($P < 0.001$; 3-way ANOVA). In the dorsal and intermediate segments, both lower (3-4 SD) and large (≥ 7 SD) amplitude events dominated, whereas in the ventral segment smaller amplitude ripples occurred most frequently (Fig. 3F). The dorsal-ventral difference of rate in the three SD groups could largely be explained by the decreased amplitude of the ripple events in the ventral segment.

3.2.3.2 Spread of ripples along the septo-temporal axis

The single site analyses above suggested that ripples could emerge at any level along the septo-temporal axis (Fig. 4). From the seed, the activity could propagate toward both septal and temporal directions. Along the path of the travel, the amplitude of the ripple event could either increase or decrease non-monotonically, indicating that the

propagating activity is not just an amplitude spread but can be either attenuated or amplified along its course. Both the amplitude and spatial extent of ripple showed variability, from strongly localized to spatially widespread events (Fig. 4). Ripples could emerge at two or more locations either relatively simultaneously or with delays. In such cases, certain recording locations were invaded from both directions, either giving rise to a prolonged or a double ripple event or the earlier ripple could suppress the later arriving one. Occasionally, a secondary seed induced a “reflected” event propagating in the opposite direction (Fig. 4). Selecting a given recording site as the reference, the event-to-event variability of both the amplitude and latency of ripples could increase in both septal and temporal directions.

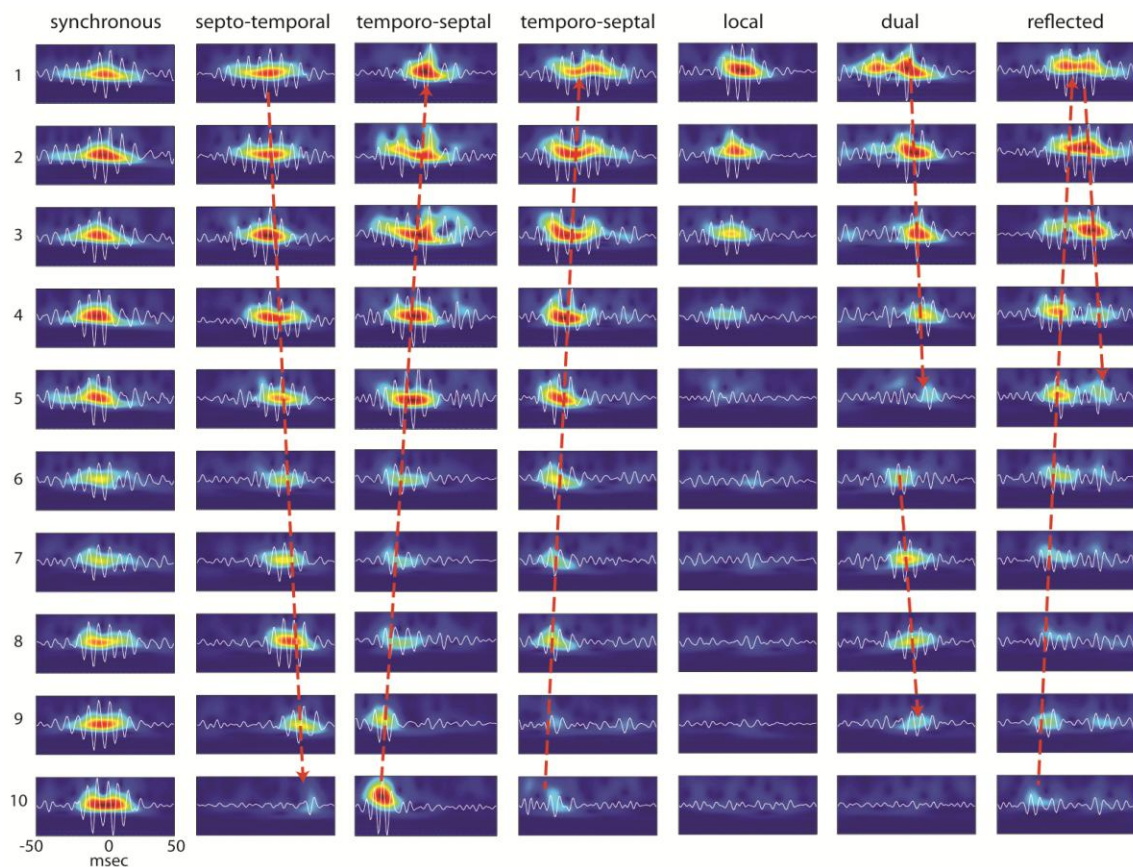


Fig. 4. Spatial extent and propagation of ripple events. Examples of single ripple events and their wavelet maps recorded from 10 sites in the dorsal and intermediate segments of the hippocampus (as in Fig. 2). Ripple events can spread in a septo-temporal or temporo-septal direction (long arrow) but multiple other forms, such as synchronous or locally confined events are also present. Occasionally, ripples emerge from two seeds simultaneously (dual; two arrows) or travel in opposite directions (reflected), leading to prolongation or doubling of ripple events at certain locations.

These qualitative observations were quantified by determining the probability of co-occurrence ('synchrony') and the change of ripple amplitudes between pairs of recording sites at all available septo-temporal distances (Fig. 5). Because of the similarity of ripples in the dorsal and intermediate segments (Fig. 3), pairs from these segments were combined as one group and compared to pairs that spanned both the dorsal/intermediate and ventral segments. In the first comparison ('ripple wave synchrony'), the trough of largest ripple wave in each ripple event was detected and the fraction of co-occurring events was plotted as a function of distance (Fig. 5A-D). Strongly synchronous ripple waves, as detected within ± 1 msec windows were confined largely to neighboring sites ("ripple wave jitter"). Co-incident large amplitude ripple waves (>7 SD events at *both* sites) occurred mainly at short distances and the percentage of coincident ripple waves decreased with ripple event amplitude. Intermediate (5-7 SD events) and small size (3-5 SD events) ripple waves were essentially non-correlated at distances >2 mm (Fig. 5C). In the second comparison, co-occurrence of troughs of ripple waves in ± 50 msec windows are plotted ("ripple event synchrony"; Fig. 5D). Ripple event synchrony was spatially more widespread, and approximately 40% of the large amplitude events (>7 SD at both

reference and referred sites) expanded up to 5 mm, while the majority of smaller amplitude events (<5 SD) remained largely local. Beyond 2 mm distance, fewer than 20% of the smaller events were synchronous (Fig. 5D). The extent of synchrony was not uniform in the septo-temporal axis. If one of the recording sites of the pair was in the ventral segment, ripple event synchrony was smaller and associated with a larger variance at nearly all distances compared to similar distances within the same hippocampal segment (red dots compared to blue dots in Fig. 5D).

The third comparison examined the amplitude attenuation of the ripple events. The strength of the correlation between ripple events was determined by comparing the amplitude of the morlet wavelet transform at the time of peak amplitude in the reference ripple event and then taking a mean between 120-180 Hz (Fig. 5E). The amplitude of the

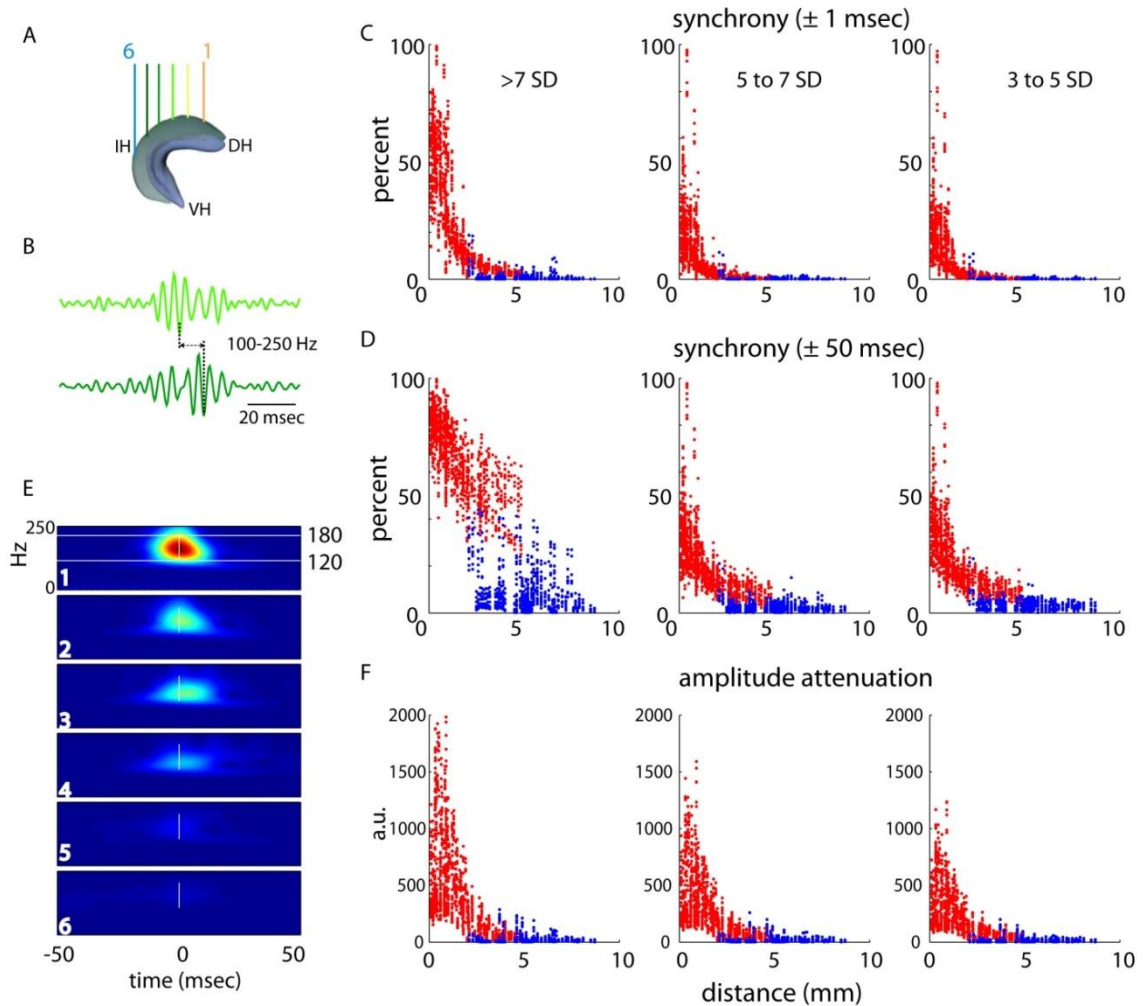


Fig. 5. Most CA1 ripples are spatially confined. (A) An example rat showing the recording locations along the septo-temporal axis. (B) Single ripple events recorded from 2 sites. The temporal delay between the largest amplitude troughs are measured (C) Spatial synchrony of ripple waves. Percent of ripple events detected in the referred electrode within ± 1 msec of ripple event in the reference electrode is plotted as a function of distance between the electrodes. Each dot is based on a single recording session. Dots are colored red if both electrodes of the recording pair were located in the dorsal-intermediate hippocampus and blue if one of the electrodes in the pair was in the ventral hippocampus and the other in the dorsal-intermediate hippocampus. Note that ripple waves in large amplitude ripple events (>7 SD group; left column) spread larger distances than the medium or small ripple events (middle column, 5-7SD; right column, 3-5SD).

(D) Spatial synchrony of ripple events. Same as C but the referred events were detected within ± 50 msec of the ripple event in the reference electrode. Note large spatial coverage of large amplitude ripples ($<7SD$) in the dorsal-intermediate hippocampus (red dots). In contrast, ripple event synchrony between dorsal-intermediate and ventral sites at similar distances (2.5 to 5 mm) was low (blue). (E) An example continuous morlet wavelet transform during a single ripple event centered on the ripple at site 1 (as in A). Note rapid attenuation of the ripple event amplitude with distance. (F) Ripple event amplitude attenuation over distance. Ripple amplitude (at zero time bin and mean over 120-180 Hz range) was measured at all referred sites during each ripple event in the reference channel and the means are plotted as a function of distance between the reference and referred electrodes (same color code as in C, D).

ripple event showed a rapid decrease with distance, indicating that ripple events are locally generated. When large amplitude ripple events ($>7SD$ at both reference and referred sites) were compared, the relative attenuation with distance was steeper compared to smaller amplitude ripple events (Fig. 5F).

For the quantification of the speed of ripple event propagation, we measured either the time shift of the first peak of the cross-correlation of ripple waves (Fig. 6) or the time difference between the peak morlet wavelet amplitude between two recording sites and plotted them as a function of distance (Fig. 7A). Although, ripples could propagate either in the septo-temporal and temporo-septal directions (Fig. 4 and Fig. 6), interestingly, the seed of activity of successive events was not completely random but showed some direction bias. In the example session shown in Fig. 6, the majority of ripples initiated ventrally and spread septally in the first sleep session (Fig. 6B - PrS1 and PrS2; Fig. 6C).

In the sleep session following a maze performance (RUN), a pronounced septo-temporal bias of ripple spread is seen followed by a gradual return to a more temporo-septal direction bias (Fig. 6B - PoS1 and PoS2; Fig. 6C). Although these qualitative observations need to be confirmed, they support the hypothesis that the site of ripple initiation is flexible. They also illustrate that averaging across all trials may not reveal the true propagation speed, because this averages over ripples traveling in each direction. Therefore, we first separated the septo-temporally propagating and temporo-septally propagating events before measuring the absolute time difference between the ripple amplitude maxima at pairs of recording sites against the distance between sites (Xu et al., 2007). The estimated speed of propagation in the septo-temporal direction was somewhat faster for the largest amplitude ripple events ($> 7SD$, 0.373 mm/msec) than for the smaller amplitude events (5-7 SD, 0.358 mm/msec; 3-5 SD,

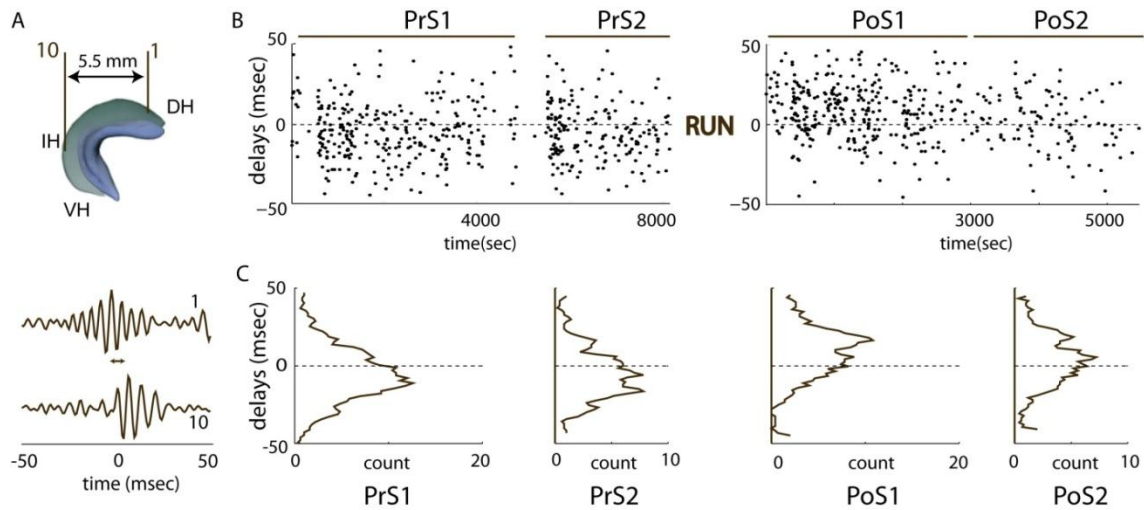


Fig. 6. Direction of ripple spread can be biased. (A) Cartoon showing recording sites in dorsal and intermediate hippocampus. Time lag between the largest trough of a co-

occurring ripple events at two sites (filtered) is shown (double arrow). (B) Positive or negative time lags for each ripple event during successive sleep sessions, separated by a maze run session (RUN). (C) Smoothed distribution curves of the delays in the first and second parts of the sleep session during both pre and post-RUN sleep sessions. Note that most ripples in pre-RUN sleep are initiated at the temporal site but after RUN they are biased towards septal initiation.

0.333 mm/msec). The propagation speed for >7 SD events differed significantly from the speed of 3-5 SD events ($P<0.02$; shuffling test; see Methods). The ripple propagation speed in the temporo-septal direction were similar (>7 SD, 0.40 mm/msec; 5-7 SD, 0.359 mm/msec and 3-5 SD, 0.333 mm/msec; <7 SD events speed differed from 5-7 SD events; $P<0.006$ and from 3-5 SD events; $P<0.001$). When comparing ripple propagation speed for the septo-temporal versus temporo-septal directions for same amplitude events, only the large amplitude events (>7 SD) showed a significant effect ($P<0.001$; shuffling test). The spread of activity across the dorsal/intermediate and ventral segments was quite variable (blue dots in Fig. 7B, C).

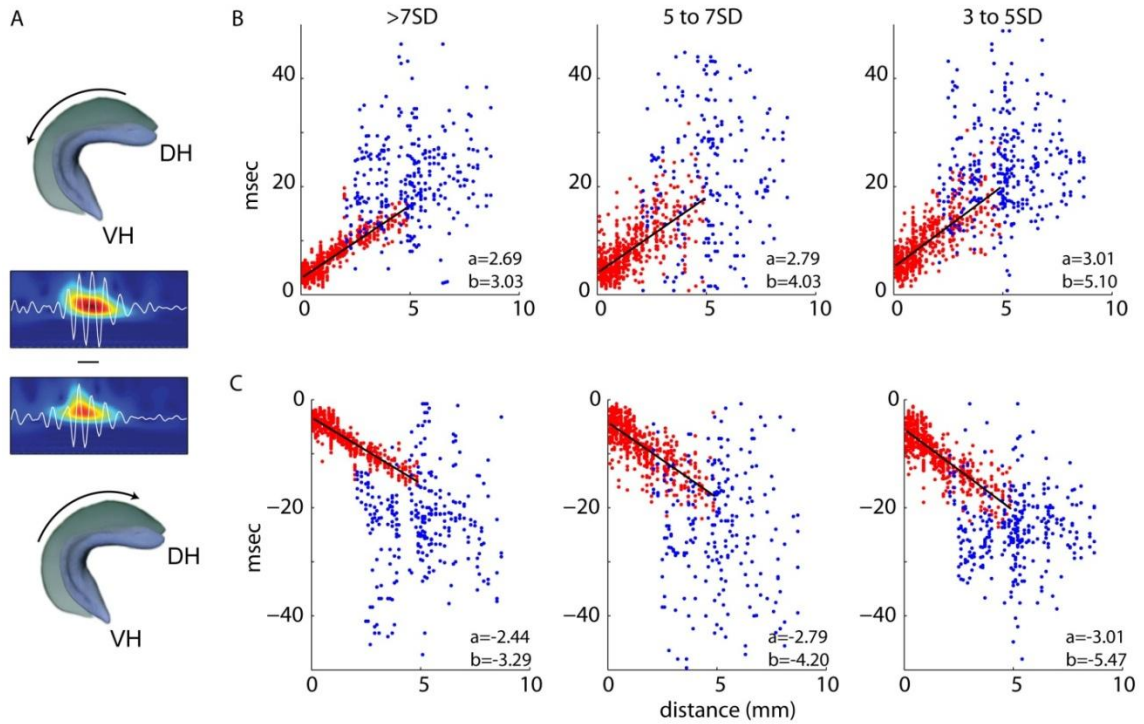


Fig. 7. Propagation of ripple events. (A) Ripple events recorded on electrode pairs and propagating in the temporo-septal (top) and septo-temporal (bottom) direction were separated. Examples show ripples at a more septal and temporal sites. Horizontal line indicates time delay between the trough of the largest ripple wave at each site. (B) Delays between more dorsal reference electrode and more ventral referred electrode, obtained from wavelet amplitude maxima. (C) Same as B but shows delays between more ventral reference location and more dorsal referred location. Blue dots indicate that one electrode of the pair was in the ventral and the other in the dorsal-intermediate hippocampus. Regression lines for red dots (pairs from the dorsal and intermediate hippocampus) are shown in black. b, y coordinate intercept. a, slope.

Chapter 4.0 - Discussion

The studies described in this thesis examined the organization of theta and sharp-wave associated ripples along the entire septo-temporal axis of the hippocampus in behaving rats. In addition we also studied how neurons at different levels of the septo-temporal axis relate to the ongoing oscillatory patterns recorded locally or at more distant sites.

The main findings of my two completed studies are:

4.1 Main Results: Theta oscillations

- 1) While the frequency of theta oscillations remained the same at all locations along the entire septo-temporal axis, the amplitude and coherence between recording sites decreased from the dorsal to the ventral hippocampus.
- 2) Theta phase shifted monotonically with distance along the septo-temporal axis, reaching $\sim 180^\circ$ during behavior and 150° during REM sleep, between the septal and temporal poles.
- 3) The majority of concurrently recorded local units were phase-locked to the trough of the locally recorded field theta at all septo-temporal segments. However, approximately 25% of single pyramidal cells in the ventral hippocampus fired at the peak of locally recorded theta cycle.
- 4) The power of ventral hippocampal theta oscillations had a significantly weaker correlation with locomotion velocity of the rat compared with theta in the dorsal and intermediate segments.

5) Theta amplitude in the ventral segment often varied independently from theta in the dorsal-intermediate segments. For example, during running behavior while theta oscillations were observed continuously in the septal hippocampus, theta oscillations in the ventral segment exhibited an intermittent pattern. Furthermore, the presence of theta in the ventral hippocampus did not correlate with the animals' presence in the goal/reward locations.

4.2 Main Results: Sharp-wave associated ripple oscillations

- 1) Ripples could emerge at any location along the entire longitudinal axis of the CA1 pyramidal layer.
- 2) While ripple frequency decreased monotonically from the dorsal pole to the ventral pole, ripple amplitude was significantly lower in the ventral segment.
- 3) Ripples are generated locally but sharp-wave related synchrony is spatially more widespread. Indeed, ripple wave coherence dropped precipitously ($<2\text{mm}$) but the 'ripple event' related increases in firing rates were more widespread ($\sim 5\text{mm}$).
- 4) From the local seed ripple events propagated in both septo-temporal and temporo-septal directions with an average speed of 0.35 m/sec . The spatial extent of the ripple events was proportional to the ripple magnitude. Conversely, ripples in the ventral segment most often remained isolated.
- 5) Our observations also suggest that the direction of propagation of ripples along the septo-temporal axis depends on prior behavior.

4.3 General Discussion

The hippocampus plays an important role in the formation of new episodic (memory of what, where and when), and semantic (memory for facts) memories (Squire, 1992). Apart from the well-studied spatial memories (O'Keefe and Nadel, 1978), the hippocampus is also known to be critical for a variety of other forms of memories, including recognition (Mahut et al., 1982; Wilson, 1987), recollection (Zola-Morgan and Squire, 1986), positional (Kesner et al., 1988; Parkinson et al., 1988), olfactory (Eichenbaum et al., 1988; Eichenbaum et al., 1989), verbal and visual memories (Fernandez et al., 1998; Nyberg et al., 1996; Rombouts et al., 1997; Stern et al., 1996), categories which are usually referred to as “declarative” memory in humans (Squire, 1992), as well as anxiety, emotions, and reward based memories (Bannerman et al., 2003; Bannerman et al., 2004; Degroot and Treit, 2004; Kjelstrup et al., 2002; McHugh et al., 2004; Phillips and LeDoux, 1992; Richmond et al., 1999; Royer et al., 2010). The hippocampus could serve these diverse functions in one of at least three ways. (1) In principle, the entire hippocampus could be devoted to a single general type of memory system, where each memory is represented in the activity patterns of the whole hippocampus, but in separate neuronal ensembles. (2) Alternatively, the hippocampus could be divided into separate segments, in a graded or continual manner, where each segment would then subserve a different function. (3) The diverse forms of hippocampal memories would depend on separate intra-hippocampal circuits, either overlaid or segregated (Fanselow and Dong, 2010; Hampson et al., 1999; Moser and Moser, 1998; Risold and Swanson, 1996).

Data on gene expression, anatomical connectivity, including both afferent and efferent hippocampal connections, cellular-synaptic constructs, electrophysiological properties, and lesion studies all support the hypothesis of a segmental organization of the hippocampus along its septo-temporal axis (Fanselow and Dong, 2010; Moser and Moser, 1998). In contrast, the strong and widespread CA3 recurrent connections (Amaral and Witter, 1989; Fricke and Cowan, 1978; Ishizuka et al., 1990; Li et al., 1994; Swanson et al., 1978; Wittner et al., 2007), and the sparse but nevertheless important recurrent collaterals among CA1 pyramidal cells (Christian and Dudek, 1988; Deuchars and Thomson, 1996; Thomson and Radpour, 1991) support the argument of a unified hippocampal circuit that can integrate patterns in the entire hippocampus. In the presence of such competing potential mechanisms, we investigated how theta oscillations (during overt behavior and REM sleep) and the fast frequency sharp-wave ripples (during slow wave sleep), were organized along the entire septo-temporal axis of the hippocampus. While theta oscillations occur when hippocampal circuits receive rhythmic input from neurons within the superficial layers of the entorhinal cortex, sharp waves are initiated within the hippocampus and spread to the entorhinal cortex (Buzsaki, 1986, 2002; Buzsaki et al., 1992; Chrobak and Buzsaki, 1994; Hasselmo et al., 1995). Thus, while theta oscillations are assumed to largely organize afferent patterns in the hippocampus, sharp-wave associated ripple oscillations are thought to synchronize the output pathways from the hippocampus back to the neocortical structures via the entorhinal cortex.

4.4 Theta oscillations along the entire septo-temporal axis of the hippocampus

In rodents, theta oscillations are essential for the physiological operation of the hippocampus, and abolishing the rhythm results in severe behavioral deficits (Winson, 1978). It is believed that the phasic patterning of spiking activity taking place during theta provides opportunities for spatio-temporal coding of information in the hippocampus (Huxter et al., 2003; Huxter et al., 2008; O'Keefe and Recce, 1993; Skaggs et al., 1996). Furthermore, theta oscillations have been found to compress neuronal representations from the timescale of seconds ('behavior time scale') to milliseconds (referred to as "temporal compression"), (Dragoi and Buzsaki, 2006; Skaggs et al., 1996), which may be an important mechanism for the induction of spike timing dependent plasticity (STDP), (Jensen et al., 1996; Jensen and Lisman, 1996; Magee and Johnston, 1995; Markram et al., 1997; Mehta et al., 1997) and for the proper temporal packaging and transfer of neuronal information (Buzsaki, 2005; Hasselmo et al., 2002). "The theta rhythm" is considered as the central coordinating mechanism of the hippocampal formation. Both intrinsic (Bland, 1986a; Kamondi et al., 1998; Lee et al., 1994), as well as extrinsic mechanisms, such as the medial septum (Lee et al., 1994; Stewart and Fox, 1990) and/or the supramammillary nucleus (Kocsis and Vertes, 1997) contribute to theta oscillations. Recent experiments using high-density silicon probes in different layers of the hippocampal region (Montgomery et al., 2009; Montgomery et al., 2008) or electrode arrays covering large region of the CA1 pyramidal layer (Lubenov and Siapas, 2009), clearly show that the power, coherence, and phase of theta oscillations in the hippocampus change in a layer- and behavior-specific manner, suggesting that theta oscillations should be conceived not as a rigid period generator, but as a flexible

framework of oscillators that allows different layers and regions within the hippocampus to coordinate adaptively with one another depending on the specific processing functions of the system. The present work provides a glimpse into how these ‘monolithic’ appearing oscillations also differ within the CA1 pyramidal layer along the septo-temporal axis.

Neuronal recording studies from the septal and temporal segments have been controversial and range from emphasizing the unity of hippocampal operations to more localized and specialized computations (Bullock et al., 1990; Jung et al., 1994; Kjelstrup et al., 2008; Lubenov and Siapas, 2009; Maurer et al., 2005; O'Keefe and Nadel, 1978). A recent study (Lubenov and Siapas, 2009), using recordings from the septal hippocampus (covering approximately 3.5 mm along the septo-temporal axis), reported that theta oscillations in area CA1 are traveling waves, with extrapolated septo-temporal phase offset of 360° that propagate roughly along the septo-temporal axis of the hippocampus and pattern the hippocampal activity not only in time but also across anatomical space. The authors argued that the presence of traveling waves indicates that the instantaneous output of the hippocampus is topographically organized and represents a segment, rather than a point, of physical space. The implication of a full-cycle phase shift of theta waves from the dorsal and ventral poles is that while the two poles of the hippocampus would provide temporally synchronous outputs to their targets, the large part of the intermediate hippocampus would be left temporally segregated from either pole. In contrast to the prediction of Lubenov and Siapas (2009), we recorded theta oscillations from the entire septo-temporal length of the CA1 pyramidal layer and found a linear phase shift along the

whole axis, reaching approximately 180° phase shift between the two poles during exploration, and a slower propagation of theta waves reaching approximately 150° during REM sleep (Patel et al., 2012).

Our results confirm and extend the prediction of Lubenov and Siapas (2009) that the phase of theta waves advances monotonically along the entire long axis of the hippocampus. In their ‘hippocampal circle’ model, the septal and temporal poles are functionally ‘connected’ by a full theta cycle. In contrast, we found $\sim 180^\circ$ phase offset during exploration and a slower propagation of theta waves during REM, possibly due to the lower frequency of REM theta. A potential source of discrepancy between the two studies is the different axes of phase measurements. In the experiments of Lubenov and Siapas (2009), phase was computed from the combined antero-posterior and medio-lateral propagation of theta waves in the dorsal hippocampus and extrapolated to correspond to $240^\circ - 360^\circ$ along the septo-temporal axis. Since theta waves travel not only along the long axis but also in the CA1-CA3 direction, (Dragoi and Buzsaki, 2006), the simultaneous contribution of the phase shifts in both septo-temporal and CA3-subicular axis could have resulted in overestimation of the phase advancement along the longitudinal axis.

The half-cycle theta shift between the septal and temporal poles should have important functional implications. The orderly temporal offsets between increasing septo-temporal levels of the hippocampus result in a sequence of activity maxima of CA1 pyramidal cells, corresponding to the troughs of local theta waves. Combining the delays of activity

maxima with spike-timing dependent plasticity (Magee and Johnston, 1997; Markram et al., 1997), the temporal shifts with distance suggest that the functional connections among neurons at different septo-temporal levels are mainly unidirectional during theta oscillations and that neighboring neurons are more strongly connected than distant ones. At the septal and temporal ends of the hippocampus, the half-theta cycle delay (~70 msec) may prevent the association of signals from the poles. These considerations suggest that the intermediate hippocampus is best poised to integrate diverse hippocampal representations (Bast et al., 2009), whereas neurons at the poles broadcast segregated messages to different parts of the neocortex. The relative discontinuity of coherence, phase and speed correlation between the intermediate and ventral segments also supports this notion. Locomotor velocity had a strong effect on theta power in the dorsal and intermediate hippocampus (McFarland et al., 1975; Montgomery et al., 2009), but this relationship was weak in the temporal segment (Hinman et al., 2011), suggesting that ventral hippocampal neurons are less affected by speed. Because place cells are speed-controlled oscillators (Geisler et al., 2007; Jeewajee et al., 2008), the diminishing effect of speed supports the hypothesis that inputs to the ventral hippocampus carry largely non-spatial information (Royer et al., 2010).

4.4.1 Mechanisms of traveling theta waves along the septo-temporal axis

Traveling LFP waves may arise from multiple distinct mechanisms (Ermentrout and Kleinfeld, 2001). The simplest one requires a single rhythm generator (e.g., the ‘septal

theta pacemaker’); (Petsche and Stumpf, 1962) and the (fictive) delays would emerge through a progression of increasing time delays, due to the propagation velocity of septo-hippocampal afferents. This mechanism is unlikely to play a significant role for the following reasons. First, it requires precisely tuned delays in multiple collaterals of septal afferents to the various regions of the hippocampus and matching entorhinal cortical inputs. Second, the frequency of theta oscillations depends primarily on the GABAergic neurons of the medial septal area (Lee et al., 1994; Yoder and Pang, 2005), and the conduction velocities of thickly myelinated septo-hippocampal GABAergic neurons (Freund and Antal, 1988) are an order of magnitude faster than the propagation velocity of theta waves (Bilkey and Goddard, 1985). Third, the different septo-temporal segments of the hippocampus are not innervated by axons of the same septal neurons. Instead, fibers to the septal two-thirds travel largely in the fimbria and fornix, whereas the temporal segment receives its input through a ventral pathway (Gage et al., 1983). Phase shifts could also arise from a single pacemaker (e.g., medial septum) through delays emerging from a chain of unidirectionally linked groups of neurons (Ermentrout and Kleinfeld, 2001). Another mechanism that could provide delays would be a chain of oscillators residing within the pacemaker itself (e.g., the septal area) and the phase shift observed in the hippocampus would be a reflection of the phase-delayed septal outputs. While this latter solution cannot be fully excluded, it would require a complex temporal coordination of the hippocampal and entorhinal neurons in different regions and layers with appropriate delays.

We hypothesize that traveling theta waves arise from a network of ‘weakly coupled’ (Kopell and Ermentrout, 1986) intrahippocampal and matched entorhinal cortex oscillators. In support of this hypothesis, both the CA3 recurrent system and *in-vitro* slices of the CA3 region can generate theta oscillations (Kocsis et al., 1999; Konopacki et al., 1987). In addition, delays with similar magnitudes documented here have been reported in the isolated CA3 region *in-vitro* (Miles et al., 1988).

The importance of weakly coupled oscillators in traveling waves is illustrated by the spinal cord activity of the lamprey during swimming (Cohen et al., 1992; Kopell and Ermentrout, 1986). The swim rhythm arises from inter-segmental coordination of spinal cord oscillators, connected by local connections with short delays. The dominance of forward swimming is secured by the faster oscillators in the frontal end of the cord (Grillner et al., 1995). By analogy, the oscillation frequencies of place cell assemblies decrease progressively along the septo-temporal axis of the hippocampus (Jung et al., 1994; Kjelstrup et al., 2008; Maurer et al., 2005; Royer et al., 2010) and theta oscillating cell groups are coupled by delays (Geisler et al., 2010). Similarly, the oscillation frequencies of medial entorhinal cortex neurons decrease progressively in the dorso-ventral direction (Giocomo et al., 2007), providing a frequency match between corresponding entorhinal and hippocampal neurons. Due to the delays, the faster but transient assembly oscillators produce a slower global rhythm, expressed by the coherent LFP oscillation in the entire length of the hippocampus and entorhinal cortex (Geisler et al., 2010). The progressively decreasing excitability of pyramidal neurons along the long axis (Segal et al., 2010) might further contribute to the dominantly septo-temporal spread

of activity. Finally, septally projecting long-range interneurons (Dragoi et al., 1999; Jinno et al., 2007; Toth et al., 1993), integrating the spiking activity of pyramidal cells at various septo-temporal segments, can serve as conduits to adjust the frequency and level of activity in the medial septum, which, in turn, can coordinate the frequency of global theta oscillations.

4.5 Sharp wave-associated ripple oscillations along the entire septo-temporal axis of the hippocampus

The present experiments demonstrate that ripples can occur at any level of the septo-temporal axis of the hippocampal CA1 region and the locally generated ripple events are qualitatively very similar. From the seed, the ripples can travel either septally or temporally with a speed of approximately 0.35 m/sec and invade varying segments, depending on the ripple magnitude. While large amplitude ripple events can occur synchronously over large distances or can propagate long distances, small amplitude events, in general, remain relatively local. While ripples travel smoothly across the dorsal and intermediate segments of the hippocampus, most ripples in the ventral segment occur in isolation. Ripples that emerge in the ventral and dorsal poles of the hippocampus are therefore largely independent and broadcast information to their cortical and subcortical targets at different times.

4.5.1 Ripples are locally generated

Locally confined ripples have been observed previously (Chrobak and Buzsaki, 1996; Csicsvari et al., 2000; Ylinen et al., 1995) but the spread of ripple activity along the septo-temporal axis has not been studied quantitatively. While sharp waves and ripples are strongly coupled physiological events, they can be dissociated (Maier et al., 2003; Nakashiba et al., 2008; Nimmrich et al., 2005; Traub and Bibbig, 2000; Ylinen et al., 1995). The population bursts of spatially distributed CA3 pyramidal neurons give rise to widespread depolarization and firing of CA1 (and CA3) pyramidal cells and specific classes of interneurons (Buzsaki et al., 1992; Csicsvari et al., 1999; Klausberger et al., 2003; Klausberger and Somogyi, 2008). Depending on the magnitude of the depolarization of CA1 neurons, they can generate either a fast gamma (or epsilon; 90-120 Hz) or ripple (130-200 Hz) oscillation in the dorsal CA1 region, largely reflecting the network resonance properties of this region (Sullivan et al., 2011). The extensive axon collaterals of CA3 pyramidal neurons (Li et al., 1994) exert a spatially widespread effect on CA1 neurons but ripples can emerge at single or multiple locations in CA1. Observing individual ripple events at multiple locations revealed various forms of ripple propagation, including locally confined events, propagating patterns from single or multiple locations, collision and reflection, similar to propagating events described in the neocortex (Arieli et al., 1996; Benucci et al., 2007; Roland et al., 2006; Xu et al., 2007). Although larger amplitude ripple events tended to travel further, the amplitude of the locally recorded events did not always predict whether the event will terminate or continue to travel and grow in amplitude. We hypothesize that the propagation mechanisms of ripple events largely reside in the extensive recurrent collaterals of the

CA3 neurons (Ishizuka et al., 1990; Li et al., 1994) so that each sharp wave event is a sweep in space but individual ripple waves reflect local interactions between CA1 pyramidal cells and interneurons. In support of this hypothesis, half of all large amplitude ripple events (>7 SD) occurred within a 100 msec window in the entire dorsal and intermediate segments of the hippocampus. Smaller amplitude ripple events, in general, were more spatially confined. An alternative substrate for ripple event propagation is the sparse but nevertheless important recurrent collaterals among CA1 pyramidal cells (Deuchars and Thomson, 1996; Maier et al., 2003; Memmesheimer, 2010).

The large spatial variability of ripples also suggests that widespread ripple events represent the fusion of multiple, locally emerging events. Every segment of the CA1 region along its long axis could generate ripples. Nearby ripples may be synchronized locally by interneuron or gap junction-mediated mechanisms (Nimmrich et al., 2005; Taxidis et al., 2012; Traub and Bibbig, 2000; Ylinen et al., 1995) or by the sparse CA1 collaterals (Deuchars and Thomson, 1996; Maier et al., 2003; Memmesheimer, 2010).

The lower amplitude of ripples in the ventral hippocampus can be explained by decreased synchrony of pyramidal cell spikes and/or the lower density of neurons in the ventral hippocampus (Schomburg et al., 2012). In support of the cell density hypothesis, ripples are of larger amplitude in the mouse where neurons are more densely packed in the same volume compared to the rat (Buzsaki et al., 2003). Modeling studies also demonstrate the importance of the density of neurons surrounding the recording electrodes for the amplitude of extracellular events (Schomburg et al., 2012). The mean frequency of ripples also decreased along the septo-temporal axis, which may be a result of a weaker excitatory drive in the ventral hippocampus. Reduced drive and frequency would lead to

both: fewer cells firing and reduced spike synchrony, both of which reduce ripple amplitude (Schomburg et al., 2012). The same hypothetical mechanism may also explain the decreased rate of large amplitude ripple events in the ventral hippocampus. When all ripples ($>3SD$) were considered, the mean ripple rates in the dorsal, intermediate and ventral segments were similar.

4.5.2 Propagating sharp wave ripples along the septo-temporal axis of the hippocampus

The locally emerging ripples could propagate either septally, temporally, or in both directions. The propagation speed of ripple events was approximately 0.35 m/sec. This speed is comparable to previously reported traveling waves in different cortical areas in vivo, including the primary motor cortex and the visual cortex in rats, ferrets, monkeys and cats (Arieli et al., 1996; Benucci et al., 2007; Roland et al., 2006; Rubino et al., 2006; Xu et al., 2007) and barrel cortex of guinea pigs and rats (Contreras and Llinas, 2001; Petersen et al., 2003). The speed of ripple propagation was almost twice as fast as the travel velocity of theta wave-related recruitment of neurons (0.16 m/sec), (Lubenov and Siapas, 2009; Patel et al., 2012) or in the longitudinal in vitro slice of the CA3 region (Miles et al., 1988). During ripple events, there is a 2 to 4-fold gain of excitation (Csicsvari et al., 1999), which may explain the speed acceleration relative to theta oscillations.

The perinatal form of sharp waves, known as giant depolarizing potentials (or GDPs), also shows a traveling pattern of propagation in the isolated hippocampus in vitro (Leinekugel et al., 1998). GDPs are most often initiated at the septal sites and propagated to more temporal regions but at a very low speed (0.01-0.02 m/sec), (Leinekugel et al., 1998). The large difference in the spread of activity may be partially due to the lower temperature of the in vitro situation or to maturational factors. It is possible that in the adult brain, the propagation of the CA3-initiated sharp wave sweep is accelerated by local, ripple-related mechanisms since ripples do not emerge until the third week after birth (Buhl and Buzsaki, 2005; Leinekugel et al., 1998).

4.5.3 Hippocampus-neocortical communication by ripples

A topographic organization exists between different segments of the hippocampus and the neocortex by way of the entorhinal cortical interface (Amaral, 2007; Petrovich et al., 2001; Witter et al., 1989b). The consequence of this anatomical layout is that the dorsal, intermediate and ventral segments of the hippocampus target spatially different but overlapping neocortical and subcortical domains. Under the framework that hippocampal ripples can assist with sleep and rest-related consolidation of memory traces (Buzsaki, 1989; Wilson and McNaughton, 1994), our findings suggest that the amplitude-dependent spatial spread of ripples may determine the extent of segregation and integration of hippocampal content by their cortical targets. These flexible mechanisms may assist with off-line categorization of hippocampofugal information (McClelland et al., 1995).

Alternatively, one can take the opposite or complementary view that the information from the septal and ventral poles of the hippocampus reach non-overlapping structures and the virtual lack of ripple synchrony at the two poles serves to assist in segregating neuronal patterns from these segments (Patel et al., 2012). Although spatial information is also present in the ventral hippocampus, place cells are rare (Kjelstrup et al., 2008; Royer et al., 2010). Instead, pyramidal neurons in the ventral quadrant reflect progressively increasing representations of emotional memory, and goal or reward directedness (Kjelstrup et al., 2002; Royer et al., 2010). Further support for this view comes from our observations that the ventral third of the hippocampus behaved somewhat disconnected from the rest of the structure. Synchrony of ripples between ventral sites and sites in the dorsal and intermediate hippocampus was significantly less than at identical distances in the dorsal and intermediate segments. This was also true for propagation of ripple events to and from the ventral sites. The relatively isolated nature of the ventral segment is also reflected by the abrupt decrease of theta coherence between ventral and dorsal/intermediate sites and the decreased speed-modulation of theta power in the ventral segment (Hinman et al., 2011; Patel et al., 2012). The relative functional isolation of the ventral segment is likely important because in primates the ventral segment grows disproportionally to become the uncus and body of the hippocampus, parts which communicate with the enlarged associational cortices (Amaral, 2007; Royer et al., 2010). In summary, the magnitude of ripples may be taken as an index of the intrahippocampal communication between various hippocampal segments. This local-

global dynamic could then be the mechanism of mixing spatial and non-spatial information before routing it back to the neocortex.

From the hippocampal perspective, the extent and travel direction of ripple events may determine how spatial and non-spatial information are combined within hippocampal circuits and their targets. For example, following an emotional experience, the temporo-septal dominance of ripple spread to the dorsal-intermediate segments may be taken as an indication that the emotional content propagates and mixes with place information. Our observation of sustained direction bias of ripple travel is compatible with this hypothesis but detailed verification would require specifically designed experiments. Indeed, it will be important to determine if behavioral conditions can influence the direction of travel of ripple events and the neurophysiological consequences of such bias for plasticity and memory consolidation. Our present findings show that ripple occurrence is quite flexible from strongly localized to spatially extensive events, associated with variable direction of travel. Whether or not this flexibility is utilized by the brain in a functional way remains an open question.

4.6 Outstanding Questions:

4.6.1 How strict is the dorsal-intermediate-ventral functional boundary? Is the hippocampus a functionally unified network or two relatively separate, inter-connected networks?

The entire organization of the hippocampus, including its afferent, efferent, and intrinsic connectivity (Amaral, 2007; Amaral, 1993; Amaral and Witter, 1989), neuro-modulatory influence (Roberts et al., 1984; Room and Groenewegen, 1986a), genetic make-up (Fanselow and Dong, 2010), cellular and circuit properties (Ashton et al., 1989; Gilbert et al., 1985), lesion studies (Ashton et al., 1989; Bannerman et al., 2002; Bannerman et al., 2004; Hock and Bunsey, 1998; Moser and Moser, 1998), and electrophysiological studies (Colombo et al., 1998; Jung et al., 1994; Kjelstrup et al., 2008; Maurer et al., 2005; Patel et al., 2012; Royer et al., 2010) all indicate potential functional differences between the two poles of the hippocampus. Given such an organization, an important question arises as to whether there exist a sharp sudden change along the septo-temporal axis or whether the differences noted at the poles are due to a continual change along the whole axis which when looked at the two ends of the distribution ‘appear’ different. Not surprisingly, it is difficult to answer this question with certainty. Most of the studies showing differences between the poles have in fact supported the argument that gradual changes are observed as one proceeds from one pole to the other. Although most changes noted along the axis are indeed gradual, there does seem to be some natural boundaries of connections (Fricke and Cowan, 1978), genes (Fanselow and Dong, 2010), and cellular and circuit properties (Moser and Moser, 1998), which may functionally divide the

hippocampus along the septo-temporal axis into segregated zones. Depending on the studies, they report a relatively sharp change at 2 or 3 locations, thereby dividing the hippocampus either into 2 or 3 zones along the septo-temporal axis.

In such an organization scheme with some features/properties showing gradual changes along the whole hippocampus vis-à-vis other features dividing the hippocampus into 3 zones (genetic profiles), or 2 zones (longitudinally divergent intrinsic connections, lesion studies and a few electrophysiological properties), it seems that the hippocampus along the septo-temporal axis keeps itself open to the possibility of combining information from the entire hippocampus when needed and keeping it segregated when appropriate. This flexibility would offer a mechanism by which the hippocampus could sub serve multiple forms of memories (Eichenbaum and Cohen, 1988; Gray, 1983; McClelland et al., 1995; O'Keefe and Nadel, 1978).

4.6.2 Is the ventral hippocampus functional distinction concerning sharp-wave ripples due to the 'gap' in anatomical sampling?

While some features of ripples change gradually along the large part of the septo-temporal axis (frequency, occurrence rate), other features are sharply different (amplitude, timing) and does not depend on distance but more so on the exact location along the whole septo-temporal axis. If it was simply a factor of the missed recording locations along the septo-temporal axis (where the CA1 pyramidal layer is vertical and so under sampled in our experiments), the distance dependent features should have not segregated measurements when electrode pairs came from septal only compared to when

they came from septal and ventral locations. Therefore, the functional dissociation of the hippocampus along the septo-temporal axis during offline state and ripples cannot be ascribed to the “gap” in recordings along the long axis. Instead, such functional segregation between the dorsal-intermediate and the ventral segments can likely be explained by the relative segregation of the CA3 collateral system (Ishizuka et al., 1990; Li et al., 1994; Wittner et al., 2007), differential afferent organization (Amaral and Witter, 1989; Burwell and Amaral, 1998; Dolorfo and Amaral, 1998a, b; Ruth et al., 1982; Witter et al., 1989a; Witter et al., 1989b) and perhaps the intrinsic circuit (Fricke and Cowan, 1978; Swanson et al., 1978) and neuronal features (Eichenbaum and Cohen, 1988; O'Keefe, 1999; Olton et al., 1986; Wible et al., 1986; Wiener, 1996; Wiener et al., 1989).

4.6.3 How can the dorsal and ventral hippocampal circuits influence each other?

The intermediate hippocampus may be best poised to integrate hippocampal representations from the septal and the temporal poles. The intermediate hippocampus can either help bring the entire hippocampus along the septo-temporal axis in sync or may leave the neurons at the poles to broadcast separate messages to their distinct, non-overlapping cortical targets (Amaral, 1993; Bast, 2007; Bast et al., 2009; Moser and Moser, 1998). In either scenario, it is the intermediate hippocampus which plays a crucial role when it comes to the functional dissociation of the hippocampus along the septo-temporal axis (Bast, 2007; Moser and Moser, 1998). More detailed studies will have to be performed to improve our understanding as to how the intermediate hippocampus may

play a dynamic role in integrating or segregating the hippocampal poles during different behaviors.

4.6.4 How might the hippocampal poles integrate and segregate information?

A half-cycle delay (corresponding to approximately 70 msec) between the septal and temporal poles may prevent temporal association of signals in the downstream structures with overlapping inputs from the entire hippocampus, suggesting functional physiological segmentation of the hippocampus (Royer et al., 2010). In addition, our results on theta coherence, theta intermittency, theta amplitude variability, theta-speed correlation and single unit local theta phase preference suggest a behavior-dependent dissociation of function between the intermediate and ventral segments of the hippocampus (Bannerman et al., 2004; Bannerman et al., 1999; Bast et al., 2009; Degroot and Treit, 2004; Hock and Bunsey, 1998; Moser and Moser, 1998; Pothuizen et al., 2004; Richmond et al., 1999; Risold and Swanson, 1996; Royer et al., 2010; Small, 2002). However, a small portion of ventral hippocampal neurons (approximately 25%) fire at the peak of local theta and therefore in synchrony with neurons in the septal segment. This subset could potentially be responsible for temporally uniting and helping combine distributed representations along the entire hippocampus before passing on the information to downstream targets.

In summary, our results indicate that theta oscillations can both temporally combine or segregate neocortical representations along the entire septo-temporal axis of the hippocampal CA1 pyramidal layer. Even ripples observed during off-line states support the segregation of the hippocampus into two distinct compartments along the septo-

temporal axis owing to the majority of non-overlapping ripple occurrence timing. However, the small percentage of ripples ($<7\%$) that do occur in synchrony along the whole hippocampus may permit the hippocampus to synchronize the whole structure along the septo-temporal axis during those select events. Thus, it seems that the hippocampal circuits primarily keep the information segregated during both online (theta) and offline (ripple) states, with the option to synchronize the whole structure along the septo-temporal axis during certain events/times.

4.6.5 How can these findings relate to the knowledge of theta generation?

Five decades of research on hippocampal theta oscillations still cannot provide a concrete mechanistic understanding of how hippocampal theta oscillations arise (Buzsaki, 2002; Petsche and Stumpf, 1962; Stewart and Fox, 1990; Vinogradova, 1995; Winson, 1974). Though numerous studies have supported and argued for the role of medial septum and the associated diagonal band of Broca as a pace-maker for hippocampal theta (Buzsaki, 2002; Vinogradova, 1995), these studies have not adequately addressed the complexity of phase distribution of neuronal firing in different hippocampal regions. Furthermore, subsequent research has also discovered that there are multiple intrinsic theta generators both within the hippocampus and entorhinal cortex (Brankack et al., 1993; Buzsaki, 2002; Buzsaki et al., 1986; Buzsaki et al., 1983; Kamondi et al., 1998). In addition, the supra-mammillary nucleus acts as a complimentary partner of the medial septum in the coordination of theta in the hippocampus (Vertes and Kocsis, 1997). Although relatively detailed anatomical studies inform us about the topographical connections between septum, supra-mammillary nucleus and EC with the hippocampus along with the

topography of the intrinsic connections within the hippocampus, these findings raise the question as to what supports the organization of phase (time) shifting hippocampal theta waves along the entire septo-temporal axis (Lubenov and Siapas, 2009; Patel et al., 2012). It seems that the medial septum is an interactive coordinator that plays a critical role in temporally organizing theta oscillations along the septo-temporal axis of the hippocampus and the dorso-ventral axis of the entorhinal cortex as opposed to a strict metronome-like pacemaker (Brazhnik and Fox, 1997; Stewart and Fox, 1990; Vinogradova, 1995). Both the long-range GABA-ergic hippocampo-septal fibers (Jinno et al., 2007) and the reciprocal septo-hippocampo GABA-ergic fibers (Freund and Antal, 1988; Peterson, 1994; Yoshida and Oka, 1995) are topographically organized, and this reciprocal fast conducting system can serve to coordinate neurons in the septum such that the frequency of theta along the entire septo-temporal axis remains same, even though the phase shifts monotonically along the axis reaching a maximum of half-theta cycle from pole-to-pole. The differences observed in the hippocampal theta from the dorsal 2/3rd and the ventral 1/3rd could be partly due to the different septo-hippocampo fiber pathways where the topographic septal projections to the dorsal 2/3rd travel via the fimbria/fornix while the connections to the ventral 1/3rd via a separate ventral pathway (Freund and Antal, 1988; Peterson, 1994; Petsche and Stumpf, 1960; Yoshida and Oka, 1995). The mechanism supporting the precise phase shifts observed along the septo-temporal axis of the hippocampus is likely in synchrony with a similar phase shift in theta oscillations in the entorhinal cortex along its dorso-ventral axis (Brun et al., 2008; Yoshida et al., 2011). While it is reported that putative GABA-ergic neurons in the septum fire at widely distributed phases of the hippocampal theta cycle (Borhegyi et al., 2004; Brazhnik and

Fox, 1999; Stewart and Fox, 1989), it does not directly answer the question why hippocampal theta phase shifts a half-cycle from pole-to-pole. I hypothesize that the primary mechanisms reside in the hippocampus and the hippocampo-septal GABA-ergic feedback from various segments and regions of the hippocampus set the appropriate phase of septal neurons. Local interactions of these neurons, synaptic and/or gap junction mediated, can then be responsible for adjusting the frequency of the global rhythm. Numerous tools, such as optogenetic manipulation and local cooling and heating, are now available to study the behavioral consequences of altering either the phase or frequency of theta oscillations.

4.7 Overall Summary

Overall, the work presented in this dissertation examined the organization of the theta oscillations and the sharp wave associated ripple oscillations along the entire septo-temporal axis of the hippocampus in behaving rats. These data reveal that during active behaviors such as exploration, the hippocampus can utilize traveling theta oscillations to combine or segregate information in the septo-temporal axis before passing it on to its downstream targets. During the “offline” state of the hippocampus, the propagating ripples within the septal-intermediate segments can permit integration of information from these regions and pass it on to downstream targets. On the other hand, the predominantly different timing of sharp-wave ripples and large phase shifts and relative amplitude independence of theta, in the septal-intermediate versus temporal segments suggest a relatively segregated transfer of information from these *two* hippocampal entities to their distinct cortical and sub-cortical targets.

The anatomical knowledge that the ventral hippocampus of the rodent brain enlarges disproportionately to become the large uncus and body parts of the hippocampus in primates emphasizes the need to study how the information in the entire hippocampus gets processed in our attempt to better understand the physiological mechanisms of the hippocampus. This knowledge may be instrumental to treatments for learning and memory disorders and Alzheimer’s disease. The attribution to the hippocampus in other psychiatric disorders like autism, bipolar disorder, obsessive compulsive disorder and

schizophrenia suggests a critical participation of the affective part (ventral) of the rodent hippocampus and warrants the study of the hippocampus in its entirety.

Chapter 5.0 – Bibliography

Adhikari, A., Topiwala, M.A., and Gordon, J.A. (2011). Single units in the medial prefrontal cortex with anxiety-related firing patterns are preferentially influenced by ventral hippocampal activity. *Neuron* 71, 898-910.

Amaral, D.G., Lavenex, P. (2007). Hippocampal Neuroanatomy In *The hippocampus book*, P. Andersen, ed. (New York: Oxford University Press), pp. xx, 832 p.

Amaral, D.G. (1986). Amygdalohippocampal and amygdalocortical projections in the primate brain. *Adv Exp Med Biol* 203, 3-17.

Amaral, D.G. (1993). Emerging principles of intrinsic hippocampal organization. *Curr Opin Neurobiol* 3, 225-229.

Amaral, D.G., and Kurz, J. (1985). An analysis of the origins of the cholinergic and noncholinergic septal projections to the hippocampal formation of the rat. *J Comp Neurol* 240, 37-59.

Amaral, D.G., and Witter, M.P. (1989). The three-dimensional organization of the hippocampal formation: a review of anatomical data. *Neuroscience* 31, 571-591.

Anderson, M.I., and O'Mara, S.M. (2003). Analysis of recordings of single-unit firing and population activity in the dorsal subiculum of unrestrained, freely moving rats. *J Neurophysiol* 90, 655-665.

Anderson, P.J. (1971). In memoriam Grete Globus, 1901-1970. *J Neuropathol Exp Neurol* 30, 1-2.

Arieli, A., Sterkin, A., Grinvald, A., and Aertsen, A. (1996). Dynamics of ongoing activity: explanation of the large variability in evoked cortical responses. *Science* 273, 1868-1871.

Ashton, D., Van Reempts, J., Haseldonckx, M., and Willems, R. (1989). Dorsal-ventral gradient in vulnerability of CA1 hippocampus to ischemia: a combined histological and electrophysiological study. *Brain Res* 487, 368-372.

Bannerman, D.M., Deacon, R.M., Offen, S., Friswell, J., Grubb, M., and Rawlins, J.N. (2002). Double dissociation of function within the hippocampus: spatial memory and hyponeophagia. *Behav Neurosci* 116, 884-901.

Bannerman, D.M., Grubb, M., Deacon, R.M., Yee, B.K., Feldon, J., and Rawlins, J.N. (2003). Ventral hippocampal lesions affect anxiety but not spatial learning. *Behav Brain Res* 139, 197-213.

- Bannerman, D.M., Rawlins, J.N., McHugh, S.B., Deacon, R.M., Yee, B.K., Bast, T., Zhang, W.N., Pothuizen, H.H., and Feldon, J. (2004). Regional dissociations within the hippocampus--memory and anxiety. *Neurosci Biobehav Rev* 28, 273-283.
- Bannerman, D.M., Yee, B.K., Good, M.A., Heupel, M.J., Iversen, S.D., and Rawlins, J.N. (1999). Double dissociation of function within the hippocampus: a comparison of dorsal, ventral, and complete hippocampal cytotoxic lesions. *Behav Neurosci* 113, 1170-1188.
- Bast, T. (2007). Toward an integrative perspective on hippocampal function: from the rapid encoding of experience to adaptive behavior. *Rev in Neurosci* 18, 253-281.
- Bast, T., Wilson, I.A., Witter, M.P., and Morris, R.G. (2009). From rapid place learning to behavioral performance: a key role for the intermediate hippocampus. *PLoS Biol* 7, e1000089.
- Benucci, A., Frazor, R.A., and Carandini, M. (2007). Standing waves and traveling waves distinguish two circuits in visual cortex. *Neuron* 55, 103-117.
- Berger, T.W., Rinaldi, P.C., Weisz, D.J., and Thompson, R.F. (1983). Single-unit analysis of different hippocampal cell types during classical conditioning of rabbit nictitating membrane response. *J Neurophysiol* 50, 1197-1219.
- Bilkey, D.K., and Goddard, G.V. (1985). Medial septal facilitation of hippocampal granule cell activity is mediated by inhibition of inhibitory interneurons. *Brain Res* 361, 99-106.
- Bland, B.H. (1986a). The physiology and pharmacology of hippocampal formation theta rhythms. *Prog Neurobiol* 26, 1-54.
- Blasco-Ibanez, J.M., and Freund, T.F. (1997). Distribution, ultrastructure, and connectivity of calretinin-immunoreactive mossy cells of the mouse dentate gyrus. *Hippocampus* 7, 307-320.
- Bodizs, R., Kantor, S., Szabo, G., Szucs, A., Eross, L., and Halasz, P. (2001). Rhythmic hippocampal slow oscillation characterizes REM sleep in humans. *Hippocampus* 11, 747-753.
- Borhegyi, Z., Varga, V., Szilagy, N., Fabo, D., and Freund, T.F. (2004). Phase segregation of medial septal GABAergic neurons during hippocampal theta activity. *J Neurosci* 24, 8470-8479.
- Brankack, J., Stewart, M., and Fox, S.E. (1993). Current source density analysis of the hippocampal theta rhythm: associated sustained potentials and candidate synaptic generators. *Brain research* 615, 310-327.

- Brazhnik, E.S., and Fox, S.E. (1997). Intracellular recordings from medial septal neurons during hippocampal theta rhythm. *Exp Brain Res* 114, 442-453.
- Brazhnik, E.S., and Fox, S.E. (1999). Action potentials and relations to the theta rhythm of medial septal neurons in vivo. *Exp Brain Res* 127, 244-258.
- Brazier, M.A. (1970). Regional activities within the human hippocampus and hippocampal gyrus. *Exp Neurol* 26, 254-268.
- Brun, V.H., Solstad, T., Kjelstrup, K.B., Fyhn, M., Witter, M.P., Moser, E.I., and Moser, M.B. (2008). Progressive increase in grid scale from dorsal to ventral medial entorhinal cortex. *Hippocampus* 18, 1200-1212.
- Buhl, D.L., and Buzsaki, G. (2005). Developmental emergence of hippocampal fast-field "ripple" oscillations in the behaving rat pups. *Neuroscience* 134, 1423-1430.
- Bullock, T.H., Buzsaki, G., and McClune, M.C. (1990). Coherence of compound field potentials reveals discontinuities in the CA1-subiculum of the hippocampus in freely-moving rats. *Neuroscience* 38, 609-619.
- Burwell, R.D., and Amaral, D.G. (1998). Perirhinal and postrhinal cortices of the rat: interconnectivity and connections with the entorhinal cortex. *J Comp Neurol* 391, 293-321.
- Buzsaki, G. (1986). Hippocampal sharp waves: their origin and significance. *Brain Res* 398, 242-252.
- Buzsaki, G. (1989). Two-stage model of memory trace formation: a role for "noisy" brain states. *Neuroscience* 31, 551-570.
- Buzsaki, G. (2002). Theta oscillations in the hippocampus. *Neuron* 33, 325-340.
- Buzsaki, G. (2005). Theta rhythm of navigation: link between path integration and landmark navigation, episodic and semantic memory. *Hippocampus* 15, 827-840.
- Buzsáki, G. (2006). *Rhythms of the brain* (Oxford ; New York: Oxford University Press).
- Buzsaki, G., Buhl, D.L., Harris, K.D., Csicsvari, J., Czeh, B., and Morozov, A. (2003). Hippocampal network patterns of activity in the mouse. *Neuroscience* 116, 201-211.
- Buzsaki, G., Czopf, J., Kondakor, I., and Kellenyi, L. (1986). Laminar distribution of hippocampal rhythmic slow activity (RSA) in the behaving rat: current-source density analysis, effects of urethane and atropine. *Brain Res* 365, 125-137.
- Buzsaki, G., Horvath, Z., Urioste, R., Hetke, J., and Wise, K. (1992). High-frequency network oscillation in the hippocampus. *Science* 256, 1025-1027.

- Buzsaki, G., Leung, L.W., and Vanderwolf, C.H. (1983). Cellular bases of hippocampal EEG in the behaving rat. *Brain Res* 287, 139-171.
- Caffe, A.R., van Leeuwen, F.W., and Luiten, P.G. (1987). Vasopressin cells in the medial amygdala of the rat project to the lateral septum and ventral hippocampus. *J Comp Neurol* 261, 237-252.
- Cantero, J.L., Atienza, M., Stickgold, R., Kahana, M.J., Madsen, J.R., and Kocsis, B. (2003). Sleep-dependent theta oscillations in the human hippocampus and neocortex. *J Neurosci* 23, 10897-10903.
- Cenquizca, L.A., and Swanson, L.W. (2007). Spatial organization of direct hippocampal field CA1 axonal projections to the rest of the cerebral cortex. *Brain Res Rev* 56, 1-26.
- Christian, E.P., and Dudek, F.E. (1988). Electrophysiological evidence from glutamate microapplications for local excitatory circuits in the CA1 area of rat hippocampal slices. *J Neurophysiol* 59, 110-123.
- Chrobak, J.J., and Buzsaki, G. (1994). Selective activation of deep layer (V-VI) retrohippocampal cortical neurons during hippocampal sharp waves in the behaving rat. *J Neurosci* 14, 6160-6170.
- Chrobak, J.J., and Buzsaki, G. (1996). High-frequency oscillations in the output networks of the hippocampal-entorhinal axis of the freely behaving rat. *J Neurosci* 16, 3056-3066.
- Cohen, A.H., Ermentrout, G.B., Kiemel, T., Kopell, N., Sigvardt, K.A., and Williams, T.L. (1992). Modelling of intersegmental coordination in the lamprey central pattern generator for locomotion. *Trends Neurosci* 15, 434-438.
- Colombo, M., Fernandez, T., Nakamura, K., and Gross, C.G. (1998). Functional differentiation along the anterior-posterior axis of the hippocampus in monkeys. *J Neurophysiol* 80, 1002-1005.
- Contreras, D., and Llinas, R. (2001). Voltage-sensitive dye imaging of neocortical spatiotemporal dynamics to afferent activation frequency. *J Neurosci* 21, 9403-9413.
- Csicsvari, J., Hirase, H., Czurko, A., and Buzsaki, G. (1998). Reliability and state dependence of pyramidal cell-interneuron synapses in the hippocampus: an ensemble approach in the behaving rat. *Neuron* 21, 179-189.
- Csicsvari, J., Hirase, H., Czurko, A., Mamiya, A., and Buzsaki, G. (1999). Fast network oscillations in the hippocampal CA1 region of the behaving rat. *J Neurosci* 19, RC20.
- Csicsvari, J., Hirase, H., Mamiya, A., and Buzsaki, G. (2000). Ensemble patterns of hippocampal CA3-CA1 neurons during sharp wave-associated population events. *Neuron* 28, 585-594.

- Csicsvari, J., Jamieson, B., Wise, K.D., and Buzsaki, G. (2003). Mechanisms of gamma oscillations in the hippocampus of the behaving rat. *Neuron* 37, 311-322.
- de Hoz, L., Knox, J., and Morris, R.G. (2003). Longitudinal axis of the hippocampus: both septal and temporal poles of the hippocampus support water maze spatial learning depending on the training protocol. *Hippocampus* 13, 587-603.
- Deadwyler, S.A., Bunn, T., and Hampson, R.E. (1996). Hippocampal ensemble activity during spatial delayed-nonmatch-to-sample performance in rats. *J Neurosci* 16, 354-372.
- DeCoteau, W.E., Thorn, C., Gibson, D.J., Courtemanche, R., Mitra, P., Kubota, Y., and Graybiel, A.M. (2007). Oscillations of local field potentials in the rat dorsal striatum during spontaneous and instructed behaviors. *J Neurophysiol* 97, 3800-3805.
- Degroot, A., and Treit, D. (2004). Anxiety is functionally segregated within the septo-hippocampal system. *Brain Res* 1001, 60-71.
- Deuchars, J., and Thomson, A.M. (1996). CA1 pyramid-pyramid connections in rat hippocampus in vitro: dual intracellular recordings with biocytin filling. *Neuroscience* 74, 1009-1018.
- Diba, K., and Buzsaki, G. (2007). Forward and reverse hippocampal place-cell sequences during ripples. *Nat Neurosci* 10, 1241-1242.
- Dolorfo, C.L., and Amaral, D.G. (1998a). Entorhinal cortex of the rat: organization of intrinsic connections. *J Comp Neurol* 398, 49-82.
- Dolorfo, C.L., and Amaral, D.G. (1998b). Entorhinal cortex of the rat: topographic organization of the cells of origin of the perforant path projection to the dentate gyrus. *J Comp Neurol* 398, 25-48.
- Dong, H.W., Swanson, L.W., Chen, L., Fanselow, M.S., and Toga, A.W. (2009). Genomic-anatomic evidence for distinct functional domains in hippocampal field CA1. *Proc Natl Acad Sci U S A* 106, 11794-11799.
- Dragoi, G., and Buzsaki, G. (2006). Temporal encoding of place sequences by hippocampal cell assemblies. *Neuron* 50, 145-157.
- Dragoi, G., Carpi, D., Recce, M., Csicsvari, J., and Buzsaki, G. (1999). Interactions between hippocampus and medial septum during sharp waves and theta oscillation in the behaving rat. *J Neurosci* 19, 6191-6199.
- Dupret, D., O'Neill, J., Pleydell-Bouverie, B., and Csicsvari, J. (2010). The reorganization and reactivation of hippocampal maps predict spatial memory performance. *Nat Neurosci* 13, 995-1002.

- Ego-Stengel, V., and Wilson, M.A. (2010). Disruption of ripple-associated hippocampal activity during rest impairs spatial learning in the rat. *Hippocampus* 20, 1-10.
- Eichenbaum, H., and Cohen, N.J. (1988). Representation in the hippocampus: what do hippocampal neurons code? *Trends Neurosci* 11, 244-248.
- Eichenbaum, H., Fagan, A., Mathews, P., and Cohen, N.J. (1988). Hippocampal system dysfunction and odor discrimination learning in rats: impairment or facilitation depending on representational demands. *Behav Neurosci* 102, 331-339.
- Eichenbaum, H., Kuperstein, M., Fagan, A., and Nagode, J. (1987). Cue-sampling and goal-approach correlates of hippocampal unit activity in rats performing an odor-discrimination task. *J Neurosci* 7, 716-732.
- Eichenbaum, H., Mathews, P., and Cohen, N.J. (1989). Further studies of hippocampal representation during odor discrimination learning. *Behav Neurosci* 103, 1207-1216.
- Ermentrout, G.B., and Kleinfeld, D. (2001). Traveling electrical waves in cortex: insights from phase dynamics and speculation on a computational role. *Neuron* 29, 33-44.
- Fanselow, M.S., and Dong, H.W. (2010). Are the dorsal and ventral hippocampus functionally distinct structures? *Neuron* 65, 7-19.
- Ferino, F., Thierry, A.M., and Glowinski, J. (1987). Anatomical and electrophysiological evidence for a direct projection from Ammon's horn to the medial prefrontal cortex in the rat. *Exp Brain Res* 65, 421-426.
- Fernandez, G., Weyerts, H., Schrader-Bolsche, M., Tendolkar, I., Smid, H.G., Tempelmann, C., Hinrichs, H., Scheich, H., Elger, C.E., Mangun, G.R., and Heinze, H.J. (1998). Successful verbal encoding into episodic memory engages the posterior hippocampus: a parametrically analyzed functional magnetic resonance imaging study. *J Neurosci* 18, 1841-1847.
- Foster, D.J., and Wilson, M.A. (2006). Reverse replay of behavioural sequences in hippocampal place cells during the awake state. *Nature* 440, 680-683.
- Freund, T.F., and Antal, M. (1988). GABA-containing neurons in the septum control inhibitory interneurons in the hippocampus. *Nature* 336, 170-173.
- Fricke, R., and Cowan, W.M. (1978). An autoradiographic study of the commissural and ipsilateral hippocampo-dentate projections in the adult rat. *J Comp Neurol* 181, 253-269.
- Fujisawa, S., Amarasingham, A., Harrison, M.T., and Buzsaki, G. (2008). Behavior-dependent short-term assembly dynamics in the medial prefrontal cortex. *Nat Neurosci* 11, 823-833.

- Gage, F.H., Bjorklund, A., and Stenevi, U. (1983). Reinnervation of the partially deafferented hippocampus by compensatory collateral sprouting from spared cholinergic and noradrenergic afferents. *Brain Res* 268, 27-37.
- Gage, F.H., and Thompson, R.G. (1980). Differential distribution of norepinephrine and serotonin along the dorsal-ventral axis of the hippocampal formation. *Brain Res Bull* 5, 771-773.
- Gall, C., Brecha, N., Karten, H.J., and Chang, K.J. (1981). Localization of enkephalin-like immunoreactivity to identified axonal and neuronal populations of the rat hippocampus. *J Comp Neurol* 198, 335-350.
- Geisler, C., Diba, K., Pastalkova, E., Mizuseki, K., Royer, S., and Buzsaki, G. (2010). Temporal delays among place cells determine the frequency of population theta oscillations in the hippocampus. *Proc Natl Acad Sci U S A* 107, 7957-7962.
- Geisler, C., Robbe, D., Zugaro, M., Sirota, A., and Buzsaki, G. (2007). Hippocampal place cell assemblies are speed-controlled oscillators. *Proc Natl Acad Sci U S A* 104, 8149-8154.
- Gilbert, M., Racine, R.J., and Smith, G.K. (1985). Epileptiform burst responses in ventral vs dorsal hippocampal slices. *Brain Res* 361, 389-391.
- Giocomo, L.M., Zilli, E.A., Fransen, E., and Hasselmo, M.E. (2007). Temporal frequency of subthreshold oscillations scales with entorhinal grid cell field spacing. *Science* 315, 1719-1722.
- Girardeau, G., Benchenane, K., Wiener, S.I., Buzsaki, G., and Zugaro, M.B. (2009). Selective suppression of hippocampal ripples impairs spatial memory. *Nat Neurosci* 12, 1222-1223.
- Gray, J.A. (1982). *The neuropsychology of anxiety : an enquiry into the functions of the septo-hippocampal system* (Oxford New York: Clarendon Press ; Oxford University Press).
- Gray, J.A. (1983). A theory of anxiety: the role of the limbic system. *Encephale* 9, 161B-166B.
- Green, J.D., and Arduini, A.A. (1954). Hippocampal electrical activity in arousal. *J Neurophysiol* 17, 533-557.
- Grillner, S., Deliagina, T., Ekeberg, O., el Manira, A., Hill, R.H., Lansner, A., Orlovsky, G.N., and Wallen, P. (1995). Neural networks that co-ordinate locomotion and body orientation in lamprey. *Trends Neurosci* 18, 270-279.
- Hampson, R.E., Simeral, J.D., and Deadwyler, S.A. (1999). Distribution of spatial and nonspatial information in dorsal hippocampus. *Nature* 402, 610-614.

- Hargreaves, E.L., Rao, G., Lee, I., and Knierim, J.J. (2005). Major dissociation between medial and lateral entorhinal input to dorsal hippocampus. *Science* 308, 1792-1794.
- Haring, J.H., and Davis, J.N. (1985). Differential distribution of locus coeruleus projections to the hippocampal formation: anatomical and biochemical evidence. *Brain Res* 325, 366-369.
- Harris, K.D., Henze, D.A., Csicsvari, J., Hirase, H., and Buzsaki, G. (2000). Accuracy of tetrode spike separation as determined by simultaneous intracellular and extracellular measurements. *J Neurophysiol* 84, 401-414.
- Hasselmo, M.E., Hay, J., Ilyn, M., and Gorchetchnikov, A. (2002). Neuromodulation, theta rhythm and rat spatial navigation. *Neural Netw* 15, 689-707.
- Hasselmo, M.E., Schnell, E., and Barkai, E. (1995). Dynamics of learning and recall at excitatory recurrent synapses and cholinergic modulation in rat hippocampal region CA3. *J Neurosci* 15, 5249-5262.
- Hazan, L., Zugaro, M., and Buzsaki, G. (2006). Klusters, NeuroScope, NDManager: a free software suite for neurophysiological data processing and visualization. *J Neurosci Methods* 155, 207-216.
- Hinman, J.R., Penley, S.C., Long, L.L., Escabi, M.A., and Chrobak, J.J. (2011). Septotemporal variation in dynamics of theta: speed and habituation. *J Neurophysiol* 105, 2675-2686.
- Hock, B.J., Jr., and Bunsey, M.D. (1998). Differential effects of dorsal and ventral hippocampal lesions. *J Neurosci* 18, 7027-7032.
- Hughes, K.R. (1965). Dorsal and ventral hippocampus lesions and maze learning: influence of preoperative environment. *Can J Psychol* 19, 325-332.
- Huxter, J., Burgess, N., and O'Keefe, J. (2003). Independent rate and temporal coding in hippocampal pyramidal cells. *Nature* 425, 828-832.
- Huxter, J.R., Senior, T.J., Allen, K., and Csicsvari, J. (2008). Theta phase-specific codes for two-dimensional position, trajectory and heading in the hippocampus. *Nat Neurosci* 11, 587-594.
- Insausti, R., Amaral, D.G., and Cowan, W.M. (1987). The entorhinal cortex of the monkey: II. Cortical afferents. *J Comp Neurol* 264, 356-395.
- Ishizuka, N., Weber, J., and Amaral, D.G. (1990). Organization of intrahippocampal projections originating from CA3 pyramidal cells in the rat. *J Comp Neurol* 295, 580-623.

- Jacobson, L., and Sapolsky, R. (1991). The role of the hippocampus in feedback regulation of the hypothalamic-pituitary-adrenocortical axis. *Endocr Rev* 12, 118-134.
- Jay, T.M., Glowinski, J., and Thierry, A.M. (1989). Selectivity of the hippocampal projection to the prelimbic area of the prefrontal cortex in the rat. *Brain Res* 505, 337-340.
- Jay, T.M., and Witter, M.P. (1991). Distribution of hippocampal CA1 and subicular efferents in the prefrontal cortex of the rat studied by means of anterograde transport of Phaseolus vulgaris-leucoagglutinin. *J Comp Neurol* 313, 574-586.
- Jeewajee, A., Barry, C., O'Keefe, J., and Burgess, N. (2008). Grid cells and theta as oscillatory interference: electrophysiological data from freely moving rats. *Hippocampus* 18, 1175-1185.
- Jensen, O., Idiart, M.A., and Lisman, J.E. (1996). Physiologically realistic formation of autoassociative memory in networks with theta/gamma oscillations: role of fast NMDA channels. *Learning & memory* 3, 243-256.
- Jensen, O., and Lisman, J.E. (1996). Theta/gamma networks with slow NMDA channels learn sequences and encode episodic memory: role of NMDA channels in recall. *Learning & memory* 3, 264-278.
- Jinno, S., Klausberger, T., Marton, L.F., Dalezios, Y., Roberts, J.D., Fuentealba, P., Bushong, E.A., Henze, D., Buzsaki, G., and Somogyi, P. (2007). Neuronal diversity in GABAergic long-range projections from the hippocampus. *J Neurosci* 27, 8790-8804.
- Jung, M.W., Wiener, S.I., and McNaughton, B.L. (1994). Comparison of spatial firing characteristics of units in dorsal and ventral hippocampus of the rat. *J Neurosci* 14, 7347-7356.
- Kahana, M.J., Seelig, D., and Madsen, J.R. (2001). Theta returns. *Curr Opin Neurobiol* 11, 739-744.
- Kamondi, A., Acsady, L., Wang, X.J., and Buzsaki, G. (1998). Theta oscillations in somata and dendrites of hippocampal pyramidal cells in vivo: activity-dependent phase-precession of action potentials. *Hippocampus* 8, 244-261.
- Karlsson, M.P., and Frank, L.M. (2009). Awake replay of remote experiences in the hippocampus. *Nat Neurosci* 12, 913-918.
- Kesner, R.P., Crutcher, K., and Beers, D.R. (1988). Serial position curves for item (spatial location) information: role of the dorsal hippocampal formation and medial septum. *Brain Res* 454, 219-226.

- Kjelstrup, K.B., Solstad, T., Brun, V.H., Hafting, T., Leutgeb, S., Witter, M.P., Moser, E.I., and Moser, M.B. (2008). Finite scale of spatial representation in the hippocampus. *Science* 321, 140-143.
- Kjelstrup, K.G., Tuvnes, F.A., Steffenach, H.A., Murison, R., Moser, E.I., and Moser, M.B. (2002). Reduced fear expression after lesions of the ventral hippocampus. *Proc Natl Acad Sci U S A* 99, 10825-10830.
- Klausberger, T., Magill, P.J., Marton, L.F., Roberts, J.D., Cobden, P.M., Buzsaki, G., and Somogyi, P. (2003). Brain-state- and cell-type-specific firing of hippocampal interneurons in vivo. *Nature* 421, 844-848.
- Klausberger, T., and Somogyi, P. (2008). Neuronal diversity and temporal dynamics: the unity of hippocampal circuit operations. *Science* 321, 53-57.
- Kocsis, B., Bragin, A., and Buzsaki, G. (1999). Interdependence of multiple theta generators in the hippocampus: a partial coherence analysis. *J Neurosci* 19, 6200-6212.
- Kocsis, B., and Vertes, R.P. (1997). Phase relations of rhythmic neuronal firing in the supramammillary nucleus and mammillary body to the hippocampal theta activity in urethane anesthetized rats. *Hippocampus* 7, 204-214.
- Kohler, C., Schultzberg, M., and Radesater, A.C. (1987). Distribution of neuropeptide Y receptors in the rat hippocampal region. *Neurosci Lett* 75, 141-146.
- Konopacki, J., Bland, B.H., MacIver, M.B., and Roth, S.H. (1987). Cholinergic theta rhythm in transected hippocampal slices: independent CA1 and dentate generators. *Brain Res* 436, 217-222.
- Kopell, N., and Ermentrout, G.B. (1986). Symmetry and phaselocking in chains of weakly coupled oscillators. *Comm Pure App Math* 39, 623-660.
- Kudrimoti, H.S., Barnes, C.A., and McNaughton, B.L. (1999). Reactivation of hippocampal cell assemblies: effects of behavioral state, experience, and EEG dynamics. *J Neurosci* 19, 4090-4101.
- Lee, A.K., and Wilson, M.A. (2002). Memory of sequential experience in the hippocampus during slow wave sleep. *Neuron* 36, 1183-1194.
- Lee, M.G., Chrobak, J.J., Sik, A., Wiley, R.G., and Buzsaki, G. (1994). Hippocampal theta activity following selective lesion of the septal cholinergic system. *Neuroscience* 62, 1033-1047.
- Leinekugel, X., Khalilov, I., Ben-Ari, Y., and Khazipov, R. (1998). Giant depolarizing potentials: the septal pole of the hippocampus paces the activity of the developing intact septohippocampal complex in vitro. *J Neurosci* 18, 6349-6357.

- Li, X.G., Somogyi, P., Ylinen, A., and Buzsaki, G. (1994). The hippocampal CA3 network: an in vivo intracellular labeling study. *J Comp Neurol* 339, 181-208.
- Lubenov, E.V., and Siapas, A.G. (2009). Hippocampal theta oscillations are travelling waves. *Nature* 459, 534-539.
- Magee, J.C., and Johnston, D. (1995). Synaptic activation of voltage-gated channels in the dendrites of hippocampal pyramidal neurons. *Science* 268, 301-304.
- Magee, J.C., and Johnston, D. (1997). A synaptically controlled, associative signal for Hebbian plasticity in hippocampal neurons. *Science* 275, 209-213.
- Maggio, N., and Segal, M. (2007). Striking variations in corticosteroid modulation of long-term potentiation along the septotemporal axis of the hippocampus. *J Neurosci* 27, 5757-5765.
- Maguire, E.A., Gadian, D.G., Johnsrude, I.S., Good, C.D., Ashburner, J., Frackowiak, R.S., and Frith, C.D. (2000). Navigation-related structural change in the hippocampi of taxi drivers. *Proc Natl Acad Sci U S A* 97, 4398-4403.
- Mahut, H., Zola-Morgan, S., and Moss, M. (1982). Hippocampal resections impair associative learning and recognition memory in the monkey. *J Neurosci* 2, 1214-1220.
- Maier, N., Nimmrich, V., and Draguhn, A. (2003). Cellular and network mechanisms underlying spontaneous sharp wave-ripple complexes in mouse hippocampal slices. *J Physiol* 550, 873-887.
- Markram, H., Lubke, J., Frotscher, M., and Sakmann, B. (1997). Regulation of synaptic efficacy by coincidence of postsynaptic APs and EPSPs. *Science* 275, 213-215.
- Maruki, K., Izaki, Y., Nomura, M., and Yamauchi, T. (2001). Differences in paired-pulse facilitation and long-term potentiation between dorsal and ventral CA1 regions in anesthetized rats. *Hippocampus* 11, 655-661.
- Maurer, A.P., Vanrhoads, S.R., Sutherland, G.R., Lipa, P., and McNaughton, B.L. (2005). Self-motion and the origin of differential spatial scaling along the septo-temporal axis of the hippocampus. *Hippocampus* 15, 841-852.
- McClelland, J.L., McNaughton, B.L., and O'Reilly, R.C. (1995). Why there are complementary learning systems in the hippocampus and neocortex: insights from the successes and failures of connectionist models of learning and memory. *Psychol Rev* 102, 419-457.
- McFarland, W.L., Teitelbaum, H., and Hedges, E.K. (1975). Relationship between hippocampal theta activity and running speed in the rat. *J Comp Physiol Psychol* 88, 324-328.

- McHugh, S.B., Deacon, R.M., Rawlins, J.N., and Bannerman, D.M. (2004). Amygdala and ventral hippocampus contribute differentially to mechanisms of fear and anxiety. *Behav Neurosci* 118, 63-78.
- Mehta, M.R., Barnes, C.A., and McNaughton, B.L. (1997). Experience-dependent, asymmetric expansion of hippocampal place fields. *Proc Natl Acad Sci U S A* 94, 8918-8921.
- Memmesheimer, R.M. (2010). Quantitative prediction of intermittent high-frequency oscillations in neural networks with supralinear dendritic interactions. *Proc Natl Acad Sci U S A* 107, 11092-11097.
- Miles, R., Traub, R.D., and Wong, R.K. (1988). Spread of synchronous firing in longitudinal slices from the CA3 region of the hippocampus. *J Neurophysiol* 60, 1481-1496.
- Milner, T.A., Loy, R., and Amaral, D.G. (1983). An anatomical study of the development of the septo-hippocampal projection in the rat. *Brain Res* 284, 343-371.
- Mitra, P.P., and Pesaran, B. (1999). Analysis of dynamic brain imaging data. *Biophys J* 76, 691-708.
- Mizuseki, K., Diba, K., Pastalkova, E., and Buzsaki, G. (2011). Hippocampal CA1 pyramidal cells form functionally distinct sublayers. *Nat Neurosci* 14, 1174-1181.
- Montgomery, S.M., Betancur, M.I., and Buzsaki, G. (2009). Behavior-dependent coordination of multiple theta dipoles in the hippocampus. *J Neurosci* 29, 1381-1394.
- Montgomery, S.M., Sirota, A., and Buzsaki, G. (2008). Theta and gamma coordination of hippocampal networks during waking and rapid eye movement sleep. *J Neurosci* 28, 6731-6741.
- Moser, E., Moser, M.B., and Andersen, P. (1993). Spatial learning impairment parallels the magnitude of dorsal hippocampal lesions, but is hardly present following ventral lesions. *J Neurosci* 13, 3916-3925.
- Moser, E.I., Kropff, E., and Moser, M.B. (2008). Place cells, grid cells, and the brain's spatial representation system. *Annu Rev Neurosci* 31, 69-89.
- Moser, M.B., and Moser, E.I. (1998). Functional differentiation in the hippocampus. *Hippocampus* 8, 608-619.
- Moser, M.B., Moser, E.I., Forrest, E., Andersen, P., and Morris, R.G. (1995). Spatial learning with a minislab in the dorsal hippocampus. *Proc Natl Acad Sci U S A* 92, 9697-9701.

- Muller, R.U., Kubie, J.L., and Ranck, J.B., Jr. (1987). Spatial firing patterns of hippocampal complex-spike cells in a fixed environment. *J Neurosci* 7, 1935-1950.
- Naber, P.A., Caballero-Bleda, M., Jorritsma-Byham, B., and Witter, M.P. (1997). Parallel input to the hippocampal memory system through peri- and postrhinal cortices. *Neuroreport* 8, 2617-2621.
- Nakashiba, T., Young, J.Z., McHugh, T.J., Buhl, D.L., and Tonegawa, S. (2008). Transgenic inhibition of synaptic transmission reveals role of CA3 output in hippocampal learning. *Science* 319, 1260-1264.
- Nimmrich, V., Maier, N., Schmitz, D., and Draguhn, A. (2005). Induced sharp wave-ripple complexes in the absence of synaptic inhibition in mouse hippocampal slices. *J Physiol* 563, 663-670.
- Nokia, M.S., Mikkonen, J.E., Penttonen, M., and Wikgren, J. (2012). Disrupting neural activity related to awake-state sharp wave-ripple complexes prevents hippocampal learning. *Front Behav Neurosci* 6, 84.
- Nyberg, L., McIntosh, A.R., Cabeza, R., Habib, R., Houle, S., and Tulving, E. (1996). General and specific brain regions involved in encoding and retrieval of events: what, where, and when. *Proc Natl Acad Sci U S A* 93, 11280-11285.
- O'Keefe, J. (1999). Do hippocampal pyramidal cells signal non-spatial as well as spatial information? *Hippocampus* 9, 352-364.
- O'Keefe, J., and Dostrovsky, J. (1971). The hippocampus as a spatial map. Preliminary evidence from unit activity in the freely-moving rat. *Brain Res* 34, 171-175.
- O'Keefe, J., and Recce, M.L. (1993). Phase relationship between hippocampal place units and the EEG theta rhythm. *Hippocampus* 3, 317-330.
- O'Keefe, J.M., and Nadel, L. (1978). *The hippocampus as a cognitive map* (Oxford New York: Clarendon Press ; Oxford University Press).
- O'Neill, J., Senior, T., and Csicsvari, J. (2006). Place-selective firing of CA1 pyramidal cells during sharp wave/ripple network patterns in exploratory behavior. *Neuron* 49, 143-155.
- O'Neill, J., Senior, T.J., Allen, K., Huxter, J.R., and Csicsvari, J. (2008). Reactivation of experience-dependent cell assembly patterns in the hippocampus. *Nat Neurosci* 11, 209-215.
- O'Keefe, J. (2006). Hippocampal Neurophysiology in the behaving animal In *The Hippocampus Book*, P. Andersen, R. Morris, D. Amaral, T. Bliss, J. O'Keefe, and Oxford University Press., eds. (New York, Oxford University Press).

- Olton, D.S., Wible, C.G., and Shapiro, M.L. (1986). Mnemonic theories of hippocampal function. *Behav Neurosci* 100, 852-855.
- Papathodoropoulos, C., Asprodini, E., Nikita, I., Koutsona, C., and Kostopoulos, G. (2002). Weaker synaptic inhibition in CA1 region of ventral compared to dorsal rat hippocampal slices. *Brain Res* 948, 117-121.
- Papathodoropoulos, C., and Kostopoulos, G. (2000a). Decreased ability of rat temporal hippocampal CA1 region to produce long-term potentiation. *Neurosci Lett* 279, 177-180.
- Papathodoropoulos, C., and Kostopoulos, G. (2000b). Dorsal-ventral differentiation of short-term synaptic plasticity in rat CA1 hippocampal region. *Neurosci Lett* 286, 57-60.
- Pare, D., Collins, D.R., and Pelletier, J.G. (2002). Amygdala oscillations and the consolidation of emotional memories. *Trends Cogn Sci* 6, 306-314.
- Parkinson, J.K., Murray, E.A., and Mishkin, M. (1988). A selective mnemonic role for the hippocampus in monkeys: memory for the location of objects. *J Neurosci* 8, 4159-4167.
- Patel, J., Fujisawa, S., Berenyi, A., Royer, S., and Buzsaki, G. (2012). Traveling theta waves along the entire septotemporal axis of the hippocampus. *Neuron* 75, 410-417.
- Paxinos, G., and Watson, C. (2007). *The rat brain in stereotaxic coordinates*, 6th edn (Amsterdam ; Boston: Elsevier).
- Petersen, C.C., Grinvald, A., and Sakmann, B. (2003). Spatiotemporal dynamics of sensory responses in layer 2/3 of rat barrel cortex measured in vivo by voltage-sensitive dye imaging combined with whole-cell voltage recordings and neuron reconstructions. *J Neurosci* 23, 1298-1309.
- Peterson, G.M. (1994). Differential projections to the hippocampus by neurons of the medial septum and vertical limb of the diagonal band. *Brain Res* 646, 129-134.
- Petrovich, G.D., Canteras, N.S., and Swanson, L.W. (2001). Combinatorial amygdalar inputs to hippocampal domains and hypothalamic behavior systems. *Brain Res Rev* 38, 247-289.
- Petsche, H., and Stumpf, C. (1960). Topographic and toposcopic study of origin and spread of the regular synchronized arousal pattern in the rabbit. *Electroencephalogr Clin Neurophysiol* 12, 589-600.
- Petsche, H., and Stumpf, C. (1962). [The origin of theta-rhythm in the rabbit hippocampus]. *Wien Klin Wochenschr* 74, 696-700.
- Phillips, R.G., and LeDoux, J.E. (1992). Differential contribution of amygdala and hippocampus to cued and contextual fear conditioning. *Behav Neurosci* 106, 274-285.

- Pitkanen, A., Pikkarainen, M., Nurminen, N., and Ylinen, A. (2000). Reciprocal connections between the amygdala and the hippocampal formation, perirhinal cortex, and postrhinal cortex in rat. A review. *Ann N Y Acad Sci* 911, 369-391.
- Pothuizen, H.H., Zhang, W.N., Jongen-Relo, A.L., Feldon, J., and Yee, B.K. (2004). Dissociation of function between the dorsal and the ventral hippocampus in spatial learning abilities of the rat: a within-subject, within-task comparison of reference and working spatial memory. *Eur J Neurosci* 19, 705-712.
- Poucet, B., and Buhot, M.C. (1994). Effects of medial septal or unilateral hippocampal inactivations on reference and working spatial memory in rats. *Hippocampus* 4, 315-321.
- Poucet, B., Herrmann, T., and Buhot, M.C. (1991). Effects of short-lasting inactivations of the ventral hippocampus and medial septum on long-term and short-term acquisition of spatial information in rats. *Behav Brain Res* 44, 53-65.
- Poucet, B., Thinus-Blanc, C., and Muller, R.U. (1994). Place cells in the ventral hippocampus of rats. *Neuroreport* 5, 2045-2048.
- Racine, R., Rose, P.A., and Burnham, W.M. (1977). Afterdischarge thresholds and kindling rates in dorsal and ventral hippocampus and dentate gyrus. *Can J Neurol Sci* 4, 273-278.
- Richmond, M.A., Yee, B.K., Pouzet, B., Veenman, L., Rawlins, J.N., Feldon, J., and Bannerman, D.M. (1999). Dissociating context and space within the hippocampus: effects of complete, dorsal, and ventral excitotoxic hippocampal lesions on conditioned freezing and spatial learning. *Behav Neurosci* 113, 1189-1203.
- Risold, P.Y., and Swanson, L.W. (1996). Structural evidence for functional domains in the rat hippocampus. *Science* 272, 1484-1486.
- Risold, P.Y., and Swanson, L.W. (1997). Connections of the rat lateral septal complex. *Brain Res Rev* 24, 115-195.
- Roberts, G.W., Woodhams, P.L., Polak, J.M., and Crow, T.J. (1984). Distribution of neuropeptides in the limbic system of the rat: the hippocampus. *Neuroscience* 11, 35-77.
- Roland, P.E., Hanazawa, A., Undeman, C., Eriksson, D., Tompa, T., Nakamura, H., Valentiniene, S., and Ahmed, B. (2006). Cortical feedback depolarization waves: a mechanism of top-down influence on early visual areas. *Proc Natl Acad Sci U S A* 103, 12586-12591.
- Rombouts, S.A., Machielsen, W.C., Witter, M.P., Barkhof, F., Lindeboom, J., and Scheltens, P. (1997). Visual association encoding activates the medial temporal lobe: a functional magnetic resonance imaging study. *Hippocampus* 7, 594-601.

- Room, P., and Groenewegen, H.J. (1986a). Connections of the parahippocampal cortex in the cat. II. Subcortical afferents. *J Comp Neurol* 251, 451-473.
- Room, P., and Groenewegen, H.J. (1986b). Connections of the parahippocampal cortex. I. Cortical afferents. *J Comp Neurol* 251, 415-450.
- Royer, S., Sirota, A., Patel, J., and Buzsaki, G. (2010). Distinct representations and theta dynamics in dorsal and ventral hippocampus. *J Neurosci* 30, 1777-1787.
- Rubino, D., Robbins, K.A., and Hatsopoulos, N.G. (2006). Propagating waves mediate information transfer in the motor cortex. *Nat Neurosci* 9, 1549-1557.
- Rudy, J.W., and Sutherland, R.J. (1989). The hippocampal formation is necessary for rats to learn and remember configural discriminations. *Behav Brain Res* 34, 97-109.
- Ruth, R.E., Collier, T.J., and Routtenberg, A. (1982). Topography between the entorhinal cortex and the dentate septotemporal axis in rats: I. Medial and intermediate entorhinal projecting cells. *J Comp Neurol* 209, 69-78.
- Sainsbury, R.S. (1998). Hippocampal theta: a sensory-inhibition theory of function. *Neurosci Biobehav Rev* 22, 237-241.
- Schomburg, E.W., Anastassiou, C.A., Buzsaki, G., and Koch, C. (2012). The spiking component of oscillatory extracellular potentials in the rat hippocampus. *J Neurosci* 32, 11798-11811.
- Scoville, W.B., and Milner, B. (1957). Loss of recent memory after bilateral hippocampal lesions. *J Neurol Neurosurg Psychiatry* 20, 11-21.
- Segal, M., Richter-Levin, G., and Maggio, N. (2010). Stress-induced dynamic routing of hippocampal connectivity: a hypothesis. *Hippocampus* 20, 1332-1338.
- Siapas, A.G., Lubenov, E.V., and Wilson, M.A. (2005). Prefrontal phase locking to hippocampal theta oscillations. *Neuron* 46, 141-151.
- Siegel, A., and Tassoni, J.P. (1971). Differential efferent projections from the ventral and dorsal hippocampus of the cat. *Brain Behav Evol* 4, 185-200.
- Singer, A.C., and Frank, L.M. (2009). Rewarded outcomes enhance reactivation of experience in the hippocampus. *Neuron* 64, 910-921.
- Sirota, A., Montgomery, S., Fujisawa, S., Isomura, Y., Zugaro, M., and Buzsaki, G. (2008). Entrainment of neocortical neurons and gamma oscillations by the hippocampal theta rhythm. *Neuron* 60, 683-697.
- Skaggs, W.E., and McNaughton, B.L. (1996). Replay of neuronal firing sequences in rat hippocampus during sleep following spatial experience. *Science* 271, 1870-1873.

- Skaggs, W.E., McNaughton, B.L., Wilson, M.A., and Barnes, C.A. (1996). Theta phase precession in hippocampal neuronal populations and the compression of temporal sequences. *Hippocampus* 6, 149-172.
- Small, S.A. (2002). The longitudinal axis of the hippocampal formation: its anatomy, circuitry, and role in cognitive function. *Rev Neurosci* 13, 183-194.
- Squire, L.R. (1992). Memory and the hippocampus: a synthesis from findings with rats, monkeys, and humans. *Psychol Rev* 99, 195-231.
- Stern, C.E., Corkin, S., Gonzalez, R.G., Guimaraes, A.R., Baker, J.R., Jennings, P.J., Carr, C.A., Sugiura, R.M., Vedantham, V., and Rosen, B.R. (1996). The hippocampal formation participates in novel picture encoding: evidence from functional magnetic resonance imaging. *Proc Natl Acad Sci U S A* 93, 8660-8665.
- Stevens, R., and Cowey, A. (1973). Effects of dorsal and ventral hippocampal lesions on spontaneous alternation, learned alternation and probability learning in rats. *Brain Res* 52, 203-224.
- Stewart, M., and Fox, S.E. (1989). Firing relations of medial septal neurons to the hippocampal theta rhythm in urethane anesthetized rats. *Exp Brain Res* 77, 507-516.
- Stewart, M., and Fox, S.E. (1990). Do septal neurons pace the hippocampal theta rhythm? *Trends Neurosci* 13, 163-168.
- Sullivan, D., Csicsvari, J., Mizuseki, K., Montgomery, S., Diba, K., and Buzsaki, G. (2011). Relationships between hippocampal sharp waves, ripples, and fast gamma oscillation: influence of dentate and entorhinal cortical activity. *J Neurosci* 31, 8605-8616.
- Sutherland, R.J., McDonald, R.J., Hill, C.R., and Rudy, J.W. (1989). Damage to the hippocampal formation in rats selectively impairs the ability to learn cue relationships. *Behav Neural Biol* 52, 331-356.
- Swanson, L.W. (1981). A direct projection from Ammon's horn to prefrontal cortex in the rat. *Brain Res* 217, 150-154.
- Swanson, L.W., Wyss, J.M., and Cowan, W.M. (1978). An autoradiographic study of the organization of intrahippocampal association pathways in the rat. *J Comp Neurol* 181, 681-715.
- Taxidis, J., Coombes, S., Mason, R., and Owen, M.R. (2012). Modeling sharp wave-ripple complexes through a CA3-CA1 network model with chemical synapses. *Hippocampus* 22, 995-1017.

- Thierry, A.M., Gioanni, Y., Degenetais, E., and Glowinski, J. (2000). Hippocampo-prefrontal cortex pathway: anatomical and electrophysiological characteristics. *Hippocampus* 10, 411-419.
- Thinus-Blanc, C., Save, E., Poucet, B., and Buhot, M.C. (1991). The effects of reversible inactivations of the hippocampus on exploratory activity and spatial memory. *Hippocampus* 1, 365-371.
- Thompson, C.L., Pathak, S.D., Jeromin, A., Ng, L.L., MacPherson, C.R., Mortrud, M.T., Cusick, A., Riley, Z.L., Sunkin, S.M., Bernard, A., *et al.* (2008). Genomic anatomy of the hippocampus. *Neuron* 60, 1010-1021.
- Thomson, A.M., and Radpour, S. (1991). Excitatory Connections Between CA1 Pyramidal Cells Revealed by Spike Triggered Averaging in Slices of Rat Hippocampus are Partially NMDA Receptor Mediated. *Eur J Neurosci* 3, 587-601.
- Toth, K., Borhegyi, Z., and Freund, T.F. (1993). Postsynaptic targets of GABAergic hippocampal neurons in the medial septum-diagonal band of broca complex. *J Neurosci* 13, 3712-3724.
- Traub, R.D., and Bibbig, A. (2000). A model of high-frequency ripples in the hippocampus based on synaptic coupling plus axon-axon gap junctions between pyramidal neurons. *J Neurosci* 20, 2086-2093.
- van Groen, T., and Wyss, J.M. (1990). Extrinsic projections from area CA1 of the rat hippocampus: olfactory, cortical, subcortical, and bilateral hippocampal formation projections. *J Comp Neurol* 302, 515-528.
- van Leeuwen, F.W., van Heerikhuize, J., van der Meulen, G., and Wolters, P. (1985). Light microscopic autoradiographic localization of [3H]oxytocin binding sites in the rat brain, pituitary and mammary gland. *Brain Res* 359, 320-325.
- Vanderwolf, C.H. (1969a). Hippocampal electrical activity and voluntary movement in the rat. *Electroen Clin Neuro* 26, 407-418.
- Vann, S.D., Brown, M.W., Erichsen, J.T., and Aggleton, J.P. (2000). Using fos imaging in the rat to reveal the anatomical extent of the disruptive effects of fornix lesions. *J Neurosci* 20, 8144-8152.
- Verney, C., Baulac, M., Berger, B., Alvarez, C., Vigny, A., and Helle, K.B. (1985). Morphological evidence for a dopaminergic terminal field in the hippocampal formation of young and adult rat. *Neuroscience* 14, 1039-1052.
- Vertes, R.P., and Kocsis, B. (1997). Brainstem-diencephalo-septohippocampal systems controlling the theta rhythm of the hippocampus. *Neuroscience* 81, 893-926.

- Vinogradova, O.S. (1995). Expression, control, and probable functional significance of the neuronal theta-rhythm. *Prog Neurobiol* 45, 523-583.
- Wible, C.G., Findling, R.L., Shapiro, M., Lang, E.J., Crane, S., and Olton, D.S. (1986). Mnemonic correlates of unit activity in the hippocampus. *Brain Res* 399, 97-110.
- Wiener, S.I. (1996). Spatial, behavioral and sensory correlates of hippocampal CA1 complex spike cell activity: implications for information processing functions. *Prog Neurobiol* 49, 335-361.
- Wiener, S.I., Paul, C.A., and Eichenbaum, H. (1989). Spatial and behavioral correlates of hippocampal neuronal activity. *J Neurosci* 9, 2737-2763.
- Wilson, F.A. (1987). Cortical and subcortical structures involved in recognition memory: neurophysiological and anatomical studies. *Int J Neurol* 21-22, 204-217.
- Wilson, M.A., and McNaughton, B.L. (1994). Reactivation of hippocampal ensemble memories during sleep. *Science* 265, 676-679.
- Winson, J. (1974). Patterns of hippocampal theta rhythm in the freely moving rat. *Electroen Clin Neuro* 36, 291-301.
- Winson, J. (1978). Loss of hippocampal theta rhythm results in spatial memory deficit in the rat. *Science* 201, 160-163.
- Witter, M.P., Groenewegen, H.J., Lopes da Silva, F.H., and Lohman, A.H. (1989a). Functional organization of the extrinsic and intrinsic circuitry of the parahippocampal region. *Prog Neurobiol* 33, 161-253.
- Witter, M.P., Van Hoesen, G.W., and Amaral, D.G. (1989b). Topographical organization of the entorhinal projection to the dentate gyrus of the monkey. *J Neurosci* 9, 216-228.
- Wittner, L., Henze, D.A., Zaborszky, L., and Buzsaki, G. (2007). Three-dimensional reconstruction of the axon arbor of a CA3 pyramidal cell recorded and filled in vivo. *Brain Struct Funct* 212, 75-83.
- Womelsdorf, T., Schoffelen, J.M., Oostenveld, R., Singer, W., Desimone, R., Engel, A.K., and Fries, P. (2007). Modulation of neuronal interactions through neuronal synchronization. *Science* 316, 1609-1612.
- Xu, W., Huang, X., Takagaki, K., and Wu, J.Y. (2007). Compression and reflection of visually evoked cortical waves. *Neuron* 55, 119-129.
- Ylinen, A., Bragin, A., Nadasdy, Z., Jando, G., Szabo, I., Sik, A., and Buzsaki, G. (1995). Sharp wave-associated high-frequency oscillation (200 Hz) in the intact hippocampus: network and intracellular mechanisms. *J Neurosci* 15, 30-46.

- Yoder, R.M., and Pang, K.C. (2005). Involvement of GABAergic and cholinergic medial septal neurons in hippocampal theta rhythm. *Hippocampus* 15, 381-392.
- Yoshida, K., and Oka, H. (1995). Topographical projections from the medial septum-diagonal band complex to the hippocampus: a retrograde tracing study with multiple fluorescent dyes in rats. *Neurosci Res* 21, 199-209.
- Yoshida, M., Giocomo, L.M., Boardman, I., and Hasselmo, M.E. (2011). Frequency of subthreshold oscillations at different membrane potential voltages in neurons at different anatomical positions on the dorsoventral axis in the rat medial entorhinal cortex. *J Neurosci* 31, 12683-12694.
- Young, B.J., Fox, G.D., and Eichenbaum, H. (1994). Correlates of hippocampal complex-spike cell activity in rats performing a nonspatial radial maze task. *J Neurosci* 14, 6553-6563.
- Zhang, W.N., Pothuizen, H.H., Feldon, J., and Rawlins, J.N. (2004). Dissociation of function within the hippocampus: effects of dorsal, ventral and complete excitotoxic hippocampal lesions on spatial navigation. *Neuroscience* 127, 289-300.
- Zola-Morgan, S., and Squire, L.R. (1986). Memory impairment in monkeys following lesions limited to the hippocampus. *Behav Neurosci* 100, 155-160.

Chapter 6.0 - Appendix

Chapter 7.0 - Curriculum Vitae

Jagdish Patel

Born 7/7/77 Bhayavadar, Rajkot District, Gujarat, India

Prior Education and Work Experience

University of Oxford	MSc in Pharmacology with Distinction	2004-2005
Quintiles India	Associate – Regulatory Affairs	2002-2004
Triumphant Institute of Management Education	Visiting Faculty	2003-2004
Eli-Lilly India	Trainee Territory Manager	2001-2002
LM College of Pharmacy	Bachelor of Pharmacy with Distinction	1997-2001
LM College of Pharmacy	Diploma in Pharmacy with Distinction	1995-1997

Teaching

2008 Spring semester, Psychology – I, TA, Rutgers – The State Univ of NJ
 2008 Fall semester, Mathematical Biology, TA, NJ Institute of Technology
 2009 fall Semester, Critical Thinking, TA, Rutgers – The State Univ of NJ

Awards

- 1) Scholarship from MBL, to attend the “Neuroinformatics”, a 2-week summer program (Aug, 2011) organized by the Marine Biological Laboratory at MBL, Woods Hole.
- 2) Departmental Funding from Behavioral Neuroscience, Rutgers Univ., to attend the “Cognitive and Computational Neuroscience”, a 2-week summer program (in July 2011) organized by Cold Spring Harbor Asia Conference in Suzhou, China.
- 3) Invited by Temporal Dynamics for Learning Center (TDLC), San Diego to give a talk during the National Science Foundation site visit at San Diego in May 2012.
- 4) Funding from Temporal Dynamics for Learning Center (TDLC) to present a poster during a National Science Foundation site visit at San Diego in Aug 2010.
- 5) Scholarship fund from the Department of Pharmacology for MSc studies at the University of Oxford.
- 6) Chess trophy from LMCP (May, 2001), Gujarat University for winning 3 consecutive annual chess tournaments.